MEASUREMENT CALIBRATION/TUNING & TOPOLOGY PROCESSING IN POWER SYSTEM STATE ESTIMATION

A Dissertation

by

SHAN ZHONG

Submitted to the Office of Graduate Studies of
Texas A&M University
in partial fulfillment of the requirements for the degree of

DOCTOR OF PHILOSOPHY

December 2003

Major Subject: Electrical Engineering

MEASUREMENT CALIBRATION/TUNING & TOPOLOGY PROCESSING IN POWER SYSTEM STATE ESTIMATION

A Dissertation

by

SHAN ZHONG

Submitted to Texas A&M University
in partial fulfillment of the requirements
for the degree of

DOCTOR OF PHILOSOPHY

Approved as to style and content by:

_____	_____
Ali Abur (Chair of Committee)	Mladen Kezunovic (Member)
_____	_____
Don R. Halverson (Member)	Vivek Sarin (Member)
_____	
Chanan Singh (Head of Department)	

December 2003

Major Subject: Electrical Engineering

ABSTRACT

Measurement Calibration/Tuning & Topology Processing in Power System State Estimation. (December 2003)

Shan Zhong, B.S., Huazhong University of Science and Technology, China;
M.S., Tsinghua University, China

Chair of Advisory Committee: Dr. Ali Abur

State estimation plays an important role in modern power systems. The errors in the telemetered measurements and the connectivity information of the network will greatly contaminate the estimated system state. This dissertation provides solutions to suppress the influences of these errors.

A two-stage state estimation algorithm has been utilized in topology error identification in the past decade. Chapter II discusses the implementation of this algorithm. A concise substation model is defined for this purpose. A friendly user interface that incorporates the two-stage algorithm into the conventional state estimator is developed.

The performances of the two-stage state estimation algorithms rely on accurate determination of suspect substations. A comprehensive identification procedure is described in chapter III. In order to evaluate the proposed procedure, a topology error library is created. Several identification methods are comparatively tested using this library.

A remote measurement calibration method is presented in chapter IV. The un-calibrated quantities can be related to the true values by the characteristic functions. The conventional state estimation algorithm is modified to include the parameters of these functions. Hence they can be estimated along with the system state variables and used to calibrate the measurements. The measurements taken at different time instants are utilized to minimize the influence of the random errors.

A method for auto tuning of measurement weights in state estimation is described in chapter V. Two alternative ways to estimate the measurement random error variances are discussed. They are both tested on simulation data generated based on IEEE systems. Their performances are compared. A comprehensive solution, which contains an initialization process and a recursively updating process, is presented.

Chapter VI investigates the errors introduced in the positive sequence state estimation due to the usual assumptions of having fully balanced bus loads/generations and continuously transposed transmission lines. Several tests are conducted using different assumptions regarding the availability of single and multi-phase measurements. It is demonstrated that incomplete metering of three-phase system quantities may lead to significant errors in the positive sequence state estimates for certain cases. A novel sequence domain three-phase state estimation algorithm is proposed to solve this problem.

ACKNOWLEDGMENTS

First and foremost, I would like to express my sincere gratitude to my advisor, Dr. Ali Abur, for his inspiring guidance, encouragement, and support. His ardor and earnestness for studies are respected and will never be forgotten.

I also want to extend my gratitude and appreciation to many people who made this dissertation possible. Special thanks are due to all of my committee members, Dr. Mladen Kezunovic, Dr. Don R. Halverson, and Dr. Vivek Sarin. They gave me many invaluable suggestions during these three years. I am grateful to Prof. Marshall S. Poole, my Graduate Council Representative. Special thanks goes to the Power System Engineering Research Center (PSERC) and the National Science Foundation (NSF) for the support to work on the research.

Finally, I would like to thank my parents and my dear girl friend, Shaobo Du, for their unbounded love and encouragement.

TABLE OF CONTENTS

Page

Page

CHAPTER

Page

CHAPTER

Page

CHAPTER

LIST OF TABLES

TABLE Page

TABLE Page

LIST OF FIGURES

FIGURE Page

FIGURE Page

CHAPTER I

INTRODUCTION

Since electric power system state estimation (SE) was introduced by Fred Schweppe of MIT in 1969 [1], it has remained an extremely active and contentious area. At present, state estimation plays an essential role in modern Energy Management systems (EMS) providing a complete, consistent, accurate and reliable database for other key functions of the EMS system, such as security monitoring, optimal power flow, security analysis, on-line power flow studies, supervisory control, automatic voltage control and economic dispatch control [2]-[3].

Power system state estimation is the process carried out in the energy control centers in order to provide a best estimate of the system state based on the real-time system measurements and a pre-determined system model. A redundant set of real-time measurements, including bus voltage magnitudes, real and reactive power injections at the buses, real and reactive line power flows, and sometimes line current magnitudes, are collected from the entire network through the Supervisory Control and Data Acquisition (SCADA) system. These telemetered raw measurements are usually corrupted by different kinds of errors. State estimator is a digestive system that removes these impurities statistically to determine the state of the system. In formulating power system state estimation problem, the complex bus voltages (bus voltages magnitudes and phase angles) are commonly used as the state variables. Once system state is determined, the entire system quantities such as line power flows, line current magnitudes and bus power injections can be calculated.

The deregulation of the electric power industry has transformed state estimation from an important application into a critical one. Many critical commercial issues in the power market, such as congestion management, need to be founded and justified on a precise model of power system, which is derived from the state estimation process. Hence, the improvement of the state estimation to achieve a more accurate and more reliable system

---

This thesis follows the style and format of *IEEE Transactions on Power Delivery*.

state is a timely task.

Although the role of a state estimator is clear, there is much freedom of choice in its practical implementation. One of the important options is that of the statistical methodology used to purify the measured data. Various methods for state estimation have been introduced [5]-[7] in the past decades. Among those methods, Weighted Least Squares (WLS) algorithm is the most popular one. The objective function to be minimized of this method is chosen as the weighted sum of squares of the measurement residuals. Since this kind of problem can be solved by efficient numerical techniques, state estimators based on WLS approach have been installed in almost all the EMS systems all over the world. However, WLS method is highly sensitive to bad data in the measurement set [8]. In order to solve this problem, an alternative formulation of the state estimation problem, Weight Least Absolute Values (WLAV) [8]-[10], has been used. It defines the sum of the weighted absolute values of the measurement residuals as the objective function. Although this method is not widely used in the industry due to slower speed compared to WLS method, its capability of automatic bad data rejection makes it useful in some special issues such as topology error identification.

When a state estimation model fails to yield estimates within a degree of accuracy compatible with the standard deviations of the quantities estimated, one must conclude either that the measured quantities contain spurious data or that the model is unfit to explain the measured quantities. The procedure to identify and solve the former problem is called bad data analysis [4] while for the later one is topology error detection/identification. There exist many bad data analysis techniques [4], [11] and they are successfully utilized. However, the conventional state estimators are still vulnerable to errors in the topology of the system, which show up when the assumed status of the circuit breakers and switches do not coincide with their true statuses.

Observability analysis is another important procedure closely related to state estimation. Sometimes state estimation is not possible if it is not given enough measurements. If all the state variables (bus voltage magnitudes and relative phase angles) can be estimated using the available measurements, a system is said to be observable. Various methods proposed for network observability analysis have been well document in the literature [12]-[14].

Usually the following assumptions are made in formulating the conventional static power system state estimation problem [15]:

1) The three-phase power system network is balanced. Thus, a single-phase equivalent circuit can represent the system.
2) The system is operating in the steady state.
3) The parameters of the network are known and accurate.
4) The real-time topology of the network is precisely known.
5) All measurements are collected at the same instant and represent a true snapshot of the system state.
6) Measurement errors are independent random variables with zero mean Gaussian distribution.
7) Variances (σ^2) of the measurement errors are exactly known.

In a real power system, some of these assumptions may not always hold, which will result in erroneous estimates. The difficulties of solving this kind of problems give rise to the so-called Generalized State Estimation algorithm. Proposed by Alcir Monticelli [4] and others, the generalized approach takes into account that the network impedances and topology are not accurately known. They insisted that, in order to construct the best power flow model, the device statuses and impedance values must be regarded as subject to statistical errors. Likewise, all other potentially imprecise data sources, including transformer taps, phase shifter angles, voltage regulation set points, interchange schedules, equipment limits and plausibility criteria have to be factored into the estimation process.

The first application of the generalized state estimation approach is identification of topology error. In a conventional EMS system, the topology issue is mainly addressed by topology processor. It runs before the state estimator. All the switch statuses will be input into topology processor and the output is the system model in bus/branch level. The detailed substation models will be ignored. It is easy to image that sometimes the switch statuses are incorrect. Most of topology processors can handle these errors by simple consistency check. It will identify some of this kind of errors and can still provide a correct system model. However, once this function fails, the topology error will go into the state estimator, which result in erroneous estimates. This requires state estimator capable of ability to detect and identify topology error. The topic of detection and

identification of topology errors has been addressed in many papers in the past decades. There are several rule-based methods [16]-[18] and methods using correlation index [19] as an indication of possible topology errors. Other approaches [20], [21] utilize normalized measurement residuals to identify topology errors. In early 1990', Alcir Monticelli presented a new modeling method, which includes switches directly in the system model by incorporating their power flows within the state estimation formulation [22], [23]. Several topology error identification algorithms [24]-[28] are proposed based on this model. The main idea is to augment the state vector with the power flows through the circuit breakers and identify the status of the breakers based on the estimated flows through them. This is accomplished by representing the substations in detail using circuit breaker models. However, in order to keep the computational cost within reasonable limits, detailed substation models are employed only for a few substations suspected of having topological errors. A two-stage state estimation [8], [24] is used for this purpose. A small set of suspect substations will be identified after the first stage estimation. The second stage state estimation will incorporate the detailed model of the suspected substations and yield the estimated statuses of the CBs.

Chapter II focuses on the implementation of this proposed two-stage state estimation algorithm based on a conventional state estimator. A simplified substation model that contains only a minimum amount of required data for the second stage state estimation is defined. A small set of data is also added to the conventional bus/branch model to establish the relationships between all substations. Using these extra data structures, the two-stage state estimator and its associated user interface are implemented and tested. The implementation is carried out in such a way that future revisions to the estimation and/or identification algorithms can easily be incorporated and arbitrary topologies for new substations can be defined as needed. It can serve as a test platform for any further developments in this topic.

The success of the two-stage state estimator in identifying the topology errors depends on the correct identification of the suspect substations after the first stage. Currently used identification methods do not have satisfied performance under some circumstances. Chapter III describes an improved identification strategy, which utilizes the calculated state estimation residuals of the first stage and the associated network

configuration. In order to investigate and comparatively evaluate the performances of different identification methods, a topology error library containing 50 scenarios are built based on the IEEE 30 bus test system. The simulation results of different methods on this library will be compared and the best method will be selected. In addition, the new identification method will be implemented in an adaptive way. User in the practical system can modify some parameters to fit their needs.

As mentioned above, one of the assumptions of the conventional state estimation is that measurement errors are independent random variables with zero mean Gaussian distribution. The telemetered measurements used in power system state estimation are final products of a chain of instruments, including instrument transformer, transducer, A/D (D/A) convertor, etc. Hence the uncertainties in the measurements are due to combination of random and systematic errors caused by those instruments. The raw measurements need to be calibrated before used by state estimator to satisfy the "zero mean error" requirement. On-site adjustment process can correct some of the systematic errors, such as model errors, erroneous instrument ratios and transducer ratings and scaling procedures. However, due to the diversity of error sources, the on-site calibration procedure, which is untimely and labor intensive, cannot get satisfactory result. It also cannot handle time dependent errors and some temporary errors, such as failure of the metering gear, intermittent error due to the interference in communication. Chapter IV will investigate how to utilize state estimation approach to process the on-line measurement calibration.

While the systematic error might be eliminated by calibration methods, random error will always remain. The conventional state estimation assumes the variances of the random errors are known and the measurements will be weighted by the inverses of random error variances to suppress their influences. No matter using WLS method or WLAV method, the accuracy of the estimate results is greatly influenced by the weight vector. However, the random errors of measurements presented in control system are the combination of different sources of random errors, which come from different devices throughout the processing procedure. It is very difficult to precisely determine the variances of these random errors in advance. Moreover, some of the random error sources, such as those come from communication process, may be influenced by some

real-time factors. This results in the time dependent property of variances. In this case, state estimation should be capable of setting measurement weight adaptively. The estimation and the auto-tuning of the variances of the measurements are necessary. This topic will be discussed in Chapter V.

Power systems are generally configured in three phases, and are designed to operate in an almost balanced manner. Analysis of balanced three-phase systems is relatively simple compared to the full detailed three-phase solution of the network equations. A symmetrical component transformation will decompose the balanced three-phase system into three independent systems, commonly referred to as the positive, negative and the zero sequence networks. Absence of negative and zero sequence signals under perfectly balanced three-phase operating conditions, allows the analysis to be carried out in the single phase, using only the positive sequence model. State estimators are no exception, making use of the positive sequence network model and the measurements in solving for the best estimate for the system state. In a realistic system, there will be imbalances between three phases, such as non-transposed transmission line and unbalanced load distribution. This may introduce errors into the estimate of state estimator, which assume the system is fully symmetrical. Chapter VI will discuss the influences of this kind of modeling errors and discuss the solution to eliminate them.

Finally, as a summary, Chapter VII will draw the conclusions of this dissertation, outline its main contributions and provide suggestions about possible future work.

CHAPTER II

IMPLEMENTATION OF TWO-STAGE METHOD FOR TOPOLOGY ERROR DETECTION/IDENTIFICATION

2.1 Introduction

Topology error identification is an important issue in the real time operation and control of power systems. These errors will lead to inaccurate state estimates and furthermore will not be easily identified by the conventional bad data processing methods. The common cause of topology errors is the incorrect status information about the circuit breakers (CB) at the substations. Since such information may not be monitored on-line for each and every breaker in the system, there may be situations where the actual and assumed status of a breaker may differ after the occurrence of a substation reconfiguration event.

Several methods have been proposed in order to identify topology errors. Among them, there are those, which are rule-based [16]-[18] and others that are based on modified formulation of the state estimation algorithm [8], [24], [25]-[28]. The latter ones incorporate the circuit breaker models of [22]-[23] (zero impedance branches) into the state estimation formulation. The main idea is to augment the state vector with the power flows through the circuit breakers and identify the status of the breakers based on the estimated flows through them. This is accomplished by representing the substations in detail using these circuit breaker models. While it is possible to reduce the computational complexity of this formulation by cleverly manipulating the substation equations [28], including all the circuit breakers within the system model may not always be practical. In this dissertation, in order to keep the computational cost within reasonable limits, detailed substation models are employed only for a few substations suspected of having topological errors. A two-stage state estimation approach [24] is employed for this purpose. A small set of suspect substations will be identified after the first stage estimation. The second stage will incorporate the detailed model of the suspected substations and yield the estimated status of the CBs.

A simplified substation model that contains only a minimum amount of required data for the second stage state estimation is defined. A small set of data is also added to the conventional bus/branch model to establish the relationship between all substations. Using these extra data structures, the two-stage state estimator and its associated user interface are implemented and tested. The implementation is carried out in such a way that future revisions to the estimation and/or identification algorithms can easily be incorporated and arbitrary topologies for new substations can be defined as needed.

2.2 Formulation of State Estimation and Bad Data Detection

The problem of state estimation is usually formulated as a weighted least squares (WLS) problem [29], which is solved by efficient numerical techniques. The objective function to be minimized is chosen as the weighted sum of squares of the measurement residuals. However, WLS method is highly sensitive to bad data in the measurement set [8]. In order to avoid this, a different formulation of the state estimation problem has been used. It defines the sum of the weighted absolute values of the measurement residuals as the objective function. Due to its automatic bad data rejection property, WLAV estimation method will be used in topology errors identification. In the following parts of this section, we will describe these two methods briefly.

2.2.1 WLS Methods

The measurement equation for a system modeled at the bus/branch level will take the following form:

$$z = h(x) + e \tag{1}$$

where:

z is the measurement vector of dimension m;

h(x) is the nonlinear relating the error free to the system states;

x is the state vector of dimension n;

e is the measurement noise vector;

n,m: the number of the state variables and measurement respectively.

Substituting the first order Taylor expansion of h(x) around some x_0 in (1), we will have:

$$\Delta z = H \cdot \Delta x + e \tag{2}$$

where:

$\Delta z = z - h(x_0)$

$H = \frac{\partial h}{\partial x}$ at x_0

$\Delta x = x - x_0$

The weighted least square (WLS) estimate for x can be found by minimizing the following objective function:

$$J(x) = \sum_{i=1}^{m} \omega_i^2 (z_i - h_i(x))^2 \tag{3}$$

With the first order of Taylor expansion of h(x) shown in (2), the following equation will be solved iteratively to find the solution minimizing (3).

$$\left.\frac{\partial J(x)}{\partial x}\right|_{x=x^k} = H' \cdot W \cdot H \cdot \Delta x^k - H' \cdot W \cdot \Delta z^k = 0 \tag{4}$$

where: W is the diagonal weight matrix.

Equation (4) can be rewritten as:

$$\Delta x^k = G^{-1} \cdot H' \cdot W \cdot \Delta z^k = 0 \tag{5}$$

where: $G = H' \cdot W \cdot H$ is called the gain matrix.

The WLS estimation problem given by (3) and (5) can be solved iteratively until $|\Delta x^k|$ become smaller than a threshold.

2.2.2 WLAV Methods

The weighted least absolute value (WLAV) estimate for x can be found by minimizing the following objective function:

$$J(x) = \sum_{i=1}^{m} \omega_i |z_i - h_i(x)| \tag{6}$$

This is accomplished by iteratively solving the following linear programming (LP) problem at each iteration k:

$$\min J(x) = \sum_{i=1}^{m} \omega_i (u_i + v_i) \tag{7}$$

$$subject\ to \quad \Delta z^k = H(x^k) \cdot \Delta x^k + u - v \tag{8}$$

Where:

$\Delta z^k = z - h(x^k)$

$H(x^k) = \dfrac{\partial h}{\partial x}$ at x^k

ω_i : measurement weight assigned to the i^{th} measurement;

u, v = nonnegative slack variables such that *(u-v)* represents the measurement residuals. The WLAV program represented by (7) and (8) can be solved using the linear programming (LP) method.

2.2.3 Bad Data Detection/Identification

When a state estimation program fails to yield accurate estimates, it is either due to the erroneous measurements or due to a modeling error or both. The former is normally known as bad data, and the latter is called the topology error.

A common technique used for bad data processing is the normalized residuals test (r^n test). In this section, we will describe the r^n test used in WLS method and WLAV method, respectively.

1) Normalized residuals in WLS method

Assume that the state estimate $\hat{x}$ has already been computed from (5). The residuals of the measurements are defined as:

$$\hat{r} = z - h(\hat{x}) \tag{9}$$

The relationship between the residuals and the measurement errors can be obtained as:

$$\hat{r} = S \cdot e \tag{10}$$

where: $S = I - H \cdot G^{-1} \cdot H' \cdot W$

Then the covariance matrix of the residuals can be computed by:

$$R_{\hat{r}} = S \cdot R_z \cdot S = S \cdot R_z \tag{11}$$

The normalized residuals can be obtained as:

$$r^n = (diag(R_{\hat{r}}))^{-1/2} \cdot \hat{r} \tag{12}$$

If there exist some normalized residuals greater than the probability threshold, bad data will be detected in the measurement set. Further more, the measurement with the largest r^n will be identified as bad data in most of the cases.

2) Normalized residuals in WLAV method

The bad data processing in WLAV method follows the same procedure as in the WLS method. A detailed description of how to detect/identify bad data in WLAV method can be found in [29].

2.3 State Estimation Using the Substation Model

Regardless of the solution method used, the conventional state estimation formulation is based on the bus/branch model obtained from the topology processor. The circuit breakers will not appear in the model. Estimation of the power flows through circuit breakers has first been suggested for data validation at the substation by Irving and Sterling [30]. This requires the detailed topology of the substation, including the circuit breakers, to appear in the system model. Circuit breakers are modeled as zero impedance branches. Their flows are treated as additional state variables [22] because the conventional SE cannot handle the zero impedance branches. Correspondingly, the formulation of the SE must be modified. In the following part, we will discuss how to include the substation model in the WLAV state estimation formulation.

If a substation is to be modeled in detail, representing the individual circuit breakers and their configuration, then the linearized measurement equations shown in (2) will take the following form:

$$\Delta z = H \cdot \Delta x + M \cdot f + e \tag{13}$$

where:

[M] is a $(m \times l)$ measurement to circuit breaker incidence matrix defined by:

if the measurement *i* is an injection:

$$M_{ij} = \begin{cases} 1 & \text{if the injection is at the to - end of the breaker j} \\ -1 & \text{if the injection is at the from - end of the breaker j} \\ 0 & \text{otherwise} \end{cases}$$

if the measurement *i* is a line flow:

$$M_{ij} = \begin{cases} -1 & \text{if the flow is at the to - end of the breaker j} \\ 1 & \text{if the flow is at the from - end of the breaker j} \\ 0 & \text{otherwise} \end{cases}$$

l is the number of the circuit breakers,

f is a $(l \times 1)$ vector of power flows through the circuit breaker.

When all circuit breakers are open, then $f=0$, and (13) reduces to (2). To simplify the notation, a new vector is defined to designate the state vector augmented by the circuit breaker power flows:

$$\Delta y = \left[\Delta x^T f^T\right]^T \tag{14}$$

Now, the LP problem given by (7),(8) can be modified to include the breaker flow variables f, yielding:

$$\min J(x) = \sum_{i=1}^{m} \omega_i (u_i + v_i) \tag{15}$$

$$\textit{subject to} \quad \Delta z^k = H(x^k) \cdot \Delta y^k + u - v \tag{16}$$

Additional constraints are appended to the LP problem in form of zero voltage drops across closed circuit breakers. It is very easy to add the constraints into the measurement set in WLAV formulation. Since the status of the breakers are not known a priori, such constraints are made soft by introducing a pair slack variables so that the constraints will be disregarded if the breakers are actually open. For a circuit breaker between buses j and k, the following equation will be appended to (16):

$$x_j - x_k + u_{m+1} - v_{m+1} = 0 \tag{17}$$

Here u_{m+1} and v_{m+1} are the nonnegative slack variables for the newly added pseudo-measurement.

Depending on the column rank of the matrix $[H|M]$, some or all entries in f will be observable. The unobservable states can be identified by the WLAV estimator during the initial phase of the solution. The details of the WLAV estimator implementation are given in [8].

2.4 Two-Stage State Estimation Algorithm

A two-stage state estimation algorithm was proposed in [8], [24] to detect/identify the topology error. This algorithm normally includes three parts.

1) The First Stage State Estimator

The first stage state estimation is nothing but a conventional one, which is based on the bus/branch model. Most of the conventional state estimation methods capable of bad data processing could be used directly. In our study we use WLAV method due to its ability to exclude bad data.

2) Suspect Substations Identification

After the first stage state estimation, we need to detect and identify any existing topology errors. Normally, this detection/identification procedure is based on the normalized residual analysis. In [8],[24], the number of times for each bus to which the suspect measurements of stage 1 are incident is used as the identification criterion. However, experience shows that this identification method may fail for certain cases. The identification of the suspect area is the crucial step for the two-stage algorithm. We will further discuss this topic in Chapter III.

3) Second Stage State Estimation and Correction of Topology Errors

The detailed models of suspect substations are incorporated into the bus/branch model in this stage. There are lots of algorithms which can handle the detailed substation model [24]-[28]. Most of those second stage's algorithms will work well given a correctly identified sub-area. In our implementation of the two-stage algorithm, the generalized WLAV method [24] is used.

The detailed procedure of this two-stage algorithm is given below:

- **Stage1**

1. Run the WLAV estimator using the bus/branch level system model formed by the topology processor based on the telemetered or assumed statuses of the circuit breakers in the system.
2. Compute the normalized residuals by using the measurement residual covariance matrix developed in [8]. The normalized residuals are computed only for those measurements that are rejected by the WLAV estimator.

3. Identify the suspect measurements with significant normalized residuals (in all simulations a threshold of 1.0 was used). If there are none, it will be decided that no topology or analog measurement error is present. Else, go to Stage 2.

- **Stage2**

1. Identify the suspicious buses based on the normalized residual analysis.
2. Introduce the detailed substation models using zero impedance branches to represent the circuit breakers based on the configuration of the corresponding suspicious substations. Use all available measurements from the substations including the circuit breaker power flows, which may not have been explicitly used in Stage 1. For instance a flow through a circuit breaker that connects two bus sections inside the same substation, may get lost if the two bus sections are modeled as a single node in the bus level model.
3. Run the WLAV estimator for the entire system. Repeat the normalized residual test. Flag those measurements failing the test and declare these errors as analog measurement errors. The true topology of the system will be determined according to the estimated statuses of the circuit breakers based on the normalized flows through them.

The flowchart of this program is shown in Fig. 1.

2.5 Modeling of the Substation

The fully blown substation model is very complex. It is impossible and not necessary to include all the circuit breakers/switches in the system. A simplified version of the substation model that satisfies the requirements of second state estimation will be defined. Further more, this simplified model must fit into all of the existing substation schemes [31]. The simplified model will have the following properties:

1) *Every substation will be assigned a unique global number;*
2) *A substation is precisely defined as that which is considered one electrical node when all breakers or switches are closed;*
3) *All the non-independent switches and circuit breakers will be considered as one zero impedance branch;*

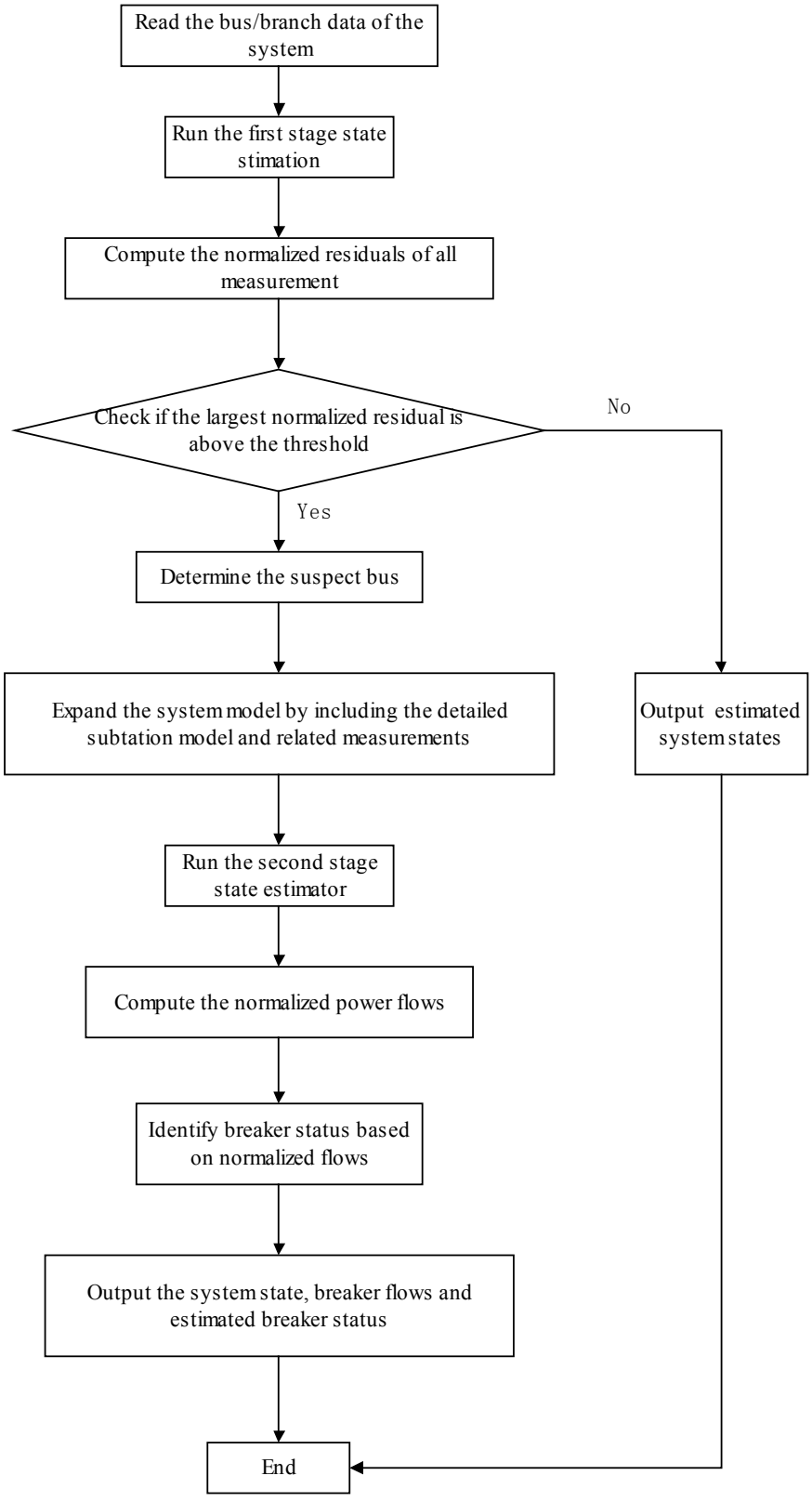

Fig. 1. Flowchart for two-stage state estimation

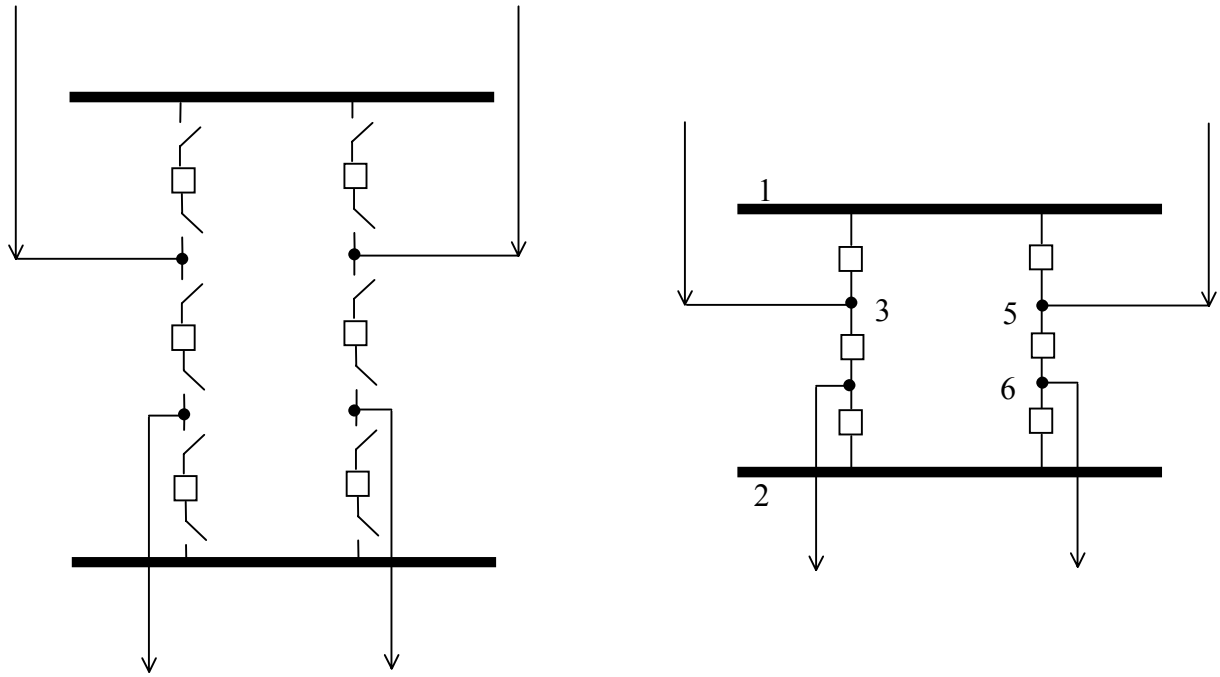

a) Original topology b) Simplified model

Fig. 2. Simplified substation model

Fig. 2 is an example of how to simplify a substation with a breaker and half scheme. The substation will be assigned a unique global number. The topology information of the simplified substation model, for instance Fig. 2 (b), will be saved in a data structure associated with this number. The measurement data structure is similar to the one in the conventional bus/branch model. That is, there will be power injection and voltage measurements associated with nodes, and power flow measurements associated with breakers. Some of these measurements within a substation will not be used in the conventional state estimator based on the bus/branch model. However, they will be used in the second stage to make the system observable and increase the local redundancy.

2.6 Data Files Format for Simplified Substation Model

The topology data and measurement data for a substation will be separated in two different files. The advantage is we can store only one copy of topology data file for

those substations which have the same configuration. The format of topology data file and measurement data file will be shown in following sections, respectively.

2.6.1 Substation Topology Data File

The purpose of this data file is to describe the nodes and the connections between them. It is composed of two sections.

- **Node Data Section**

Total Number of Nodes
NodeNumber Type
……..

NodeNumber: Node number is unique in a specified substation;
Type: The type of a node will be busbar (1), external (2) or internal(3);

- **Zero Impedance Branch Data Section**

Total Number of Zero Impedance Branches
From To
……..

From: From node number of this branch;
To: To node number of this branch;

The topology data file corresponding to the substation shown in Fig. 2 is given below.

*6 **Total number of nodes*
*1 1 ** NodeNumber Type*
2 1
3 2
4 2
5 2

*6 2 ** End of node data section*

*6 **Total number of zero impedance branches*

*1 3 **From To*

1 5

2 4

2 6

3 4

*5 6 ** End of Zero Impedance Branch Data Section*

2.6.2 Measurement Data File for a Substation

This file contains the measurement data for a single substation. The first two sections are used to describe the topology information. Other sections describe the branch status and measurement data.

- **File Name of Substation Topology Data File**

Topology Data File Name

Topology Data File Name: A string, which refers to the data file name containing the substation topology;

- **Inter-substation Connectivity Data**

ConSubNo ConNodeNo

……..

ConSubNo: The global number of the neighboring substation connected to this node; if none, this value will be -1;

ConNodeNo: The node number of the neighboring substation connected to this node; if none, this value will be -1;
(Remark: The number of rows in the section and the order they are listed should be identical to the number of external nodes defined in the topology data file.)

- **Branch Status**

Status WSta

……..

Status: The status of this set of switches, 1: closed; 0:open; 2: unknown
WSta: Standard deviation will be assigned to the equality constraint pseudo-measurement;
(Remark: In the same order as listed in topology data file)

- **Voltage Measurement**

Total Number of Voltage Measurements
NodeNo VMag SubWV
……..

NodeNo: Node number of this measurement;
VMag: The value of this measurement;
SubWV: standard deviation of this measurement;

- **Power Injection Measurement**

Total Number of Power Injection Measurements
NodeNo Pinj Qinj WInj
……..

NodeNo: Node number of this measurement;
PInj: Measurement of active power injection of this node;
QInj: Measurement of reactive power injection of this node;

WInj: standard deviation of this measurement;

- **Power Flow Measurement**

Total Number of Power Flow Measurements
BranNoPFlow QFlow WFlow
……..

BranNo: Branch number of this measurement (if greater than 0, the power flow will be at the from end; if less than zero, the power flow will be at the to end);
PFlow: Measurement of active power flows of this branch;
QFlow: Measurement of reactive power flows of this branch;
WFlow: Standard deviation of this measurement;

- **Current Measurement**

Total Number of Current Measurements
BranNoBranCur WCur
……..

BranNo: Branch number of this measurement (if greater than 0, the power flow will be at the from end; if less than zero, the power flow will be at the to end);
BranCur: Measurement of current magnitude of this branch;
WCur: Standard deviation of this measurement;

Consider the substation shown in Fig. 2 with the following information:
Topology data file: type1.otp
Connectivity: As shown in Fig.3-1
Branch Status: Closed: (1-3)(2-4)(1-5)(2-6); Opened: (3-4)(5-6)
Voltage Measurement: At node 1,2,3,4
Power Injection Measurement: At Node 2,5,6
Power Flow Measurement: At branches (1-3)(3-4)

Current Measurement: At branches (2-4)(5-6)

Then, the corresponding measurement data file will be given as:

Type1.top

12 3

18 2

17 5

28 8

1 0.001000

1 0.001000

1 0.001000

1 0.001000

0 0.001000

0 0.001000

4

1 1.05294 0.001000

2 0.99874 0.001000

3 1.05294 0.001000

4 0.99874 0.001000

3

2 -0.08200 -0.02500 0.001000

5 0.00000 0.00000 0.001000

6 0.00000 0.00000 0.001000

2

1 -0.09003 -0.02462 0.001000

5 0.00804 -0.00037 0.001000

2

3 -0.26052 0.001000

6 0.45768 0.001000

2.7 Other Data Structure

A small set of extra data is also needed to store the relationship between the substations and the bus/branch system model. First of all, the following properties will be added to each bus in the bus/branch system model.

1) ***Substation NO****: The unique number of the substation model related to this bus.*
2) ***Node NO:*** *The node number in the substation model where this bus belongs. If more than one node is combined to form this bus, the node number can be chosen arbitrarily from the list of nodes.*

Similarly, some connectivity information is also needed for the node in the substation model.

1) ***Node type:*** *There are three kinds of nodes in a substation:* ***Busbar, External Node,*** *which is connected to a transmission line, and* ***Internal Node,*** *which is connected to the elements within a substation (loads, shunt, etc). For example, in fig. 1 (b), node 1 and 2 will be* ***Busbars,*** *while node 3,4,5 and 6 will be* ***External Nodes.***
2) ***Connected Substation NO.:*** *The number of the substation, which is connected to this node by a transmission line.*
3) ***Connected Substation Node:*** *The number of the node connected to this node in the Connected Substation.*

The data set listed above is the essential data required by a two-stage state estimation algorithm. Only a small modification is needed in the conventional state estimator database, in order to create the current bus/branch data structure. In practice, the extra data structure may be further modified or expanded corresponding to the data structure of the existing state estimator and also for other application functions.

2.8 Graphical Interface for the Two-Stage State Estimation Program

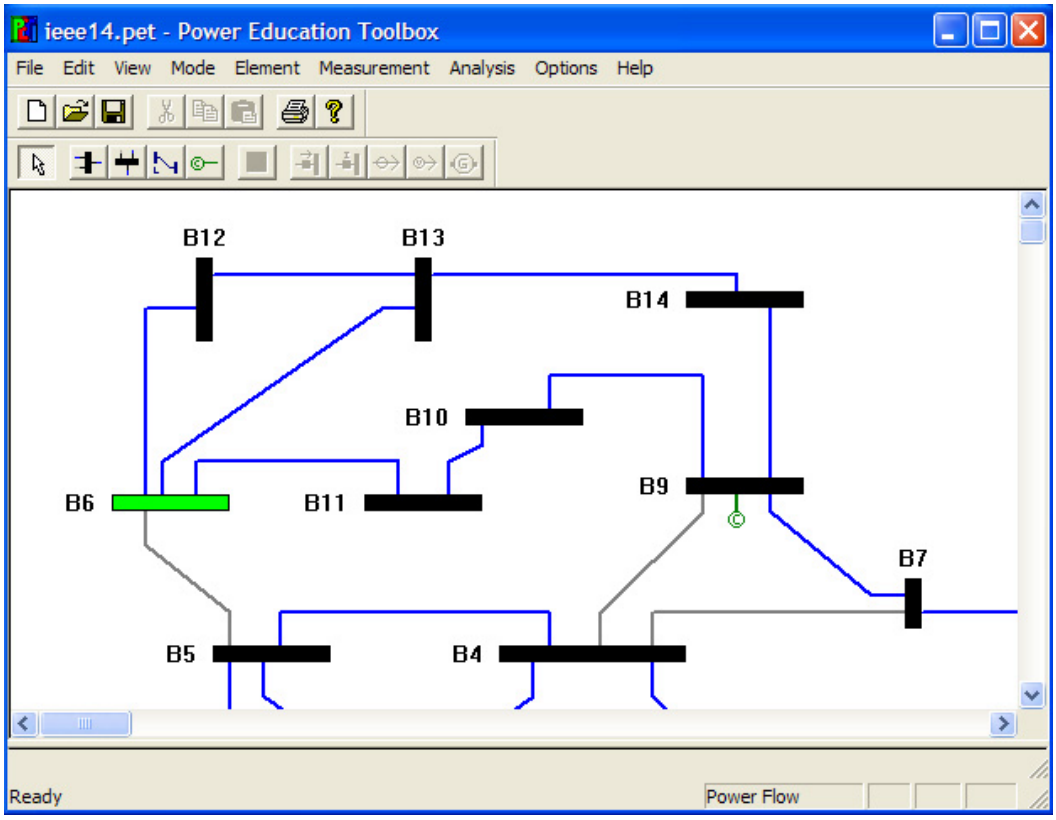

Fig. 3. The main window of power education toolbox (PET)

Power Education Toolbox (PET) [32], [33] is a user-friendly software package that is developed at Texas A&M University primarily as a teaching tool. The software is designed to provide easy access to several commonly used application functions, such as power flow analysis, state estimation, etc, using the same user interface and power system diagrams. A Windows based graphical user interface program provides the link between the user and the various application programs. PET models the system in bus/branch level thus can be treated as a conventional state estimator. The main window of this program is shown in Fig. 3.

The two-stage state estimation will be implemented based on this package. This includes the integration of the extra interface, data structure and program. At the same

time, the modification of the old program must be limited in minimum in order to keep the compatibility. The open interfaces to the algorithm programs, including the first and second stage state estimator, suspect area identification procedure, are also requirements. Hence any new algorithms can be tested using this platform.

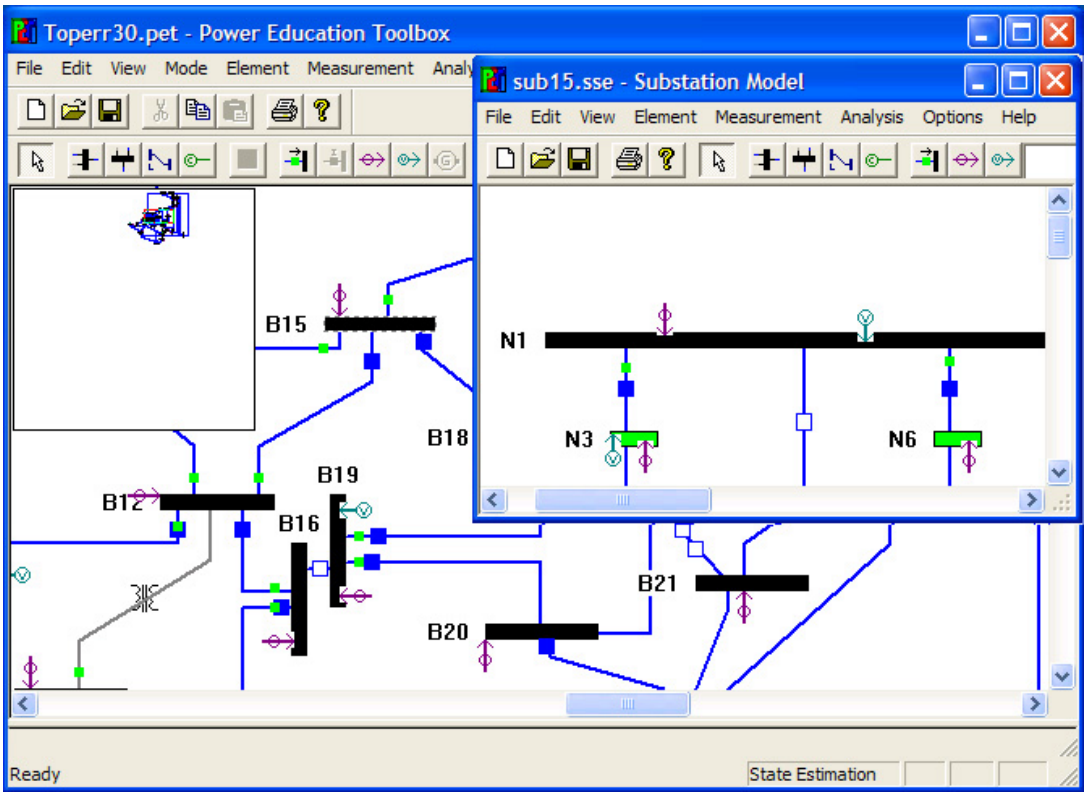

Fig. 4. User interface with the auxiliary substation window

As discussed above, for purpose of topology error identification, the two-stage algorithm needs the detailed substation models for suspect substations. Correspondingly, an auxiliary substation window for editing and setting the substation models is created first. Fig. 4 shows the screenshot of the interface of the program with the auxiliary window opened. The bus/branch system model shown in the main window is the IEEE 30 bus system. The substation shown in the auxiliary window is a pseudo-substation created for bus 15 based on the topology of IEEE 30 bus system. In addition, a navigator window,

which is opened on the left-top corner of Fig. 4, is implemented to facilitate locating the individual element when the one-line diagram is too big for single screen.

The data structures of this substation model include topology information, measurement arrangement and extra data for nodes described in the former section.

1) Creation of the substation model from scratch.

The substation model can be edited and set in the auxiliary window directly. The editing procedures, including the topology configuration and measurement arrangement, are quite the same as the editing procedure of the one line diagram in the main window. In addition, the finished substation model can be stored as a template for substation with similar configuration.

2) Creation of the substation model by template.

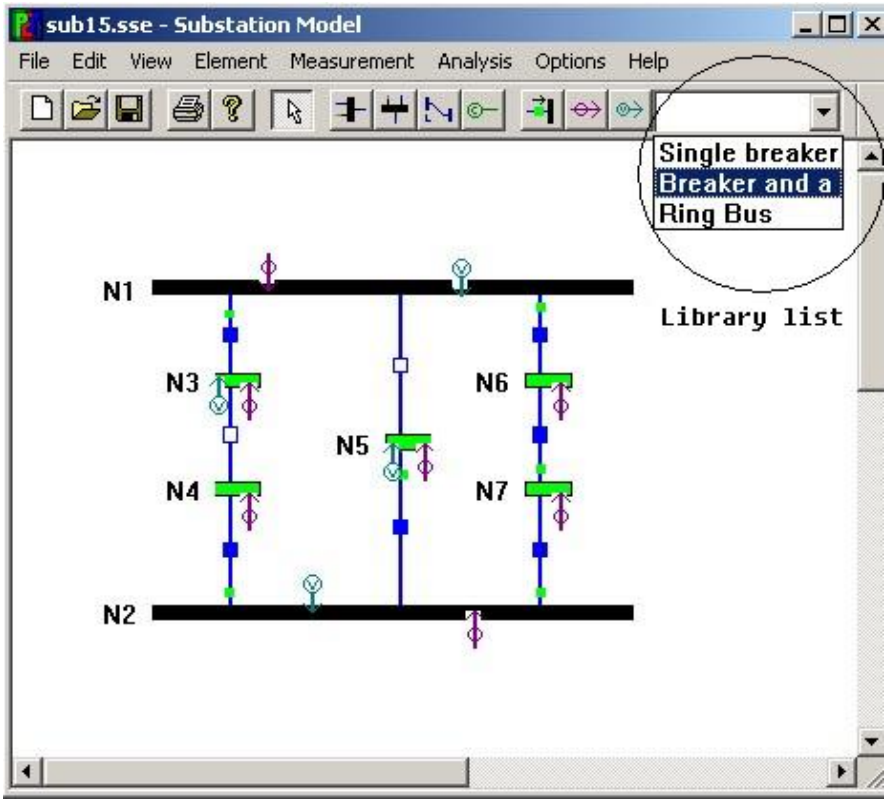

Fig. 5. The library list of substation models

There are only a limited number of substation schemes in a real power system. Hence many substations will have similar topological structures. It is more convenient to create models for those substations by templates. Fig. 5 shows the substation window with the list of substation library. Simply clicking on the name of correct template can create a substation model. The network elements and measurement configurations can then be changed to fit certain substation.

3) Automatic Generation of Substation Measurements.

The measurement values in the substation can be automatically generated. Set the relation parameters for the main system and the substation carefully and make sure it is correct. The program can utilize the power flow results of the main system and the topology information of the substation to calculate the measurement values for every meter in the substation. Note that in order to get the correct result, the status of all the circuit breakers should be set corresponding to the connection in the main system.

2.9 Procedure to Test the Two-Stage State Estimation

Two-stage state estimation method is tested using this program. The steps of testing for topology error identification are described below:

1) Create the main system

Use the main window of PET program to create the basic main system, including the network connections, generation and load setting. Place the measurements properly.

2) Create the substation model

Use substation model introduced in the former section to represent the actual substation. Create the substation data file for specified buses using the auxiliary window. There is no need to create the substation data files for all the buses. Only the substation models in the areas of interest are needed.

3) Set the correct measurement values based on the correct network

Make sure the connection information for those buses in the main system and nodes in the substation models are correctly specified. The status of the circuit breakers must correspond to the current connection of the main system. Compute the correct values of all measurements, including the measurements in the bus/branch model and the substation, by running power flow program based on the correct topology.

4) Set up the topology error

Set up the desired topology error by changing the connections in the bus/branch model and the statuses of corresponding circuit breakers in the substation.

5) Run the two-stage program

After introducing the topology error, load the two-stage state estimator. After the first stage, if there is topology error detected, the system will run the second stage state estimation. If there are mismatches between the assumed status and estimated status of circuit breakers included in those suspect substations, the location of the topology error will be shown.

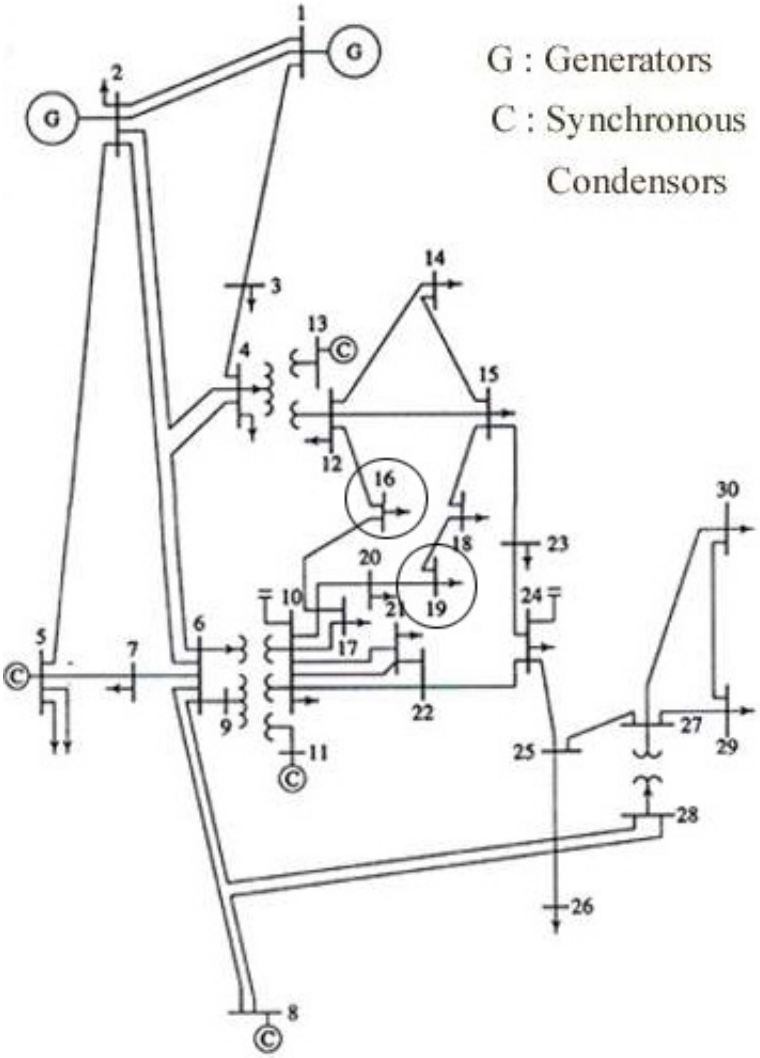

Fig. 6. IEEE 30 bus system

2.10 Simulation Result

In this section, the simulation results of two different kinds of topology scenarios will be presented to demonstrate the two-state state estimation program's operation.

These cases are based on the IEEE 30 bus system (Fig. 6). We suppose bus 16 and bus 19, which are circled in Fig. 6, belong to the same substation.

2.10.1 Case1: Bus Split Case

Fig. 7 shows the detailed topology of this substation with the status of the circuit breakers. The scenario of this demo is described as the following:

- The true status of the CB N5-N2 is open, which makes this substation appears as two split buses in the bus/branch model;
- Assume that the operation of the CB N5-N2 is not reported to the control center. The control center still assumes the status of N5-N2 as closed. Then this substation will appear only as one bus in the bus/branch model.

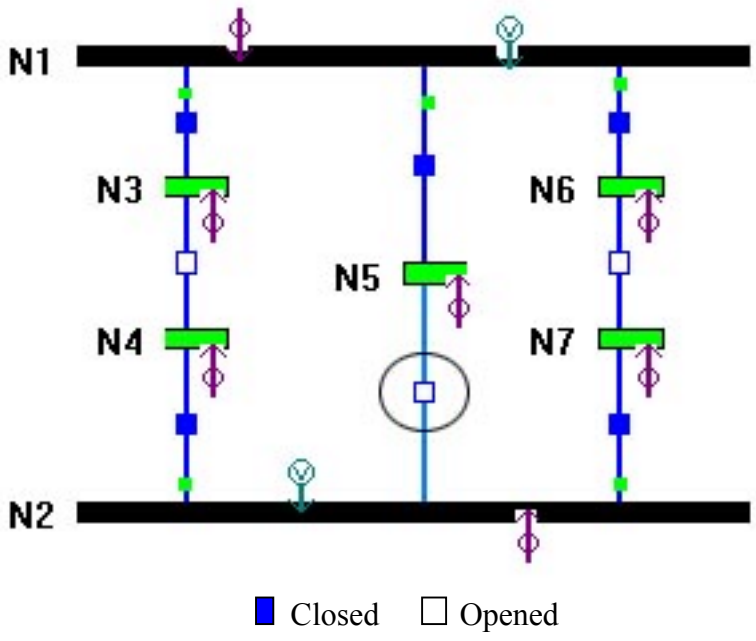

Fig. 7. Substation model consists of bus 16 and bus 19 (case1)

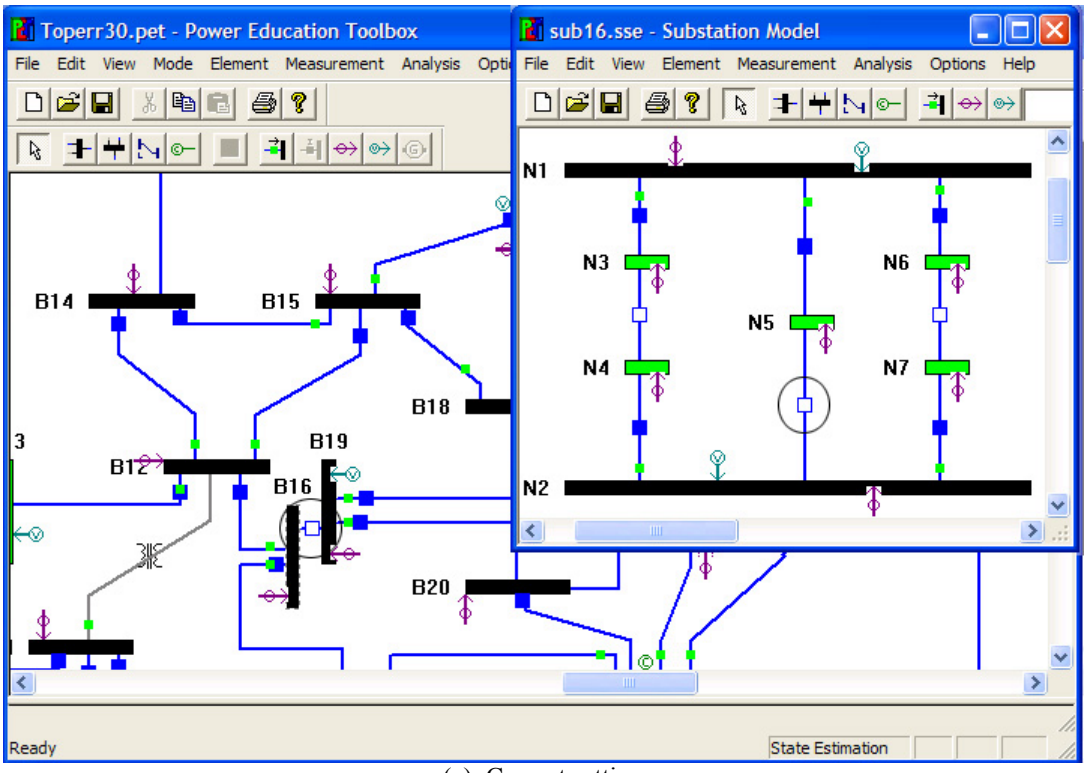

(a). Correct setting

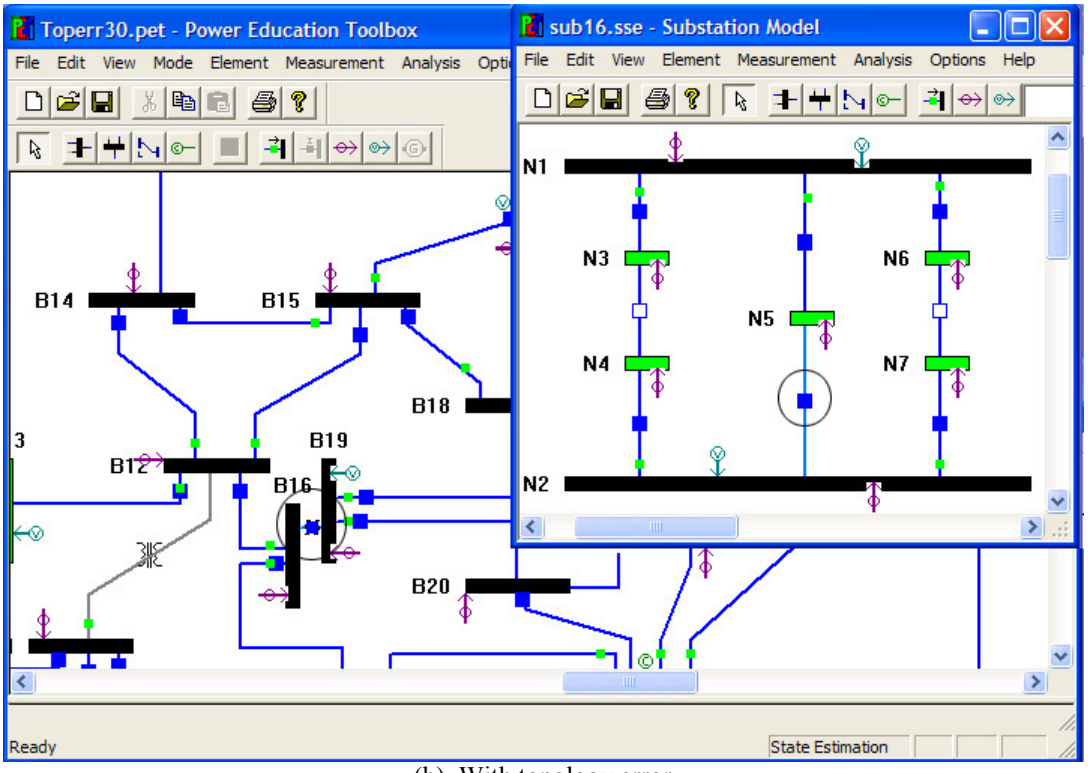

(b). With topology error

Fig. 8. Illustration of the topology error (bus split case)

For convenience, a pseudo-switch with very small impedance is added between bus 16 and 19 to simulate the connectivity. Fig. 8 shows the diagram with correct topology and after introduction of topology error.

The first stage state estimation run using the bus/branch model which assumes no split in bus 16 and bus 19, as shown in Fig. 8 (b). We can get the normalized residuals of each measurement after the first stage state estimation. The measurements that have significant normalized residuals (greater than 1.0) are listed in Table I in descending order.

The suspect area identification procedure will choose several buses by their statistical property as the suspect buses (The details of the suspect area identification procedure will be given in Chapter III). In this case, buses 16, 17 and 18 are chosen, as shown Fig. 9. The substations represented by these buses are then modeled in detail in the second stage state estimation.

TABLE I
SIGNIFICANT NORMALIZED RESIDUALS AFTER FIRST STAGE (CASE1)

Meas #	***Type***	***Location***	***Normalized Residuals***
107	QFLOW	19-20	3.2460
104	QFLOW	16-12	2.8501
103	QFLOW	16-17	2.7613
91	QFLOW	15-18	2.7361
87	QFLOW	17-10	2.3581
106	QFLOW	19-18	2.2334
35	PFLOW	16-12	2.1546
38	PFLOW	19-20	2.0952
36	PFLOW	16-17	1.8711
26	PFLOW	15-12	1.8699
22	PFLOW	15-18	1.6871
18	PFLOW	17-10	1.6140
37	PFLOW	19-18	1.5055
142	VOLTAGE	19	1.0545

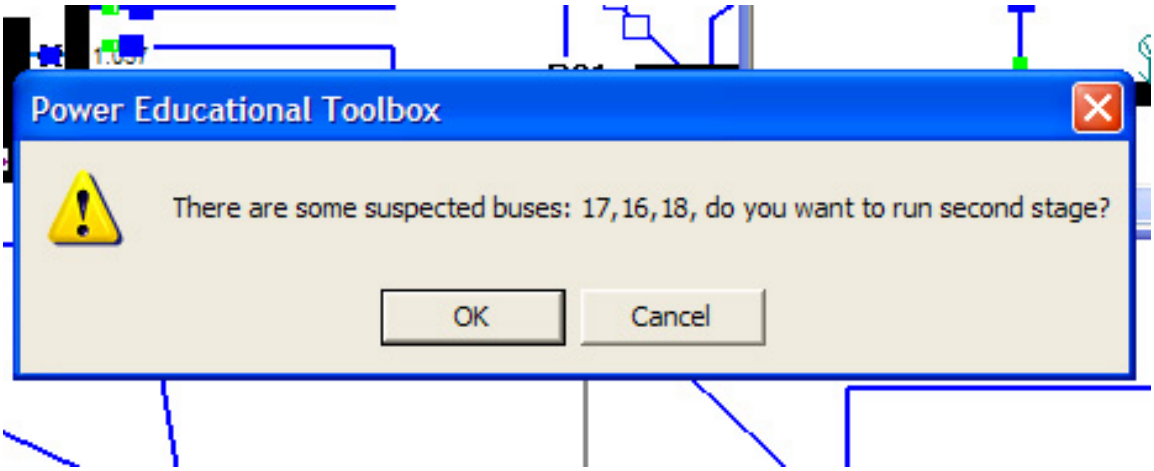

Fig. 9. Simulation result after first stage state estimation (case1)

After second stage, the normalized power flows through all the switch branches inside the suspect substation are estimated. Table II shows the estimated result for the substation represented by bus 16, which is shown in Fig. 7. If the value of normalized power flow is greater than threshold (3.0 for this case), the estimated status of corresponding branch will be closed, otherwise the estimated status will be open. The estimated statuses for all the branches inside this substation are also shown in the last column of Table II. It can be seen that only the status of branch N2-N5 is different from the assumed status. The program alarms that there is topology error detected and indicates the location as shown in Fig. 10.

TABLE II
ESTIMATED STATE OF CIRCUIT BREAKER (CASE1)

CBs	***Normalized P Flow***	***Normalized Q Flow***	***Estimated Status***
N1-N3	-115.2171	-49.0266	Closed
N3-N4	0.1701	-0.0076	Open
N2-N4	12.7813	5.6847	Closed
N1-N5	125.4597	55.9197	Closed
N2-N5	0.0987	0.0987	*Open*
N1-N6	-4.6246	-6.7945	Closed
N6-N7	-0.0568	0.0137	Open
N2-N7	-12.7813	-5.6847	Closed

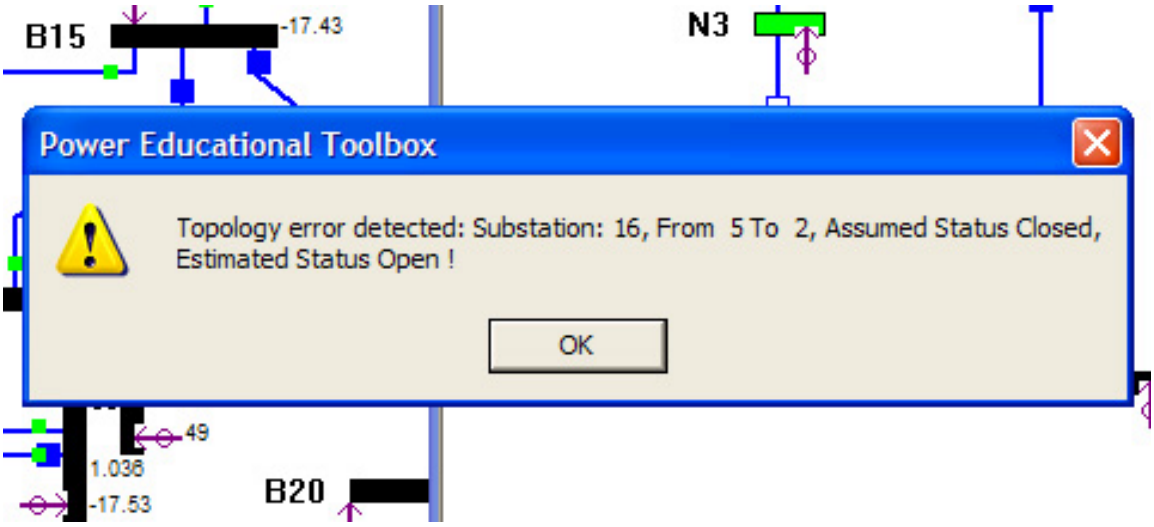

Fig. 10. Simulation result after second stage state estimation (case1)

2.10.2 Case2: Line Outage Case

Fig. 11 shows the detailed topology of this substation with the status of the circuit breakers. The scenario of this demo is described as the following:

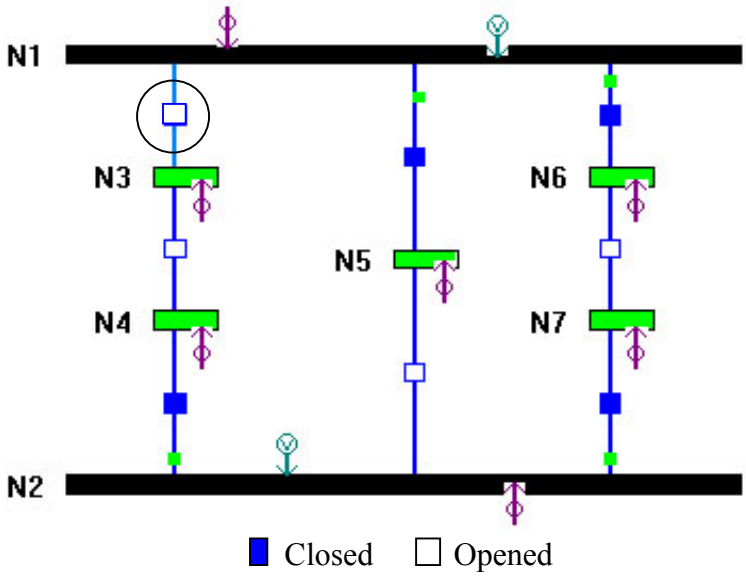

Fig. 11. Substation model consists of bus 16 and bus 19 (case2)

- The true status of the CB N1-N3 is open, which mean the transmission line 12-16 is outage in the bus/branch model;
- Assume that the operation of the CB N1-N3 is not reported to the control center. The control center still assumes the status of N5-N2 as closed. The transmission line 12-16 is still assumed on use in the system model.

For convenience, a pseudo-switch is added into transmission line 12-16 to simulate the connectivity. Fig. 12 shows the diagram with correct topology and after introduction of topology error.

The first stage state estimation run using the bus/branch model which assumes branch 12-16 is still in service, as shown in Fig. 12 (b). We can get the normalized residuals of each measurement after the first stage state estimation. The measurements that have significant normalized residuals (greater than 1.0) are listed in Table III in descending order.

The suspect area identification procedure will choose several buses by their statistical property as the suspect buses (The details of the suspect area identification procedure will be given in Chapter III). In this case, buses 16, 17 and 20 are chosen, the screenshot of the output is ignored here. The substations represented by these buses are then modeled in detail in the second stage state estimation.

After second stage, the normalized power flows through all the switch branches inside the suspect substation are estimated. Table IV shows the estimated result for the substation represented by bus 16, which is shown in Fig. 11. The estimated statuses for all the branches inside this substation are also shown in the last column of Table IV. It can be seen that only the status of branch N1-N3 is different from the assumed status. The program alarms that there is topology error detected and indicates the location as shown in Fig. 13.

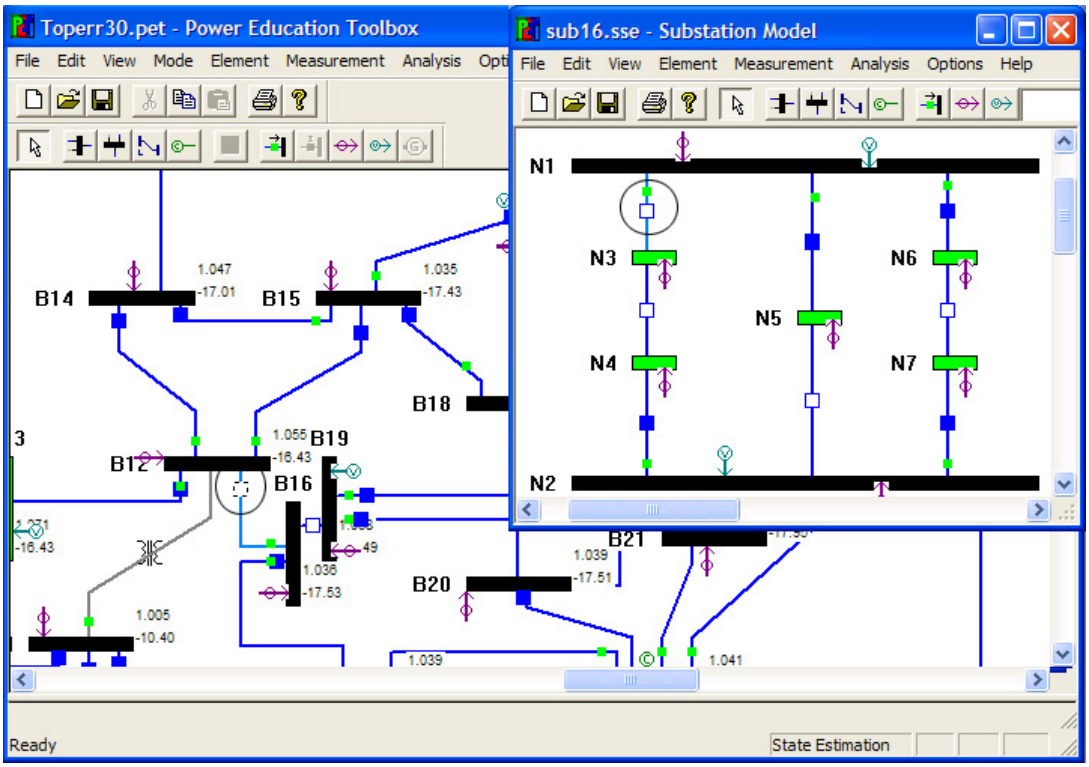

(a). Correct setting

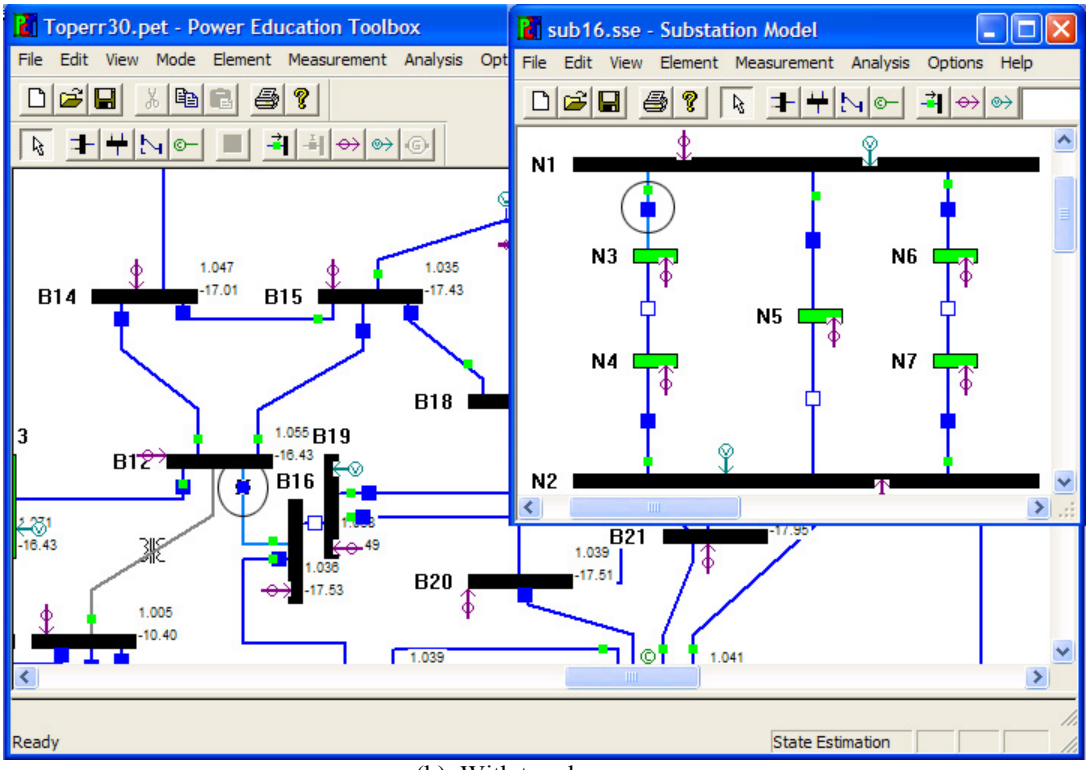

(b). With topology error

Fig. 12. Illustration of the topology error (bus split case)

TABLE III
SIGNIFICANT NORMALIZED RESIDUALS AFTER FIRST STAGE (CASE2)

Meas #	*Type*	*Location*	*Normalized Residuals*
24	PFLOW	12 – 15	-63.9720
36	PFLOW	16 – 17	-62.5336
28	PINJ	12	-27.8090
29	PINJ	16	23.0791
141	VOLTAGE	16	-13.0589
93	QFLOW	12 – 15	-11.7973
106	QFLOW	16 – 17	-10.3564
97	QINJ	12	-6.3620

TABLE IV
ESTIMATED STATE OF CIRCUIT BREAKER (CASE2)

CBs	*Normalized P Flow*	*Normalized Q Flow*	*Estimated Status*
N1-N3	0.0963	0.0963	*Open*
N3-N4	-0.0556	0.0565	Open
N2-N4	-20.7539	4.3846	Closed
N1-N5	129.8345	57.8696	Closed
N2-N5	-0.0577	0.1444	Open
N1-N6	-129.8386	-57.8714	Closed
N6-N7	0.0589	0.0570	Open
N2-N7	20.7550	-4.3849	Closed

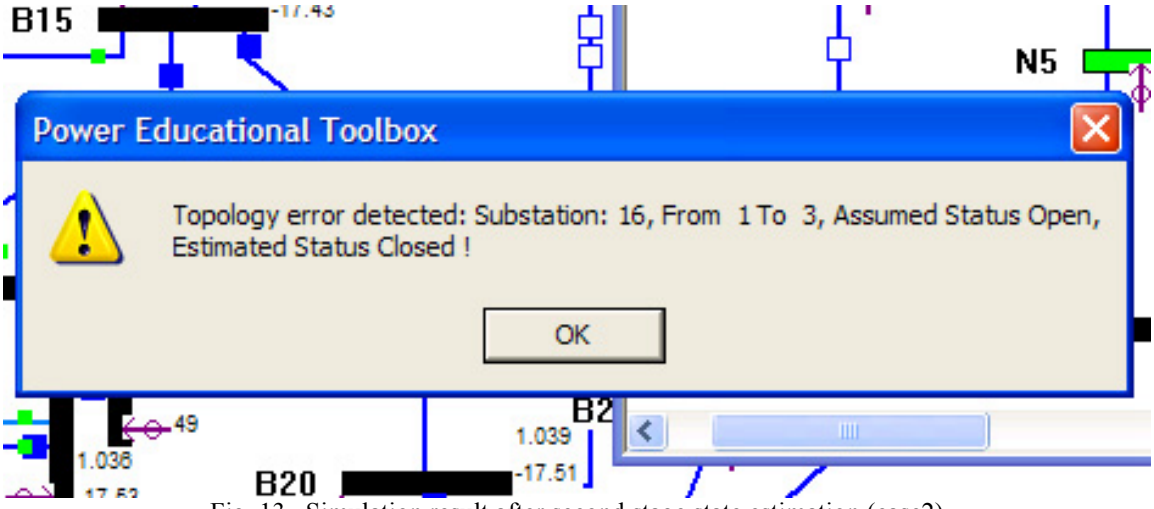

Fig. 13. Simulation result after second stage state estimation (case2)

2.11 Conclusion

The implementation of a two-stage state estimation algorithm capable of topology error identification is discussed in this chapter. A concise substation model and the minimum required extra data set needed to run the two-stage state estimation are defined. With these data structures, a conventional state estimator is updated to support the two-stage algorithm.

CHAPTER III

ROBUST IDENTIFICATION OF THE SUSPECT AREA

3.1 Introduction

The success of the two-stage state estimator in identifying the topology errors depends on the correct identification of the suspect substations after the first stage. Given correctly identified area and sufficient local redundancy, most of the second-stage state estimation program can successfully identify the topology error. Currently used identification methods do not have satisfied performance under some circumstances. An improved identification strategy, which utilizes the calculated state estimation residuals of the first stage and the associated network configuration, is described in this chapter. In order to investigate and comparatively evaluate the performances of different identification methods, a topology error library containing 50 scenarios are built based on the IEEE 30 bus test system. The simulation results of different methods on this library will be compared and the best method will be selected. In addition, the new identification method can be implemented in an adaptive way. User in the practical system can modify the parameters to fit their needs. Simulations have been done using Weighted Least Absolute Values (WLAV) method and Weighted Least Squares (WLS) methods, respectively. The results are compared and shown in the last section of this chapter.

3.2 New Identification Method

The following index *NI*, is defined in [24] as a criterion to identify those buses which may represent a substation with topology errors:

$$NI^i = \sum_{k=1}^{m1} I^i(z^k), i = 1...n \tag{18}$$

where:

NI^i : Index for bus i;

n : Total number of system buses;

$m1$: Number of suspect measurements;

z^k : *kth* suspect measurement;

$$I^i(z^k) = \begin{cases} 1 & z_k \text{ is incident to bus } i \\ 0 & \text{otherwise} \end{cases} \tag{19}$$

Those buses having the largest NI index are identified as suspect substations. While this index appears to correlate with the suspect buses quite well in most cases, there are cases where the index may fail to indicate all suspect buses. Extensive simulation studies reveal that there is still room for improvement in order to develop a highly reliable identification procedure. The identification capability might be improved through following directions.

3.2.1 Normalized Index for Suspect Buses

The index defined in (18) is modified as below:

$$NI^i_{Total} = \sum_{k=1}^{m} I^i(z^k), i = 1...n \tag{20}$$

where:

NI^i_{Total} : New modified index for bus i,

m : Total number of measurements;

It directly follows from (18) that the larger the value of NI^i_{Total}, the larger the corresponding index NI^i. Using their ratio, a normalized index can be defined as:

$$NI^i_n = NI^i / NI^i_{Total} \tag{21}$$

where:

NI^i_n : Normalized index for bus i,

The new index NI^i_n will be shown to outperform the previous index in identifying suspect buses.

3.2.2 Limiting the Number of Suspect Measurements

In choosing the suspect measurements, two approaches are possible. In the first one, all measurements with normalized residuals greater than a threshold will be considered as suspects and taken into account during the identification procedure. The other option is to choose a fixed number of measurements having the largest normalized residuals. This second approach is observed to provide better selectivity.

3.2.3 Increasing the Number of Suspicious Buses

Theoretically, if all the substations are modeled in detail (breaker level), and redundant substation measurements from all substations are available, topology errors can be identified using the second stage estimator only. In practice, for very large power networks, this may not be practical. On the other hand, limiting the suspect substation to a single bus may limit the ability to identify the true topology error. In order to make sure that the substation with topology error is included in the suspect list, the number of suspicious buses can be considered to be larger than one. Representing several substations in detail may increase the computation burden slightly, but this will be more than compensated by the increase in the possibility of correct identification of topology errors.

In practice the maximum number of suspicious buses can be left as a parameter for the user. With the help of the topology library discussed next, a confidence level can be calculated and associated with each chosen "*MaxBusNumber*", which stands for the maximum number of suspect buses. Then this parameter can be specified corresponding to the required accuracy and available computation capacity.

In our study, several alternative identification strategies are designed based on the above considerations. For all of those strategies, an index for each bus is computed utilizing the normalized residuals after the first stage estimation. The index vector is sorted and is used as an identification criterion. The following strategies of choosing the suspect substations are designed based on different assumptions and choice of parameters.

1) Choosing buses with the largest index (*MaxBusNumber = 0*).

In this category, those buses having the largest chosen index are identified. The following four possible combinations for the computation of this index yield the four strategies below:

A. *Method 0A*: Take into account all the suspect measurements and use NI as the identification index. This is the method used in [24].

B. *Method 0B*: Take into account only the top five suspect active and reactive measurements. Use NI as the identification index.

C. *Method 0C*: Take into account all the suspect measurements and use NI_n as the index.

D. *Method 0D*: Take into account only the top five suspect active and reactive measurements. Use NI_n as the identification index.

2) Choosing *n* suspect buses (*MaxBusNumber* = *n*).

In this category, up to the user specified *n* buses having the largest indices will be identified as suspicious buses. Similar to the previous category, there will be four different possibilities to implement:

A. *Method nA*: Take into account all the suspect measurements and use NI as the index.

B. *Method nB*: Take into account only the top five suspect active and reactive measurements. Use NI as the index.

C. *Method nC*: Take into account all the suspect measurements and use NI_n as the index.

D. *Method nD*: Take into account only the top five suspect active and reactive measurements. Use NI_n as the index.

These methods will be tested using the topology error library described in the following section.

3.3 Topology Error Scenarios' Library

In order to test the performance of different identification methods, a library of topology error scenarios is built based on IEEE 30 bus system. Every electrical bus has been expanded and modeled as a hypothetical but realistic substation. All typical substation schemes have been employed in the model: ring, one-and-a half CB, etc. Fig. 14 shows part of the expanded test system.

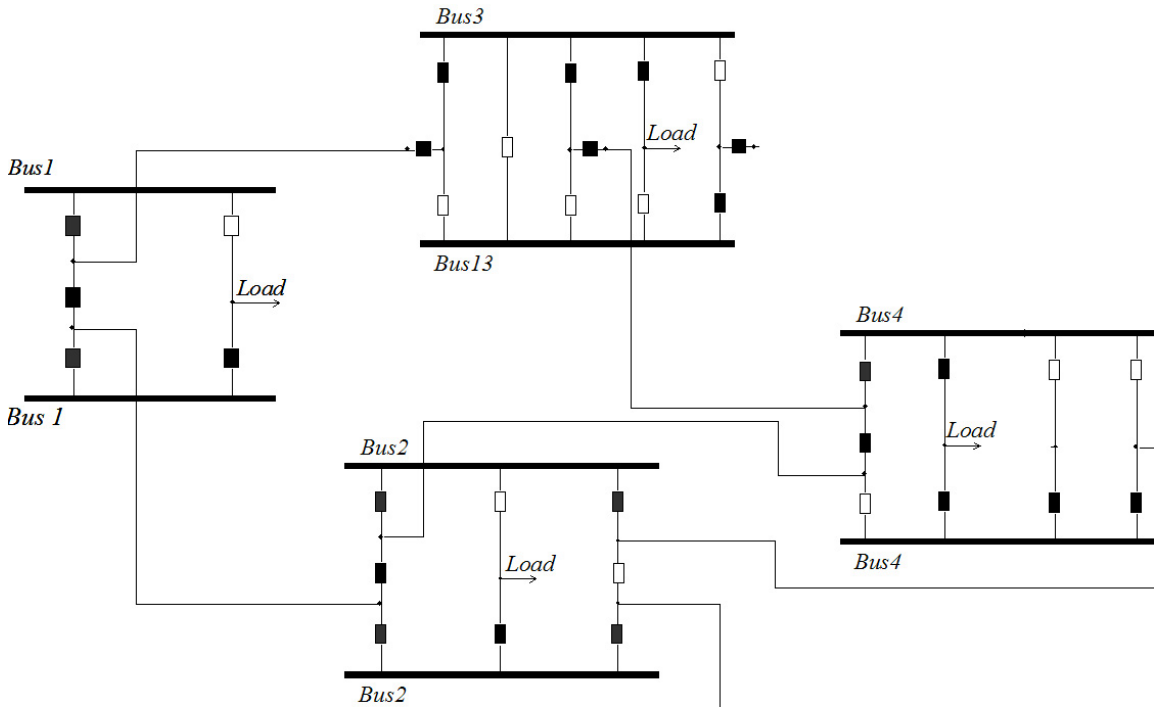

Fig. 14. One-line diagram of part of the test system

For each topology error scenario, the power flow result based on the correct topology is generated. Then the first stage state estimation is run with the correct measurements and the wrong topology. Finally, the identification procedure of different technique will be test.

The library contains 50 topology error cases of four types. Each type will be briefly described in the following sections along with a simple substation model.

1) Type 1: Merged Bus

This case could be shown in Fig. 15. The correct status of CB1 is close. In the bus/branch model, bus bar 1 and 2 should be merged as one electrical node. But the system considers the status of it as open and split busbar1 and 2 in the bus/branch model.

2) Type 2: Split Bus

This case is the counterpart of type 1. In Fig. 15, the correct status of CB1 is open. In the bus/branch model, bus bar 1 and 2 should be split. But the system considers the status of it as close and merges them incorrectly.

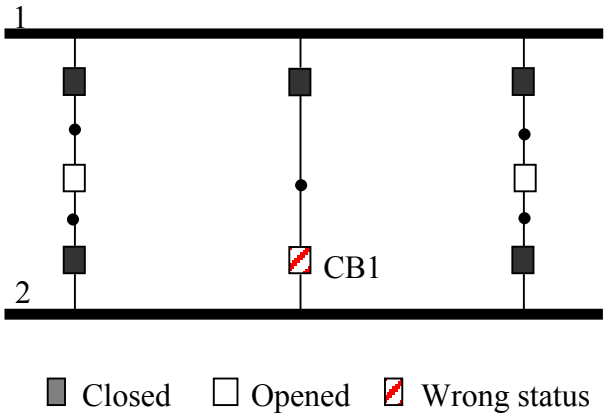

Fig. 15. Illustration of topology error in a simple substation model

3) Type 3: Open ended line

In this case, one or both of the CBs on the ends of a transmission line is actually open, which result in outage of this line. The system considers it is in service wrongly.

4) Type 4: Closed ended line

This case is the counterpart of type 3. Both of the CBs on the ends of a transmission line are actually closed. The system has the wrong status of CB in one or both ends and considers it is outage wrongly.

50 scenarios with different kinds of topology error described above are built. The positions of the CBs with wrong statuses are selected arbitrarily throughout the system. Table V shows the type configuration of the library.

TABLE V
DISTRIBUTION OF THE LIBRARY

Type	1	2	3	4
Number of cases	10	10	15	15

3.4 Simulation Results for Suspect Substation Identification Methods

The first stage state estimation algorithm can be any conventional state estimation algorithm. The suspect area identification capabilities of different algorithms, such as

WLAV and WLS, are different. Usually WLAV method has better performance than WLS for this purpose [24]. The proposed library is tested using both techniques.

3.4.1 Simulation Result of WLAV

Simulation results using WLAV for methods with MaxBusNumber = 0(Method 0A-0D) and MaxBusNumber = 3(Method 3A-3D) are showed in Table VI and Table VII respectively.

Column 2 in the result tables lists the bus numbers which should be identified as suspect buses. Columns 4-7 list the suspicious buses get from different methods. If at least one bus in column 2 is included in the result bus list, we will say the identification process is successful for this case. Otherwise it fails and the results are underlined and italicized. The final rows of the tables are the statistic results of each method. The numerator represents the number of cases which can be identified correctly by this method while the denominator represents the total number of cases.

It is easy to see from the result that for different types of topology error, the identification methods show different performances. For those cases where status of the CB is assumed to be open while it is actually closed (*type 1* and *type 4*), all of the methods can identify the suspect buses correctly for every case. On the other hand, for the opposite scenarios (*type 2* and *type 3*), some of the methods show bad performance. For instance, Method 0A can only correctly identify 9 cases out of 25. Obviously, the difficulty of identification of suspect area sits on topology error of *type 2* and *type 3*. However, slightly increasing the number of suspicious buses can solve this problem.

The results also show improvements in the identification capability when the normalized index NI_n is used and also when the top five suspect measurements instead of all are used. The best strategy is found as given by *Method 3D*, which assumes a maximum of 3 suspect buses. Using this strategy correctly identifies all 50 tested cases.

We can conclude that the procedure using normalized index NI_n and only taking into account top five suspect measurements instead of all is the best one in the simulation. A maximum of 3 suspect buses make this procedure correctly identify all the cases in the library. In practical implementation, we can even increase this number to make the identification procedure more robust.

TABLE VI
TEST RESULT FOR METHODS WITH *MAXBUSNUMBER = 0 (WLAV)*

CaseNO	*Correct Bus*	*Type*	*Suspect Buses*			
			Method 0A	*Method 0B*	*Method 0C*	*Method 0D*
1	3;13	2	*12;*	*4;*	*12;20;*	3;4;
2	8;29	2	*27;*	*27;*	8;	*27;*
3	9;24	2	*10;*	*22;*	22;24;28;	*22;*
4	11;26	2	*25;28;*	*25;*	*25;28;*	9;11;25;26;
5	14;30	2	*27;*	*27;*	*27;*	*27;*
6	16;19	2	19;	16;	19;	16;
7	18;21	2	*10;*	*10;15;*	*20;*	21;
8	20;23	2	*10;*	23;	*18;*	23;
9	5;17	2	*6;*	5;7;10;	*2;*	5;7;
10	12;31	2	*14;15;*	*14;15;*	*14;*	*14;*
11	3;13	1	3;13;	3;13;	13;	13;
12	8;29	1	8;29;	8;29;	8;29;	8;29;
13	9;24	1	9;24;	9;24;	9;	9;
14	11;26	1	11;26;	11;26;	11;26;	11;26;
15	14;30	1	14;30;	14;30;	14;30;	14;30;
16	16;19	1	16;	16;	16;	16;
17	18;21	1	21;	21;	21;	21;
18	20;23	1	20;23;	20;23;	20;	20;
19	5;17	1	5;17;	5;17;	5;17;	5;17;
20	12;31	1	12;	12;	12;	12;
21	1;3;13	4	1;3;	1;3;	3;	3;
22	2;6	4	2;6;	2;6;	2;	2;
23	4;6	4	4;6;	4;6;	4;	4;
24	6;8;29	4	6;8;	6;8;	8;	8;
25	10;22	4	10;22	10;22	10;	10;
26	20;10;23	4	20;	20;	20;	20;
27	14;15;30	4	14;15;	14;15;	14;	14;
28	9;22;24	4	22;24;	22;24;	22;24;	22;24;
29	14;27;30	4	27;30;	27;30;	30;	30;
30	9;24;25	4	24;25;	24;25;	24;25;	24;25;
31	1;3;13	3	*2;*	*2;*	*2;*	*2;*
32	2;6	3	2;	2;	*5;7;*	*5;*
33	4;6	3	4;	*2;*	4;	*2;3;*
34	10;22	3	*21;23;24;*	*21;23;*	*21;*	*21;*
35	12;16;19	3	*10;*	*17;*	*4;*	*17;*
36	15;20;23	3	23;24;	23;	23;	23;
37	5;7;17	3	*2;*	*6;*	*2;*	2;7;
38	9;22;24	3	24;	*15;23;25;27;*	24;	*23;*
39	14;27;30	3	*29;*	*29;*	*29;*	*29;*
40	9;24;25	3	24;25;27;28;	24;25;27;28;	24;25;28;	24;25;28;
41	9;20;23;24	3	*15;*	*15;*	*15;*	*15;*
42	14;15;30	3	15;	15;	14;15;	14;
43	18;21;22	3	10;22;	*10;*	21;22;	*22;*
44	6;10	3	6;10;	6;10;	6;10;	6;10;
45	6;9;24	3	*10;*	*10;*	*10;*	9;16;17;
46	9;20;23;24	4	24;	24;	24;	24;
47	18;21;22	4	21;22;	21;22;	21;	21;
48	6;10	4	10;	10;	10;	10;
49	6;9;24	4	6;9;	6;9;	9;	9;
50	9;24;25	4	24;25;	24;25;	24;25;	24;25;
Total			*34/50*	*33/50*	*35/50*	*38/50*

TABLE VII
TEST RESULT FOR METHODS WITH *MAXBUSNUMBER = 3 (WLAV)*

CaseNO	*Correct Bus*	*Type*	*Suspect Buses*			
			Method 3A	*Method 3B*	*Method 3C*	*Method 3D*
1	3;13	2	*12;6;10;*	4;12;3;	*12;20;1;*	3;4;13;
2	8;29	2	27;8;28;	27;28;29;	8;27;28;	27;29;28;
3	9;24	2	*10;6;22;*	*22;10;21;*	22;24;28;	22;21;24;
4	11;26	2	*25;28;6;*	*25;9;27;*	*25;28;8;*	9;11;25;
5	14;30	2	27;14;24;	27;29;30;	27;14;29;	27;29;30;
6	16;19	2	19;16;17;	16;17;18;	19;16;17;	16;17;18;
7	18;21	2	*10;15;20;*	10;15;21;	20;21;22;	21;15;22;
8	20;23	2	*10;22;24;*	23;15;18;	*18;22;24;*	23;18;15;
9	5;17	2	*6;2;10;*	5;7;10;	*2;28;1;*	5;7;9;
10	12;31	2	14;15;31;	14;15;31;	14;31;15;	14;31;15;
11	3;13	1	3;13;	3;13;	13;3;	13;3;
12	8;29	1	8;29;	8;29;	8;29;	8;29;
13	9;24	1	9;24;	9;24;	9;24;	9;24;
14	11;26	1	11;26;	11;26;	11;26;	11;26;
15	14;30	1	14;30;	14;30;	14;30;	14;30;
16	16;19	1	16;	16;	16;	16;
17	18;21	1	21;18;	21;18;	21;18;	21;18;
18	20;23	1	20;23;	20;23;	20;23;	20;23;
19	5;17	1	5;17;	5;17;	5;17;	5;17;
20	12;31	1	12;	12;	12;	12;
21	1;3;13	4	1;3;	1;3;	3;1;	3;1;
22	2;6	4	2;6;	2;6;	2;6;	2;6;
23	4;6	4	4;6;	4;6;	4;6;	4;6;
24	6;8;29	4	6;8;	6;8;	8;6;	8;6;
25	10;22	4	10;22;	10;22;	10;22;	10;22;
26	20;10;23	4	20;	20;	20;	20;
27	14;15;30	4	14;15;	14;15;	14;15;	14;15;
28	9;22;24	4	22;24;	22;24;	22;24;	22;24;
29	14;27;30	4	27;30;	27;30;	30;27;	30;27;
30	9;24;25	4	24;25;	24;25;	24;25;	24;25;
31	1;3;13	3	2;1;3;	2;1;3;	2;1;3;	2;1;3;
32	2;6	3	2;6;5;	2;5;6;	5;7;2;	5;2;7;
33	4;6	3	4;2;6;	2;4;3;	4;2;3;	2;3;4;
34	10;22	3	*21;23;24;*	21;23;22;	*21;23;24;*	21;23;22;
35	12;16;19	3	10;4;12;	17;10;16;	*4;17;10;*	17;16;20;
36	15;20;23	3	23;24;15;	23;15;24;	23;24;15;	23;24;15;
37	5;7;17	3	*2;4;6;*	*6;2;4;*	2;4;7;	2;7;6;
38	9;22;24	3	24;23;22;	*15;23;25;*	24;23;22;	23;25;22;
39	14;27;30	3	29;27;30;	29;27;30;	29;30;27;	29;30;27;
40	9;24;25	3	24;25;27;	24;25;27;	24;25;28;	24;25;28;
41	9;20;23;24	3	15;23;12;	15;23;12;	15;23;14;	15;23;12;
42	14;15;30	3	15;12;14;	15;14;12;	14;15;12;	14;15;12;
43	18;21;22	3	10;22;21;	10;22;21;	21;22;24;	22;21;10;
44	6;10	3	6;10;	6;10;	6;10;	6;10;
45	6;9;24	3	10;6;12;	10;6;9;	10;6;12;	9;16;17;
46	9;20;23;24	4	24;23;	24;23;	24;23;	24;23;
47	18;21;22	4	21;22;	21;22;	21;22;	21;22;
48	6;10	4	10;6;	10;6;	10;6;	10;6;
49	6;9;24	4	6;9;	6;9;	9;6;	9;6;
50	9;24;25	4	24;25;	24;25;	24;25;	24;25;
Total			*42/50*	*46/50*	*44/50*	*50/50*

3.4.2 Simulation Result of WLS

The simulation result of proposed identification method using WLAV as first stage state estimation algorithm shows great performance. However, since WLS method is widely used in industry, the identification method should not only rely on WLAV method. The simulation results using WLS algorithm for proposed methods with MaxBusNumber = 0(Method 0A-0D) and MaxBusNumber = 3(Method 3A-3D) are showed in Table VIII and Table IX respectively. We can see the improvements in the identification capability when the normalized index NI_n is used and also when the top five suspect measurements instead of all are used. The performance of the identification process can also be greatly improved by slight increase of the maximum number of suspected buses. All these conclusions are similar to those got form simulation result of WLAV algorithm.

Comparing Table VIII and Table IX with Table VI and Table VII, we can find that the proposed identification method has better performance with WLAV than WLS. For the same methods, using WLAV can correctly identify more cases. As we can see in Table VII and Table IX, using Method 3D with WLAV can identify all the cases in the library while using WLS can only identify 47 out of 50. Fortunately, by further slightly increasing the maximum number of suspected buses, we can also get the best performance. As shown in Table X, when we set MaxBusNumber = 5(Method 5A-3D), both Method 5B and Method 5D can identify all of the 50 cases.

3.5 Conclusions

Topology errors can be identified by a two-stage state estimation algorithm that is proposed earlier. This chapter investigates the part of the algorithm involving the suspect bus identification procedure following the first stage estimation. Several possible strategies are developed and comparatively tested by using a topology error library that is created for this purpose based on IEEE 30 bus test system. The performance of each method is evaluated by simulation results using this library.

For those cases where status of the CB is assumed to be open while it is actually closed (*type2* and *type3*), most of the methods can identify the suspect buses correctly. On the other hand, for the opposite scenarios, not all of the methods show equally good performance. However, by increasing the maximum number of suspected buses slightly,

one of the developed methods appears to remain robust by performing consistently well under all studied scenarios. This method is the main contribution of this study and is expected to enhance the performance of the two-stage topology error identification method significantly.

The proposed identification method has different performances when using different first stage state estimation algorithm. Generally to say, using WLAV is better than WLS for suspected area identification purpose. However, since WLS is widely used in the industry, the identification should not only rely on WLAV. Fortunately, it shows that by further increasing the maximum number of suspected buses slightly, the proposed identification method can also get the best performance with WLS algorithm.

TABLE VIII
TEST RESULT FOR METHODS WITH *MAXBUSNUMBER = 0 (WLS)*

CaseNO	*Correct Bus*	*Type*	*Suspect Buses*			
			Method 0A	*Method 0B*	*Method 0C*	*Method 0D*
1	3;13	2	*6;*	*4;*	*6;*	*4;*
2	8;29	2	*27;*	*27;*	*24;*	*27;*
3	9;24	2	*6;*	10;22;24;	*6;*	24;
4	11;26	2	*6;*	*25;*	*24;*	*25;*
5	14;30	2	*27;*	*27;*	*24;*	30;
6	16;19	2	18;19;20;	*20;*	*18;*	*18;20;*
7	18;21	2	*10;15;*	*20;*	*18;*	*20;*
8	20;23	2	*10;*	*15;18;*	*10;*	*18;*
9	5;17	2	*6;*	*7;*	*6;*	5;
10	12;31	2	*15;*	12;14;15;	*15;*	14;31;
11	3;13	1	*6;*	12;13;	*6;*	12;13;
12	8;29	1	*6;*	8;	*6;*	8;
13	9;24	1	*6;*	9;	6;24;	9;
14	11;26	1	*25;*	11;	*24;*	11;
15	14;30	1	*27;*	14;	14;30;	14;
16	16;19	1	12;16;19;	12;16;	16;	16;
17	18;21	1	15;18;19;	18;	18;	18;
18	20;23	1	*10;*	23;	*10;24;*	23;
19	5;17	1	*10;*	17;	*10;*	17;
20	12;31	1	12;	12;	12;	12;
21	1;3;13	4	*6;*	1;2;	*6;*	1;2;31;
22	2;6	4	6;	6;	6;	6;31;
23	4;6	4	6;	4;12;	4;6;	4;
24	6;8;29	4	6;	8;	6;	8;
25	10;22	4	10;	10;21;22;	10;	10;21;22;
26	20;10;23	4	*12;*	*12;14;*	*14;*	*14;*
27	14;15;30	4	12;15;	12;14;	15;	14;
28	9;22;24	4	*10;*	22;	*10;*	22;
29	14;27;30	4	27;	30;	27;	30;
30	9;24;25	4	24;25;	12;24;25;	24;	24;31;
31	1;3;13	3	*6;*	1;2;3;	*6;*	1;2;3;
32	2;6	3	6;	6;	6;	6;
33	4;6	3	6;	4;	6;	4;
34	10;22	3	10;	21;22;	*10;*	21;22;
35	12;16;19	3	*6;*	16;17;	6;	16;
36	15;20;23	3	*10;*	*12;*	*10;24;*	*24;*
37	5;7;17	3	*6;*	7;	6;	7;
38	9;22;24	3	*10;*	*23;*	24;	*23;*
39	14;27;30	3	27;	29;30;	30;	30;
40	9;24;25	3	24;	*27;*	24;	*27;*
41	9;20;23;24	3	12;24;	*12;*	*24;*	*12;*
42	14;15;30	3	15;	*12;*	14;	*12;*
43	18;21;22	3	*10;*	*10;*	*10;*	*10;*
44	6;10	3	6;10;	*12;*	6;10;	*12;*
45	6;9;24	3	6;	9;12;	6;	9;12;
46	9;20;23;24	4	19;20;	19;20;	19;20;	19;20;
47	18;21;22	4	10;19;20;22;	*19;20;*	21;	19;20;21;
48	6;10	4	10;	6;10;12;19;	10;24;	6;10;12;19;
49	6;9;24	4	6;	9;	6;	9;
50	9;24;25	4	*27;*	25;	24;	25;
Total			*24/50*	*33/50*	*27/50*	*36/50*

TABLE IX
TEST RESULT FOR METHODS WITH *MAXBUSNUMBER = 3 (WLS)*

CaseNO	*Correct Bus*	*Type*	*Suspect Buses*			
			Method 3A	*Method 3B*	*Method 3C*	*Method 3D*
1	3;13	2	*6;12;15;*	4;12;3;	*6;12;15;*	4;12;3;
2	8;29	2	*27;6;10;*	*27;28;6;*	24;27;8;	*27;28;6;*
3	9;24	2	*6;10;15;*	10;22;24;	6;10;24;	24;10;22;
4	11;26	2	*6;10;24;*	25;9;11;	*24;6;10;*	25;9;11;
5	14;30	2	*27;15;12;*	27;30;14;	24;27;14;	30;27;14;
6	16;19	2	18;19;20;	*20;15;18;*	18;16;19;	*18;20;15;*
7	18;21	2	*10;15;12;*	*20;10;15;*	18;10;15;	20;18;10;
8	20;23	2	10;19;23;	15;18;23;	*10;24;18;*	18;15;23;
9	5;17	2	*6;2;4;*	7;5;6;	*6;24;2;*	5;7;6;
10	12;31	2	15;23;12;	12;14;15;	*15;18;14;*	14;31;12;
11	3;13	1	*6;4;2;*	12;13;3;	*6;4;2;*	12;13;3;
12	8;29	1	*6;27;28;*	8;6;12;	6;8;27;	8;6;12;
13	9;24	1	*6;10;22;*	9;10;12;	6;24;10;	9;24;10;
14	11;26	1	*25;6;9;*	11;9;12;	*24;25;6;*	11;26;9;
15	14;30	1	27;12;14;	14;12;30;	14;30;27;	14;12;30;
16	16;19	1	12;16;19;	12;16;19;	16;12;19;	16;12;19;
17	18;21	1	15;18;19;	18;12;15;	18;15;19;	18;12;15;
18	20;23	1	*10;15;19;*	23;12;15;	*10;24;15;*	23;12;15;
19	5;17	1	*10;2;6;*	17;5;10;	*10;2;6;*	17;5;10;
20	12;31	1	12;	12;	12;	12;
21	1;3;13	4	*6;2;4;*	1;2;12;	*6;2;4;*	1;2;31;
22	2;6	4	6;4;12;	6;2;4;	6;4;5;	6;31;2;
23	4;6	4	6;2;10;	4;12;6;	4;6;2;	4;12;31;
24	6;8;29	4	6;4;12;	8;28;12;	6;4;24;	8;28;31;
25	10;22	4	10;21;22;	10;21;22;	10;24;21;	10;21;22;
26	20;10;23	4	*12;14;15;*	12;14;10;	*14;12;15;*	*14;12;31;*
27	14;15;30	4	12;15;14;	12;14;13;	15;12;14;	14;12;31;
28	9;22;24	4	*10;25;21;*	22;12;24;	10;22;24;	22;24;31;
29	14;27;30	4	27;12;14;	30;12;29;	27;14;30;	30;31;12;
30	9;24;25	4	24;25;12;	12;24;25;	24;14;25;	24;31;12;
31	1;3;13	3	*6;2;4;*	1;2;3;	*6;2;4;*	1;2;3;
32	2;6	3	6;2;4;	6;2;12;	6;2;4;	6;2;12;
33	4;6	3	6;2;4;	4;2;12;	6;24;2;	4;2;12;
34	10;22	3	10;22;17;	21;22;10;	10;22;24;	21;22;10;
35	12;16;19	3	6;10;12;	16;17;10;	6;10;12;	16;17;10;
36	15;20;23	3	10;12;15;	12;23;24;	*10;24;12;*	24;12;23;
37	5;7;17	3	*6;2;4;*	7;2;5;	*6;2;4;*	7;5;2;
38	9;22;24	3	*10;6;15;*	*23;12;15;*	24;10;6;	23;24;12;
39	14;27;30	3	27;29;30;	29;30;12;	30;27;29;	30;29;12;
40	9;24;25	3	24;22;25;	27;12;22;	24;22;25;	27;24;12;
41	9;20;23;24	3	12;24;15;	*12;15;22;*	24;12;15;	12;15;24;
42	14;15;30	3	15;12;14;	12;15;14;	14;15;12;	12;14;15;
43	18;21;22	3	10;22;21;	10;21;12;	10;22;21;	10;21;12;
44	6;10	3	6;10;12;	12;6;10;	6;10;24;	12;6;10;
45	6;9;24	3	6;10;12;	9;12;4;	6;10;24;	9;12;4;
46	9;20;23;24	4	19;20;12;	19;20;12;	19;20;24;	19;20;12;
47	18;21;22	4	*10;19;20;*	19;20;12;	21;10;19;	19;20;21;
48	6;10	4	10;6;4;	6;10;12;	10;24;6;	6;10;12;
49	6;9;24	4	6;10;4;	9;6;10;	6;10;4;	9;6;10;
50	9;24;25	4	*27;22;19;*	25;12;24;	24;27;22;	25;24;12;
Total			*30/50*	*45/50*	*36/50*	*47/50*

TABLE X
TEST RESULT FOR METHODS WITH *MAXBUSNUMBER = 5 (WLS)*

CaseNO	*Correct Bus*	*Type*	*Suspect Buses*			
			Method 5A	***Method 5B***	***Method 5C***	***Method 5D***
1	3;13	2	*6;10;12;4;15;*	4;12;3;13;9;	*6;24;10;12;4;*	4;12;3;13;9;
2	8;29	2	*27;6;10;22;24;*	27;28;6;25;29;	24;27;8;30;6;	27;28;6;25;29;
3	9;24	2	*6;10;15;22;12;*	10;22;24;9;21;	6;10;24;15;22;	24;10;22;9;21;
4	11;26	2	*6;10;24;25;28;*	25;9;11;26;27;	*24;6;10;25;28;*	25;9;11;26;27;
5	14;30	2	*27;15;12;24;28;*	27;30;14;25;12;	24;27;14;30;15;	30;27;14;25;24;
6	16;19	2	18;19;20;15;16;	20;15;18;19;16;	18;16;19;20;15;	18;20;15;19;16;
7	18;21	2	10;15;12;19;21;	20;10;15;18;19;	18;10;15;12;19;	20;18;10;15;19;
8	20;23	2	10;19;23;24;15;	15;18;23;19;10;	10;24;18;19;23;	18;15;23;19;24;
9	5;17	2	*6;2;4;10;12;*	7;5;6;10;17;	6;24;2;4;5;	5;7;6;10;17;
10	12;31	2	15;23;12;18;14;	12;14;15;31;	15;18;14;23;12;	14;31;12;15;
11	3;13	1	*6;4;2;10;12;*	12;13;3;	*6;4;2;10;12;*	12;13;3;
12	8;29	1	6;27;28;8;25;	8;6;12;29;	6;8;27;28;30;	8;6;12;29;
13	9;24	1	6;10;22;24;4;	9;10;12;24;	6;24;10;22;4;	9;24;10;12;
14	11;26	1	*25;6;9;24;27;*	11;9;12;26;	24;25;6;9;11;	11;26;9;12;
15	14;30	1	27;12;14;15;30;	14;12;30;15;	14;30;27;12;15;	14;12;30;15;
16	16;19	1	12;16;19;20;	12;16;19;	16;12;19;20;	16;12;19;
17	18;21	1	15;18;19;21;22;	18;12;15;21;	18;15;19;21;22;	18;12;15;21;
18	20;23	1	10;15;19;23;24;	23;12;15;20;	10;24;15;19;23;	23;12;15;20;
19	5;17	1	10;2;6;5;7;	17;5;10;12;	10;2;6;5;16;	17;5;10;12;
20	12;31	1	12;	12;	12;	12;
21	1;3;13	4	6;2;4;12;1;	1;2;12;3;13;	*6;2;4;12;5;*	1;2;31;12;3;
22	2;6	4	6;4;12;2;15;	6;2;4;12;5;	6;4;5;12;2;	6;31;2;4;12;
23	4;6	4	6;10;2;12;27;	4;12;6;13;31;	4;6;10;2;5;	4;12;31;6;13;
24	6;8;29	4	6;4;12;2;10;	8;28;12;6;13;	6;4;24;12;5;	8;28;31;12;6;
25	10;22	4	10;21;22;17;24;	10;21;22;	10;24;21;22;17;	10;21;22;
26	20;10;23	4	12;14;15;19;20;	12;14;10;13;15;	*14;12;15;20;31;*	14;12;31;20;10;
27	14;15;30	4	12;15;14;18;23;	12;14;13;15;31;	15;12;14;18;23;	14;12;31;15;13;
28	9;22;24	4	10;25;21;22;23;	22;12;24;13;21;	10;22;24;25;14;	22;24;31;12;21;
29	14;27;30	4	27;12;14;29;25;	30;12;29;13;14;	27;14;30;12;29;	30;31;12;29;14;
30	9;24;25	4	24;25;12;14;22;	12;24;25;13;14;	24;14;25;26;12;	24;31;12;25;14;
31	1;3;13	3	6;2;4;10;1;	1;2;3;12;4;	*6;2;4;10;5;*	1;2;3;12;4;
32	2;6	3	6;2;4;12;10;	6;2;12;4;5;	6;2;4;5;12;	6;2;12;5;4;
33	4;6	3	6;10;2;4;27;	4;2;12;3;6;	6;10;24;2;4;	4;2;12;3;6;
34	10;22	3	10;22;17;24;9;	21;22;10;12;	10;22;24;17;9;	21;22;10;12;
35	12;16;19	3	6;10;12;4;9;	16;17;10;12;	6;10;12;16;4;	16;17;10;12;
36	15;20;23	3	10;12;15;6;22;	12;23;24;15;22;	10;24;12;15;6;	24;12;23;15;22;
37	5;7;17	3	6;2;4;3;5;	7;2;5;6;12;	6;2;4;5;3;	7;5;2;6;12;
38	9;22;24	3	10;6;15;12;22;	23;12;15;22;24;	24;10;6;15;12;	23;24;12;15;22;
39	14;27;30	3	27;29;30;12;25;	29;30;12;27;	30;27;29;12;25;	30;29;12;27;
40	9;24;25	3	24;22;25;28;10;	27;12;22;24;25;	24;22;25;28;10;	27;24;12;22;25;
41	9;20;23;24	3	12;24;15;22;23;	12;15;22;23;24;	24;12;15;22;23;	12;15;24;22;23;
42	14;15;30	3	15;12;14;18;19;	12;15;14;	14;15;12;18;19;	12;14;15;
43	18;21;22	3	10;22;21;12;23;	10;21;12;22;	10;22;21;24;12;	10;21;12;22;
44	6;10	3	6;10;12;28;17;	12;6;10;4;9;	6;10;24;12;16;	12;6;10;4;9;
45	6;9;24	3	6;10;12;4;15;	9;12;4;10;	6;10;24;12;4;	9;12;4;10;
46	9;20;23;24	4	19;20;12;24;15;	19;20;12;	19;20;24;12;18;	19;20;12;
47	18;21;22	4	10;19;20;22;21;	19;20;12;21;10;	21;10;19;20;22;	19;20;21;12;10;
48	6;10	4	10;6;4;12;19;	6;10;12;19;9;	10;24;6;16;4;	6;10;12;19;9;
49	6;9;24	4	6;10;4;27;2;	9;6;10;12;	6;10;4;27;5;	9;6;10;12;
50	9;24;25	4	27;22;19;24;25;	25;12;24;27;	24;27;22;19;25;	25;24;12;27;
Total			*42/50*	*50/50*	*44/50*	*50/50*

CHAPTER IV

REMOTE MEASUREMENT CALIBRATION BY STATE ESTIMATION METHOD

4.1 Introduction

Power system state estimation relies on telemetered measurements for optimal estimation of the system state. State estimators are designed to handle random as well as gross errors via appropriate bad data processing methods. These errors appear in the telemetered quantities due to their accumulation during the various stages of transforming and transmitting the raw data to the control center computer. Instrument transformers, transducers, telecommunication medium and devices may all contribute to such errors. A measurement received at the control center may have an error with both a random as well as a systematic component depending upon the source of the error.

Power system state estimation itself can filter the random errors in the telemetered quantities. Most state estimation formulations, including the popular weighted least squares (WLS) method, are developed based on the assumption that the measurements contain only random errors with zero mean and known variance. On the other hand, systematic errors can be filtered either by post WLS estimation methods or via alternative robust estimation methods. Unfortunately, performances of all of these methods are limited by the measurement redundancy. The number of bad data that can be handled by these methods cannot exceed an upper limit, which is dictated by the measurement redundancy and configuration. Therefore, in order to obtain an accurate estimation result, majority of the measurements is required to be free of gross errors. This implies that the measurements must be appropriately calibrated so that the systematic errors associated with most measurements remain small.

Manual calibration and checking of instruments at the substations are labor intensive and costly. Furthermore, identification of the source of the systematic error may not be trivial when several stages of data transformation and telemetry are involved. Quite a few papers [38]-[47] have discussed the possibility of “soft” calibration techniques which can be conducted in the control center remotely. Papers [38]-[39] utilize the residuals result from state estimator to estimate the zero-offset and linear regression relation between the estimated/measured measurement pairs. Works in [40]-[43] suggests procedures that are

executed at individual substations in order to minimize errors in the analog measurements. Papers [44]-[46] propose branch/bus by branch/bus calibration methods utilizing the local redundancy. Study in [47] describes a system wide calibration method which relies on an essential reliable measurement set. However, these previous methods either cannot get satisfied performance or are not systematical enough for easy implementation.

Other than measurement calibration topic, there are lots of papers [51]-[58] discussing the estimation of network topology parameters in state estimation, such as branch impedances or transformer tap changer position. Some of these previous works utilize techniques that augment the state vector to include those network parameters. Similarly, a new remote measurement calibration technique utilizing existing state estimation algorithms and the redundancy of the measurements is presented in [59]. The main idea is to relate the true and measured values by parametric equations and estimate these parameters simultaneously with the system states by using a modified state estimation program. In order to filter the random noise and provide the needed redundancy, the proposed technique can be implemented off-line utilizing several recorded measurement scans. This paper will further discuss this idea together with other important problems such as determination of the suspect measurement set, verification of the calibration results and observability analysis.

4.2 Method Formulation

Power system state estimation is formulated based on the measurement equation given below:

$$z = h(x) + e \tag{22}$$

where:

z : the measurement vector of dimension m ;

$h(x)$: the nonlinear function relating the error free measurements to the system states;

x : the state vector of dimension n ;

e : the measurement noise vector;

m, n : the number of state variables and measurements, respectively ($n < m$).

Consider a case where there exist systematic errors in some of the telemetered quantities. Then, assume that the measured and true values of a measurement are related through a nonlinear calibration function as given below:

$$\bar{z} = f(z, p) \tag{23}$$

where:

$\bar{z}$: the vector of telemetered quantities;

z : the vector of true (calibrated) quantities;

f : the characteristics function of the measurements need calibration.

p : the vector of parameters in the characteristics function;

The first-order Taylor series expansion of (22) and (23) for a set of value can be written as:

$$\Delta\bar{z} = F_z \cdot \Delta z + F_p \cdot \Delta p \tag{24}$$

where:

F_z : $\partial f / \partial z$;

F_p : $\partial f / \partial p$;

$\Delta\bar{z}, \Delta z, \Delta p$: Increments of $\bar{z}, z, p$, respectively.

Use of the DC measurement model yields:

$$\Delta z = H \cdot \Delta x + e \tag{25}$$

where:

H : the Jacobian matrix;

Δx : Increment of x .

Substitute (25) into (24) we have:

$$\Delta\bar{z} = F_z \cdot H \cdot \Delta x + F_p \cdot \Delta p + e' \tag{26}$$

where:

$e' = F_z \cdot e$.

In compact form (26) can be written as:

$$\Delta\bar{z} = \begin{bmatrix} F_z \cdot H & F_p \end{bmatrix} \cdot \begin{bmatrix} \Delta x \\ \Delta p \end{bmatrix} + e' \tag{27}$$

Given enough redundancy, equation (27) can be solved by the conventional techniques used by state estimation, such as weighted least square (WLS) method. Due to the similarity of the formulation in (27) to the state estimation problem, it can be easily implemented by modifying an existing state estimation code.

Using this formulation, the parameters of the chosen calibration functions can be estimated along with the system state variables. These parameters can then be used to calibrate the subsequently telemetered measurements by applying the inverse of the calibration function:

$$z_c = f^{-1}(\bar{z}, \hat{p}) \tag{28}$$

where:

z_c : vector of calibrated measurements;

$\hat{p}$: estimated p vector.

The inverse function of f may not be uniquely defined depending on the chosen expression. However, given the fact that in practical systems the calibrated values are close enough to the measured values, the correct solution can be identified by inspection.

The formulation given in (27) assumes a single scan of measurements. In general, there is not enough redundancy to allow estimation of all calibration parameters based on a single scan. The fact that systematic errors remain to appear in several consecutive measurement scans can be exploited in order to increase redundancy and further suppress the influence of the random errors. This is accomplished by using a window of k consecutive measurement scans simultaneously, where the expanded measurement and state vectors will be:

$$z = [z_1, \quad z_2, \quad \ldots \quad z_k] \tag{29}$$

$$x = [x_1, \quad x_2, \quad \ldots \quad x_k, \quad p] \tag{30}$$

Note that the calibration function parameter vector p is assumed to remain fixed from one scan to the next, while the measurements and the states are changing. Measurement equations for the k scan measurement window can be written using the expanded form of (27):

$$\begin{bmatrix} \Delta\bar{z}_1 \\ \Delta\bar{z}_2 \\ \dots \\ \Delta\bar{z}_k \end{bmatrix} = \begin{bmatrix} F_{z1}\cdot H_1 & 0 & \dots & 0 & F_{p0} \\ 0 & F_{z2}\cdot H_2 & \dots & 0 & F_{p1} \\ \dots & \dots & \dots & & \dots \\ 0 & 0 & \dots & F_{zk}\cdot H_k & F_{pk} \end{bmatrix} \cdot \begin{bmatrix} \Delta x_1 \\ \Delta x_2 \\ \dots \\ \Delta x_k \\ \Delta p \end{bmatrix} + \begin{bmatrix} e'_1 \\ e'_2 \\ \dots \\ e'_k \end{bmatrix} \tag{31}$$

Where the arrays with subscripts i ($1,2\dots k$) correspond to the equations for the i^{th} measurement scan.

Applying WLS method, (31) will yield a bordered-block-diagonal gain matrix having the following structure:

$$G = \begin{bmatrix} G_1 & & & & G_{p1} \\ & G_2 & & & G_{p2} \\ & & \ddots & & \vdots \\ & & & G_k & G_{pk} \\ G_{p1}^T & G_{p2}^T & \dots & G_{pk}^T & G_{pp} \end{bmatrix} \tag{32}$$

Incorporating several scans together as in (31) naturally increases the computational burden significantly compared to single scan estimation. The gain matrix of (32) must be built and factorized at each state estimation iteration. However, alternative implementation methods exist [50] where computational burden is significantly reduced. On the other hand, if the calibration procedure is repeated few times on a daily basis, it essentially becomes an off-line procedure making these computation issues less relevant. It may run on a batch computer without interfering with the execution of the state estimator or any other on-line application. Hence, the calibration parameters can be updated routinely using the estimated results.

4.2.1 Determination of the Suspect Measurements Set

Before the calibration process, a suspected measurements set must be identified. This can be done by inspecting trouble spots, which yield bad data flags in consecutive state estimation runs, or by setting routine maintenance schedules. Theoretically to say, for optimal results, all measurements requiring calibration should be included in this set perhaps along with some already calibrated measurements. However, it was found that including of too many measurements in the suspected set couldn't produce good results. Under this case, the calibration process can reduce the errors to some degree but the

calibration parameters may be biased. This can be solved by only including the first several identified bad data instead of the whole set in one calibration process. The uncalibrated measurements that are not included will be identified at the verification process described in section 4.2.3.

4.2.2 Detailed Calibration Procedure

The procedure for solving the expanded WLS estimation problem for the measurement model of (31) is summarized below:

1. Determine the set of measurements to be calibrated.
2. Collect *k* consecutive scans of measurements. Those scans should be made within a reasonable short window of time to ensure that the characteristics of the systematic errors in non-calibrated measurements remain the same.
3. Initialize the system state vector ($x_i^0, i = 1..k$), the calibration parameter vector (p_0) and the iteration index $j = 1$.
4. Compute $F_{zi}^j, F_{pi}^j, H_i^j, i = 1..k$. Where i and j are measurement scan and iteration indices respectively. Build the Jacobian for iteration j (H^j) as given in (31).
5. Compute the estimated measurement vector for iteration j ($\hat{z}_i^j, i = 1..k$). Calculate the measurement residuals for iteration j:

$$\Delta \bar{z}_i^j = \bar{z}_i - f(\hat{z}_i^j, p^{j-1}), i = 1..k \tag{33}$$

6. Solve the WLS state estimation problem and obtain the estimates of the system states for each scan ($\Delta x_i^j, i = 1..k$) and calibration parameters (Δp^j) for iteration j. Update both vectors by:

$$\begin{cases} x_i^j = x_i^{j-1} + \Delta x_i^j, i = 1..k \\ p^j = p^{j-1} + \Delta p^j \end{cases} \tag{34}$$

7. If converged, go to step 8. Else, update the iteration counter $j = j+1$ and go to step 4. Convergence can be checked based on the norm of the incremental changes in the estimated vectors using a pre-specified tolerance.
8. Update the calibration parameters and use them to calibrate the corresponding

measurements as given in (28).

4.2.3 Verification of the Calibration

The calibration procedure described in previous section utilizes K consecutive scans of measurements to estimate the calibration parameters of the suspect measurements. However, if some of the measurements with systematical errors are not included as suspected measurements or the calibration functions of some of the suspected measurements are not suited to the patterns of systematical errors, the calibration results may be biased. This problem can be identified by using the $k+1^{st}$ scan of the measurements: after the calibration parameters are got, run the state estimation and bad data analysis for the $k+1^{st}$ scan using the calibrated values for those suspected measurements. If there are no bad data identified, it means all the bad data have been calibrated. The calibration process is completed and valid. Otherwise, the calibration process is not completed. There are two possibilities under this case:

1) The bad data include those which have been calibrated in the previous calibration process. This means the calibration functions are not suited to the error patterns. Other better functions much be choose and the calibration process need to be rerun. For example, linear calibration function is used for one measurement in the calibration process. After the parameters have been estimated, this measurement still identified as bad data. In this case, the linear function should be replace with quadratic or some other nonlinear functions and rerun the calibration process.

2) All of the identified bad data are other than those have been calibrated in the previous process. This indicates there exist some uncalibrated bad data outside the suspected measurements set defined in the previous calibration process. In this case, another set of suspect measurements is selected based on the bad data analysis results. Rerun the calibration process. Note here that we must use the calibrated values for those measurements have been calibrated in the previous calibration process.

4.3 Implementation

The general formulation of the proposed remote measurement calibration technique has been described above. In a specific implementation, the calibration function f needs

to be determined in advance for a given system and all of its measurements. The types of systematic errors appearing in measurements that are telemetered to the control centers are typically caused by the following reasons [41]:

- Age, temperature and other ambient effects related drift and deterioration of instruments over time;
- Changes in gains, zero offsets, and nonlinear characteristics of instruments involved in the measurement process;
- Inadvertently introduced gross errors due to the wrong modeling and scaling used at the control center;
- Errors in transducer parameters, instrument transformer ratios, transformer ratings, and scaling coefficients.

The calibration function, which relates the measured and calibrated values, may be chosen as a quadratic function as below:

$$\bar{z} = a \cdot z^2 + b \cdot z + c \tag{35}$$

The first-order Taylor series expansion of (35) yields:

$$\Delta\bar{z} = (2 \cdot a \cdot z + b) \cdot \Delta z + z^2 \cdot \Delta a + z \cdot \Delta b + \Delta c \tag{36}$$

Substituting (36) into (25):

$$\Delta\bar{z} = (2 \cdot a \cdot z + b) \cdot H \cdot \Delta x + z^2 \cdot \Delta a + z \cdot \Delta b + \Delta c + e_1 \tag{37}$$

Equation (37) can be rewritten in compact form as:

$$\Delta\bar{z} = \left[(2 \cdot a \cdot z + b) \cdot H \quad I \quad D(z) \quad D(z^2)\right] \cdot \begin{bmatrix} \Delta x \\ \Delta c \\ \Delta b \\ \Delta a \end{bmatrix} + e_1 \tag{38}$$

Here *D(v)* is the operator of forming a diagonal matrix whose diagonal elements are equal to the vector *v*.

Assuming *k* scans are considered simultaneously, (38) can be expanded as:

$$\begin{bmatrix} \Delta\bar{z}_1 \\ \Delta\bar{z}_2 \\ \dots \\ \Delta\bar{z}_k \end{bmatrix} = \begin{bmatrix} (2\cdot a_1\cdot z_1 + b_1)\cdot H_{0-1} & & \dots & & I\ \mathrm{D(z_1)}\ \mathrm{D(z_1^2)} \\ & (2\cdot a_2\cdot z_2 + b_2)\cdot H_2 & \dots & & I\ \mathrm{D(z_2)}\ \mathrm{D(z_2^2)} \\ \dots & \dots & \dots & & \dots \\ & & \dots & (2\cdot a_k\cdot z_k + b_k)\cdot H_k & I\ \mathrm{D(z_k)}\ \mathrm{D(z_k^2)} \end{bmatrix} * \begin{bmatrix} \Delta x_1 \\ \Delta x_2 \\ \dots \\ \Delta x_k \\ \Delta c \\ \Delta b \\ \Delta a \end{bmatrix} + \begin{bmatrix} e_1' \\ e_2' \\ \dots \\ e_k' \end{bmatrix} \tag{39}$$

Estimation of the unknown variables in (39) will yield the sought after parameters *a, b* and *c* for the chosen calibration function of (35). Corresponding measurements can be calibrated by using the inverse of this quadratic function as in (28). Among the two possible solutions of this quadratic equation only one will be correct and needs to be identified.

The calibration function (35) has two solutions given by:

$$z^1 = (-b + \sqrt{b^2 - 4a(c - \bar{z})}) / 2a \tag{40}$$

$$z^2 = (-b - \sqrt{b^2 - 4a(c - \bar{z})}) / 2a \tag{41}$$

For a single measurement, we can define the calibrated residual for different solutions as:

$$r_i^j = z_i^j - \hat{z}_i;\ \ i = 1,2,...k;\ j = 1,2 \tag{42}$$

where:

r_i^j : The residual of j^{th} solution corresponds to i^{th} measurement scan.

z_i^j : The j^{th} solution corresponds to i^{th} measurement scan.

$\hat{z}_i$: The estimated value of this measurement corresponds to i^{th} measurement scan.

For all the possible solutions, we can calculate the sum of the squares of corresponding residuals as:

$$R^j = \sum_{i=1}^{k} (r_i^j)^2 \tag{43}$$

The correct solution can be identified by simply selecting the one has the minimum value of (43).

In an actual system, this can be further verified based on the information about the type and location of the measurements. For example, the active power injection of a generation (load) bus will always be greater (less) than zero, real power flows leaving towards the load side of the transformers must be positive, etc.

As an alternative, the calibration function can also be chosen as linear instead of quadratic, reducing the unknown parameters to *b* and *c* only:

$$\bar{z} = b \cdot z + c \tag{44}$$

This model can be implemented by simply eliminating the columns and variables corresponding to the parameter *a* in (39). Similar modifications can be made in (39) for other possible combinations of *a, b* and *c*. Certainly it is possible to employ within the same formulation, different functional forms for calibrating different measurements.

In practical implementation, the following issues must be considered:

1) If the chosen measurements have already been calibrated once earlier, the original non-calibrated values must be used when forming the measurement vector. The existing calibration parameters can be used as initial values in estimating the new parameters.
2) In case of a new calibration, initialize the parameter *b* as 1 while using zeros for *a* and *c*. However, this choice of initial values will lead to ill-conditioning of the Jacobian. This problem can be circumvented by eliminating the parameters from the calibration model in the first iteration and including them in the subsequent iterations. Another alternative is to set the initial values of system state variables to the estimated values if they are available.
3) If the values of the measurements to be calibrated include zeros, such as zero-injections and the calibration models include parameters *a* or *b*, then the gain matrix will be ill conditioned. Hence, estimation of parameters *a* or *b* for zero-valued measurements should be avoided.

4.4 Observability Analysis

Like state estimation, the proposed remote measurement calibration method is subject to observability problem. The gain matrix shown in (32) may become singular under certain circumstances:

1) The number of suspect measurements excesses the limit.
2) The number of calibration parameters excesses the limit.

Both of these problems will be addressed in this section.

4.4.1 Number of Measurements Can Be Estimated

The measurement calibration issue can be treated as a special measurement error detection/identification problem. The limitation of number of measurement can be estimated is similar to the topic in multiple bad data analysis, which has been discussed in detailed in [48]. The proposed method will encounter observability problems under the following conditions:

1) Existence of critical measurements.
2) Existence of critical *k-tuples*, which is defined as a set of *k* measurements, none of which belongs to any lower order critical tuples, whose deletion results in the loss of observability [48].

First of all, the error in the critical measurement can never be detected or identified. Hence there is no way for the critical measurement to be calibrated by remote measurement calibration method.

Secondly, as shown in [48], *k-2* gross errors in a critical *k-tuple* of measurements are detectable and identifiable while *k* and *k-1* errors in a critical *k-tuple* of measurements are detectable but not identifiable. Similar rules are also valid in remote measurement calibration.

1) *Rule 1*. Systematic errors in any *k-2* or less measurements of a critical *k-tuple* of measurements can be calibrated.
2) *Rule 2*. Systematic errors in any *k-1* measurements in a critical *k-tuple* of measurements can be detectable, but not identifiable. Including of coefficients for all of those *k-1* measurements in (31) will not result in singular matrix. We can still get the estimated results even though they might be biased.
3) *Rule 3*. Systematic errors in all measurements of a critical *k-tuple* of measurements can be detectable but not identifiable. Including of coefficients for all of those measurements in (31) will result in a singular gain matrix.

These rules will be further discussed along with the simulation result in section 4.5.5. Unfortunately, these problems cannot be solved by increase the snapshots number in the equation. The increasing of the snapshots number can only helps to suppress the influence of random errors and increase the number of coefficients for individual measurement.

From above discussion, we know that under certain circumstances, the gain matrix will be singular thus the whole procedure will fail. There are two ways to solve this numerical problem.

1) After we get the suspect measurement set, conduct an observability analysis. Exclude those measurements that will make the gain matrix singular. This method needs extra detection procedure and it is not convenience.
2) Similar to pseudo-measurement in normal state estimator, we can introduce pseudo-parameter-measurement. The value of pseudo-parameter-measurements can be set to the existed one or the "flat start" values if no extra information is available. These pseudo-parameter-measurements may be wrong in most of the cases. In order to make sure the estimated result will not be contaminated by these pseudo-parameter-measurements, they should be weighted lower compared to other measurements. Consideration must be given to avoid forming ill-condition matrix by these lower weights. This issue will be further studied along with the simulation results in section 4.5. Note here that the introduction of pseudo-parameter-measurement can solve the numerical problems but cannot solve the observability problem. Although we can get results for those measurements which cannot be estimated under current measurement configuration as well, they may be biased. However, if there exist error in those measurements and we do not have other technique to suppress the influence.

4.4.2 Number of Coefficients for Individual Measurement

As shown above, only the coefficients of the redundancy measurements can be estimated along with the system state. On the other hand, each redundancy measurement can provide the possibility to the estimation of only one coefficient. This problem can be relief by increasing the number of snapshots. Formulation of k snapshots simultaneously make it is possible to estimate at most k coefficients for single measurements.

4.5 Simulation Results

The proposed remote measurement calibration technique is tested on simulation data using different IEEE systems. The results show that the performance of this method remains insensitive to the size of the system due to the local nature of this problem. Hence, the detailed simulation results will be presented only for IEEE 14 bus system in this section.

Fig. 16 shows the one-line diagram of the studied system. The measurement configuration is also shown in the picture.

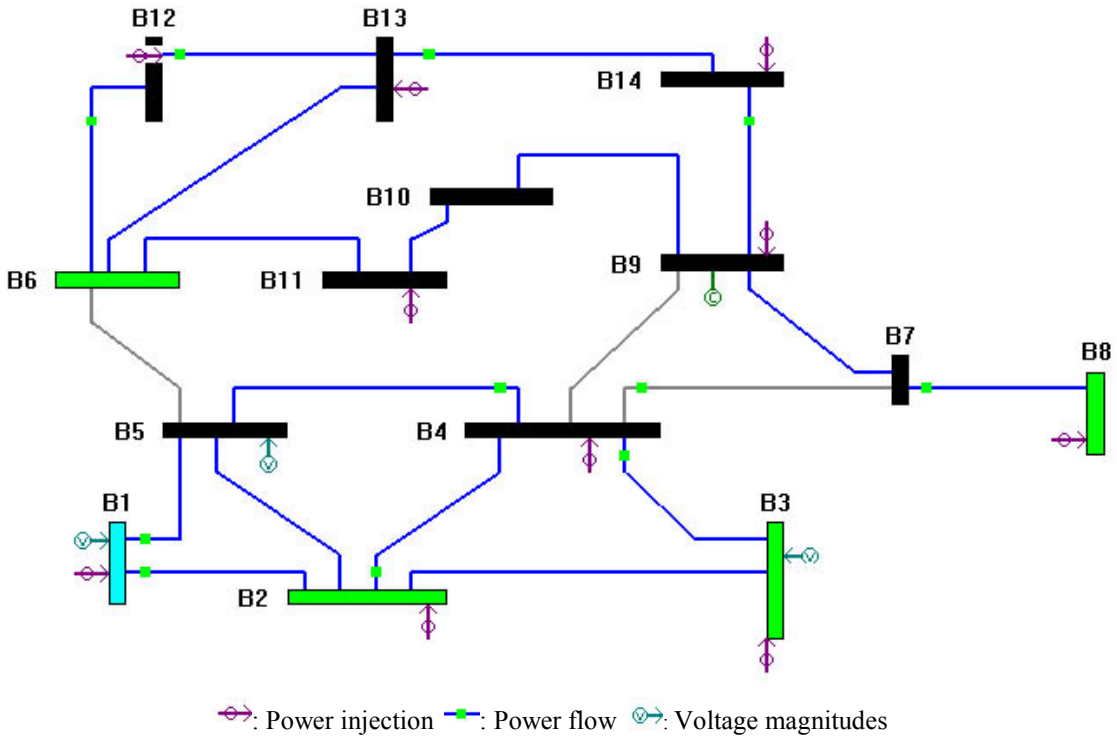

Fig. 16. Studied system of remote measurement calibration with measurement configuration

The system has the following measurements:

- 10 injections at buses 1,2,3,4,8,9,11,12,13 and 14.
- 11 flows on branches 1-2,1-5,2-4,3-4,4-5,4-7,6-12,7-8,9-14,12-13 and 13-14.
- 5 voltage magnitudes at buses 1,3,4,5 and 14.

Measurement redundancy is 21/13. The structure of the sensitivity matrix for the active part is shown in (45). For convenience, the row sequence of S_a is rearranged to form a block diagonal structure.

$$S_a = \begin{bmatrix} 0 & 0 & 0 & 0 & 0 & 0 & 0 \\ 0 & 0 & 0 & 0 & 0 & 0 & 0 \\ 0 & 0 & 0 & 0 & 0 & 0 & 0 \\ 0 & 0 & 0 & 0 & 0 & 0 & 0 \\ 0 & 0 & 0 & 0 & S_2 & 0 & 0 \\ 0 & 0 & 0 & 0 & 0 & S_3 & 0 \\ 0 & 0 & 0 & 0 & 0 & 0 & S_4 \end{bmatrix} \tag{45}$$

where:

S_2: A 2x2 sub matrix with rank 1.

S_3: A 7x7 sub matrix with rank 3.

S_4: A 8x8 sub matrix with rank 4.

As can be seen from (45), for the active sub problem, this measurement set contains the following:

1) Critical subset 1: 4 critical measurements, injections at 4,9,11 and flow 4-7. They correspond to the first four rows of S_a in (45).
2) Subset 2: Critical pair including injection 8 and flow 7-8, which correspond to the sub matrix S_2 in (45).
3) Subset 3: Residual spread component [48] containing 7 measurements, injections at 12,13,14 and flows 6-12,9-14, 12-13, 13-14. Any four of these seven measurements form a critical 4-tuple. They correspond to the sub matrix S_3 in (45).
4) Subset 4: Remaining 8 measurements. Any five of them form a critical 5-tuple. They correspond to the sub matrix S_4 in (45).

Errors having a Normal distribution with zero mean and *0.004* variance are introduced for voltage magnitude measurements and *0.01* variance for all the power measurements. The calibration results for the power injection and flow measurements

differ from those for the voltage magnitude measurements. The simulation results for both cases will be given and discussed separately in the following sections.

4.5.1 Multiple Bad Data in Power Injection/Flow Measurements

The first simulation is done for the calibration of multiple biased power injection and power flow measurements. The quadratic model shown in (35) is used for all the measurements. The following three measurements are simulated as non-calibrated measurements using quadratic calibration models with the given parameters:

- Active power injection on bus 3 ($a = 0.2; b = 1.1; c = 0.3$).
- Active power injection on bus 14 ($a = 0.0; b = 1.1; c = -0.1$).
- Active power flow on branch 3-4($a = 0.0; b = 1.1; c = -0.2$).

Based on the basic network data of IEEE 14 bus system and random load configurations, 11 scans of measurements have been created using the biased parameters. The first 10 scans will be using to implement the calibration process while the last one is used to identify the suspected measurement set and validate the calibration results.

With the uncalibrated data, the bad data analysis after state estimation produces following result:

Significant Normalized Residuals:
Measure NO= 14, PFlow 3- 4, Residual= -42.2932
Measure NO= 3, PInj at bus 3, Residual= 42.1550
Measure NO= 2, PInj at bus 2, Residual= 13.4985
Measure NO= 15, PFlow 4- 5, Residual= -9.5462
Measure NO= 10, PInj at bus 14, Residual= -6.9224
Measure NO= 19, PFlow 9- 14, Residual= -6.7008
Measure NO= 21, PFlow 13- 14, Residual= -6.1886
Measure NO= 24, QInj at bus 3, Residual= 4.5719
Measure NO= 23, QInj at bus 2, Residual= 4.0073
Measure NO= 1, PInj at bus 1, Residual= 3.0001

Here 3.0 is used as a threshold. The measurement set chosen for the first calibration process includes the top three measurements in the list: active power injections at buses 2,3 and active power flows on branches 3-4. The parameters of their calibration functions are estimated along with the system state variables using the first 10 scans. It takes 6 iterations to converge to a tolerance of 10^{-5}.

After the first calibration process, state estimation program is rerun using the calibrated measurement value for 11^{th} scans. The bad data analysis produces three more bad data:

Significant Normalized Residuals:
Measure NO= 10, PInj at bus 14, Residual= -6.9047
Measure NO= 19, PFlow 9- 14, Residual= -6.7334
Measure NO= 21, PFlow 13- 14, Residual= -6.1747

The list only contains three measurements and there are all different form the measurements which have been calibrated in the previous process. Since we still have bad data identified, the second calibration process is run. Notes here that the calibrated measurement value will be used for those measurements that already calibrated in the first process.

The state estimation following the second calibration process does not identify any bad data. This means the calibration process is complete and valid.

Table XI shows the estimated system states at the 11^{th} scan. The proposed method's results are comparatively displayed with those provided by the conventional WLS method without any measurement calibration as well as the true values of the states. The corresponding values of the objective functions are also given in the last row.

The estimated coefficients for these measurements haven been calibrated are shown in Table XII along with the measured, estimated and calibrated values of the measurements corresponding to the 11^{th} measurement scan. Since we use quadratic model shown in (35) in this case, there may be two calibrated values for each measurement. However, the calibrated values shown in Table XII are calculated by (40). The identification process always pick solutions (40) as correct one during our simulation. For example, the value of (43) for calibrated values of active power injection in bus 3 given by (40) is 3.4×10^{-5} while for (41) is 4562.35.

TABLE XI
ESTIMATED SYSTEM STATES

Bus No.	***WLS Method Without Calibration***		***Proposed Method***		***True Value***	
	|V|	**Ang.**	**|V|**	**Ang.**	**|V|**	**Ang.**
1	1.0568	*0.00*	1.0598	*0.00*	1.0600	*0.00*
2	1.0426	*-6.99*	1.0446	*-7.04*	1.0450	*-7.05*
3	1.0139	*-16.34*	1.0078	*-17.82*	1.0100	*-17.73*
4	1.0134	*-14.16*	1.0173	*-14.05*	1.0173	*-14.04*
5	1.0143	*-11.91*	1.0186	*-11.78*	1.0182	*-11.74*
6	1.0822	*-21.24*	1.0716	*-17.04*	1.0700	*-17.02*
7	1.0722	*-16.39*	1.0767	*-16.28*	1.0763	*-16.26*
8	1.0875	*-16.26*	1.0920	*-16.14*	1.0900	*-16.26*
9	1.0917	*-21.81*	1.0872	*-17.17*	1.0873	*-17.38*
10	1.0731	*-25.94*	1.0806	*-17.11*	1.0801	*-17.49*
11	1.0738	*-23.82*	1.0744	*-17.26*	1.0724	*-17.51*
12	1.0623	*-22.54*	1.0525	*-18.25*	1.0535	*-18.16*
13	1.0623	*-22.57*	1.0544	*-18.16*	1.0538	*-18.22*
14	1.0528	*-24.60*	1.0536	*-19.32*	1.0525	*-19.58*
Cost	2332.096		15.310		*N/A*	

TABLE XII
SIMULATION RESULTS FOR OBSERVABLE CASE

Meas.NO.		*Inj2*	*Inj3*	*Inj14*	*PFlow3-4*	*PFlow9-14*	*PFlow13-14*
Coeff.	*a*	0.024	0.184	-0.015	-0.030	-0.003	0.007
	b	0.999	1.079	1.122	1.082	0.984	0.995
	c	-0.004	0.290	-0.116	-0.190	0.004	0.006
Measured		0.122	-0.785	-0.383	-0.589	0.182	0.056
Estimated		0.132	-1.299	-0.233	-0.356	0.184	0.053
Calibrated		0.126	-1.273	-0.237	-0.365	0.181	0.050

The simulation results clearly favor the proposed method as evident from the close match between the true and estimated states when calibration is employed. Furthermore, for all of the three measurements with bad calibration, the estimated parameters of the calibration model are very close to the true values used in generating the simulation data. Naturally, in an actual system, the true form of the calibration model will not be known and the chosen model structure may not result in such a good match. However, since the measuring instruments are not replaced frequently, it is assumed that the correct calibration model for individual measurements can be found based on a reasonably long operating history.

In order to test different calibration models, some simulations are also carried out for the linear model shown in (44). Similar performance of the method is observed as those shown in Table XI and Table XII. In the case of the linear model, the proposed calibration method requires fewer scans and iterations to yield results of similar quality. Moreover, utilizing the linear model avoids the multiple solutions' problem. In practical implementation, in order to save computation time, most of the measurements can utilize the linear model. Quadratic model can be used on selected measurements whose characteristics show strong nonlinear behavior due to effects such as saturation, temperature dependence, etc.

4.5.2 Simulation Results for Wrong Calibration Function

Sometime the specified calibration functions may not be suitable for the measurements. This can be identified by the verification process. Assume the active power injection 3 is contaminated by (35) and the parameters are: $a = 0.2; b = 1.1; c = 0.3$.

Similar to the simulation procedure in the previous section, 11 scans are generated. Before the calibration process, the bad data analysis for the last scan is:

Significant Normalized Residuals:
Measure NO= 3, PInj at bus 3, Residual= 19.2952
Measure NO= 14, PFlow 3- 4, Residual= -17.1255
Measure NO= 2, PInj at bus 2, Residual= 10.6760
Measure NO= 15, PFlow 4- 5, Residual= -5.5081
Measure NO= 13, PFlow 2- 4, Residual= -3.5293
Measure NO= 23, QInj at bus 2, Residual= 3.2169

The first three measurements will be selected into suspected set. In the first calibration process, we assume the errors are only offsets. So only parameters *c* in (35) will be estimated.

After this calibration process, the bad data analysis for the last scan produces:

Significant Normalized Residuals:
Measure NO= 3, PInj at bus 3, Residual= -12.9601
Measure NO= 14, PFlow 3- 4, Residual= 11.6389
Measure NO= 2, PInj at bus 2, Residual= -5.8281
Measure NO= 44, Voltage at bus 3, Residual= 3.1934

Measure NO= 15, PFlow 4- 5, Residual= 3.0292

It can be seen that the top three measurements are those which have been calibrated. This means wrong calibration functions are used. Replace the calibration function with a linear function as (44). This time, *b* and *c* are both taken into account.

However, even after this calibration process, bad data are still identified:

Significant Normalized Residuals:
Measure NO= 3, PInj at bus 3, Residual= -15.3400
Measure NO= 14, PFlow 3- 4, Residual= 14.1366
Measure NO= 2, PInj at bus 2, Residual= -7.8779
Measure NO= 15, PFlow 4- 5, Residual= 3.6753
Measure NO= 11, PFlow 1- 2, Residual= -3.1420

The first three measurements are still the same. Finally, we use (35) as the calibration function. After the third calibration process, no bad data is identified and the calibration results are:

MeasureNO=3, Pinj at bus3,a=0.1974,b=1.0795,c= 0.2680
MeasureNO=14,Pflow3-4, a=-0.0089,b=0.9764,c=-0.0175
MeasureNO=2,PInj at bus2,a=0.0254,b=1.0320,c= 0.0142

The estimated parameters are close to their theoretical values.

4.5.3 Calibration of Voltage Magnitude Measurement

There are differences between the voltage magnitude measurements and others when applying the proposed method. In the per unit system, the voltage magnitudes vary only in a rather small region and they usually remain very close to 1. Utilizing of a quadratic model as (35) or a linear model as (44) may easily lead to multiple solutions of the parameters. This can be shown by a simple example. Assuming a linear model as (44) with a non-calibrated voltage magnitude measurement at bus 1 ($\bar{z} = 1.0 \cdot z + 0.2$), the estimated parameters *b* and *c* by the proposed method will be $\bar{b} = 1.5556; \bar{c} = -0.3867$. Even though these results do not match the parameters of the true (assumed) calibration model, since the true voltage magnitudes of bus 1 are very close to 1.06 in all of the snapshots, the calibrated values will still be very close to the true ones. This can be seen from the results shown in Table XIII. In this case, the parameter *b* can be fixed, simplifying it down to a single estimated bias parameter *c*.

TABLE XIII
SIMULATION RESULTS FOR VOLTAGE MAGNITUDE MEASUREMENTS

Snapshot NO.	*1*	*2*	*3*	*4*	*5*
Measured	1.2547	1.2631	1.2649	1.2555	1.2652
Estimated	1.0568	1.0606	1.0607	1.0571	1.0600
Calibrated	1.0552	1.0606	1.0617	1.0557	1.0620

4.5.4 Introduction of Pseudo-Parameter-Measurements

As suggested in section 4.4, the pseudo-parameter-measurements can be introduced to solve the numerical problem. However, the weights of these measurements will have great influence in the results. The behavior of calibration procedure under different weight settings for these pseudo-parameter-measurements is studied.

For convenience, here we take the linear model as shown in (44) instead of the quadratic model. Assume we have three bad measurements:

- Active power injection on bus 1 ($b = 1.1; c = 0.1$).
- Active power injection on bus 2 ($b = 1.2; c = 0.2$).
- Active power injection on bus 3 ($b = 1.3; c = 0.3$).

TABLE XIV
INFLUENCES OF WEIGHTS FOR PSEUDO-MEASUREMENT

Meas.NO.		*PInj1*	*PInj2*	*PInj3*	***Cost***
10^4	*b*	1.0997	1.0057	1.1862	1355.397
	c	0.0901	0.1682	0.1738	
10^3	*b*	1.1013	1.0527	1.2844	273.949
	c	0.1018	0.2105	0.2849	
10^2	*b*	1.1024	1.1904	1.3002	211.478
	c	0.1011	0.2073	0.3045	
10	*b*	1.1021	1.2695	1.3026	208.788
	c	0.1016	0.2036	0.3071	
1	*b*	1.1021	1.2832	1.3030	208.738
	c	0.1017	0.2030	0.3075	
*No**	*b*	1.1021	1.2849	1.3030	208.738
	c	0.1017	0.2029	0.3075	

**: This means do not introduce pseudo-parameter-measures*

The suspicious measurement set only includes the bad measurements. The pseudo-parameter-measurements are introduced for all the coefficients. They are weighted by different values shown in the first column of Table XIV. And their values are set as "flat start" (*b=1;c=0*), which is obviously wrong. The weights for all other measurements will be set to 10^4. The estimated coefficients and the values of objective functions under different weights setting are shown in Table XIV.

By comparing the estimated coefficients and the values of the objective functions, we can see that if the weights of the pseudo-measurements are set to 1/100 of the normal measurements, the result is pretty close to the result without those pseudo-measurements. This weight setting also avoids ill conditioning of the matrix. In the following simulation, when the pseudo-parameter-measurements are used, their weights will be set as 1/100 of other measurements.

4.5.5 Critical Measurements/Critical K-Tuple of Measurements

As mentioned in section 4.4, the proposed calibration technique has some limitation when there are critical measurements or critical *k-tuple* of measurements. Including the coefficients of the critical measurements or all the critical *k-tuple* of measurements will result in an ill-conditioned gain matrix without pseudo-parameter-measurement. The introduction of pseudo-parameter-measurement can solve the numerical problem. The coefficients of relationship functions for all the measurements can always be estimated. However, since the pseudo-parameter-measurement cannot increase the redundancy level, those "estimated" coefficients for critical measurements or critical *k-tuple* of measurements may be biased.

1) Critical measurements.

For critical measurements, the calibration procedure can only yield trivial results. The estimated coefficients are always very close to zeros. The detailed simulation results are ignored here.

2) Critical k-tuple of measurements.

If systematic errors only exist in *k-2* measurements in a Critical *k-tuple* of measurements, they can be calibrated correctly. The simulation results are similar to Table XII and will be ignored here.

A simple case is created to test the behavior for *k-1* systematic errors. The *Subset 2* of system shown in Fig. 16 contains a critical pair. Assume there is error in active power injection 8 ($\bar{z} = 1.2 \cdot z + 0.2$), we have:

- If the suspicious measurement set only contains this measurement, the estimated coefficients are: $\bar{b} = 1.1956; \bar{c} = 0.2034$.
- If the suspicious measurement set contains both measurements, the estimated coefficients are: $\bar{b}_1 = 1.1248; \bar{c}_1 = 0.1124; \bar{b}_2 = 1.0804; \bar{c}_2 = 0.0965$.

These results confirm the argument of *rule 2*. Actually, the systematic error in this case is not identifiable. We can get correct answer for the first case just because we happen to have the correct suspect measurement identification.

Assume there are errors in both measurements ($\bar{z}_1 = 1.1 \cdot z_1 + 0.1; \bar{z}_2 = 1.2 \cdot z_2 + 0.2$), we have:

- If the suspicious measurement set only contains injection 8, the estimated coefficients are: $\bar{b} = 1.3043; \bar{c} = 0.2956$.
- If the suspicious measurement set contains both measurements, the estimated coefficients are: $\bar{b}_1 = 1.1587; \bar{c}_1 = 0.1724; \bar{b}_2 = 1.1404; \bar{c}_2 = 0.1302$.

No matter what the suspicious set is, we cannot get the calibration coefficients for individual measurement correctly. The estimated results always show an "average" property.

From the simulation results, we can see that if the number of error measurement is not less than *k-1* within a critical *k-tuple* of measurement, the calibration results may be biased for single measurement. However, generally they can eliminate the systematic error to a great degree due to the "average" property. If no other calibration technique is available under these circumstances, the proposed remote calibration procedure still can help to improve the performance of state estimator.

3) The influence of voltage magnitude measurement.

Above observability analysis do not consider the voltage magnitude measurements. In fact, the existences of voltage magnitude measurements will not influence the calibration redundancy for active power measurements. However, they will increase the redundancy for reactive power measurements. In the system shown in Fig. 16, injection on bus 4 is

critical measurement. Since there is voltage magnitude measurement on bus 4, the systematic error in reactive part can be calibrated by proposed method. The voltage magnitude measurements will also increase the calibration redundancy of the reactive measurements of the critical *k-tuple* of measurements.

4.6 Conclusions

Elimination of systematic calibration errors in telemetered quantities is labor intensive and costly, if it is done at the metering site. This chapter describes an alternative remote measurement calibration approach by which calibration of measurements are done as part of the state estimation. The measured values are related to the true values by some assumed calibration functions. The details of incorporating these calibration function parameters into the normal state estimation problem are presented. The parameters will be estimated along with the system states and used to calibrate the corresponding measurements. The method can be implemented off-line using several subsequent measurement scans together to increase redundancy. It is tested on different size IEEE systems. The simulation results show that this calibration procedure can improve the performance of state estimation when there are badly calibrated measurements.

CHAPTER V

AUTO TUNING OF MEASUREMENT WEIGHT

5.1 Introduction

Measurements that are telemetered to the control center to be processed by the power system state estimator usually contain a combination of systematic and random errors. The systematic errors in the measurements can possibly be eliminated by using appropriate calibration methods [38]-[44] while the random errors will always remain and will influence the accuracy of estimated state.

The weighted least squares estimators assume a set of measurement error variances whose reciprocals are commonly chosen as the weights for the measurements. These same weights also influence the commonly employed bad data detection and identification procedures which are based on the normalized residuals. Choice of these weights is therefore an important consideration for state estimators. Furthermore, once chosen, the weights need to be continuously updated since they vary with operating conditions and aging of the instruments. Hence, this requires adaptively adjustment of measurement weights.

The measurement weights are typically assigned based on some assumed accuracy of the measuring instruments and they may be further adjusted to tune the residual based error detection tests. While these approaches may work for most systems, it is felt that they can be further improved via a tuning procedure which further reduces the degree of user intervention. Few papers [34]-[37] have so far addressed this issue. Reference [34] presents a general formulation of the parameter estimation problem and suggests that the standard deviation of measurement can also be treated as an unknown parameter; however no further details or simulation results are provided. Reference [35]-[36] uses a set of so-called test equations which include regular measurement equations as well as some consistency relations. The residuals of the test equations are then used to identify the measurement variances via the use of artificial neural networks

A novel algorithm to estimate and adaptively update measurement variances is proposed in [37]. The measurement error variances are estimated based on their

calculated residuals corresponding to several past measurement scans. The sensitivity relationship between the measurement variances and the covariance matrix of their residuals is used for this purpose. However, this method can be further improved to address the following shortcomings:

1. It requires the calculation of all the elements in the sensitivity matrix. This is computationally very expensive especially for large systems.
2. Its initialization phase is successful provided that the range of measurement variances is confined to a small region.
3. It assumes that the redundancy of the measurement set is high enough to make the Schur product (M) of the sensitivity matrix nonsingular, which is not always true. M is used for estimating measurement error variances.

In this chapter, an alternative and simpler method which avoids the above listed shortcomings is proposed and comparatively discussed with the algorithm presented in [37]. Both methods make the following two assumptions:

1. The correct network topology and parameters are known.
2. Large systematical errors have been eliminated by appropriate calibration. The measurement errors only consist of Gaussian random errors. This can be ensured by disregarding those measurement scans with identified bad data.

Initially, it is assumed that no information is available on the variances of the measurements. An off-line procedure, which is executed only for initialization purposes, is proposed. Subsequently, a recursive updating procedure which is computationally more efficient and therefore suitable for on-line implementation to update the variances is presented. It is also realized that the capability of estimating variances of the available measurements depends on the measurement configuration and types. Limitations imposed by the existing measurement structure and identification of cases for which variance estimation can not be carried out are also presented.

5.2 Problem Formulation

From the description of WLS method in chapter II, the residuals of measurements can be represented by the product of a sensitivity matrix and the measurements' vector.

$$r = S \cdot z \tag{46}$$

Covariance matrix (R_r) of measurement residual *r* can be expressed in terms of the covariance matrix (R_z) of the measurement errors as:

$$R_r = S \cdot R_z \cdot S^T \tag{47}$$

A statistically sampled covariance matrix for R_r can be calculated given enough set of historical data. Also note that, the rank of the S matrix in (47) is at most (*m-n*) making it a singular matrix [4]. Hence, given the matrix R_r, (47) cannot be directly solved to find R_z. However, using the assumption that random errors of individual measurements are not correlated, the covariance matrix R_z can be assumed to be strictly a diagonal matrix. In that case, the diagonal elements of R_z and R_r can be related by manipulating (47) and used to estimate the diagonal elements of R_z. Two alternative procedures are developed for this purpose.

5.2.1 Overview of Method 1 [37]

Let $\vec{R}_z$ be an array containing the diagonal entries of R_z which is assumed to be diagonal. Similarly define $\vec{R}_r$ to be an array containing the diagonal elements of R_r. Note that these diagonal elements are used in normalized residual test for identifying bad data. $\vec{R}_r$ can be expressed in terms of $\vec{R}_z$ by manipulating (47) as follows:

$$\begin{bmatrix} \vec{R}_{r1} \\ \vec{R}_{r2} \\ \vdots \\ \vec{R}_{rm} \end{bmatrix} = \begin{bmatrix} S_{11}^2 & S_{12}^2 & \cdots & S_{1m}^2 \\ S_{21}^2 & S_{22}^2 & \cdots & S_{2m}^2 \\ \vdots & \vdots & \ddots & \vdots \\ S_{m1}^2 & S_{m2}^2 & \cdots & S_{mm}^2 \end{bmatrix} \begin{bmatrix} \vec{R}_{z1} \\ \vec{R}_{z2} \\ \vdots \\ \vec{R}_{zm} \end{bmatrix} \Rightarrow \vec{R}_r = M\vec{R}_z \tag{48}$$

where:

$M = \begin{bmatrix} S_{11}^2 & S_{12}^2 & \cdots & S_{1m}^2 \\ S_{21}^2 & S_{22}^2 & \cdots & S_{2m}^2 \\ \vdots & \vdots & \ddots & \vdots \\ S_{m1}^2 & S_{m2}^2 & \cdots & S_{mm}^2 \end{bmatrix}$, is the Schur product of the S matrix and itself.

$\vec{R}_{ri}, i = 1..m$: The i^{th} element of vector $\vec{R}_r$.

$\vec{R}_{zi}, i = 1..m$: The i^{th} element of vector $\vec{R}_z$.

Matrix M will be non-singular provided that certain redundancy requirements, which will be elaborated on later, are met. In (48), $\vec{R}_r$ will be approximated as the sample variances of the residuals computed based on a set of historical state estimation runs. The measurement error variances may thus be estimated by solving (48) for R_z. It is noted that this will also only be a good approximation for the true measurement variance vector. The true value of R_z can not possibly be found due to the singularity of matrix S in (47).

It is further observed that the residual vector in (48) is comparably small making the numerical solution non-robust. This problem is overcome through scaling (48) as follows:

$$r^w = S^w z^w \tag{49}$$

where:

$r^w = W^{1/2} \cdot r$ is the weighted residual vector;

$S^w = W^{1/2} \cdot S \cdot W^{-1/2}$ is the weighted sensitive matrix;

$z^w = W^{1/2} z$ is the weighted residual measurement vector;

Correspondingly, equation (47) can be rewritten as:

$$R_r^w = S^w R_z^w (S^w)^T \tag{50}$$

where:

R_r^w, R_z^w : are the covariance matrix of weighted residual vector and weighted measurement vector respectively.

Thus the weighted form of (48) is obtained as:

$$\vec{R}_r^w = M^w \vec{R}_z^w \tag{51}$$

where:

M^w: The weighted form of matrix M .

Once $\vec{R}_z^w$ is calculated by solving (51), R_z can be recovered by the inverse transformation as:

$$\vec{R}_z = W^{-1/2} \vec{R}_z^w \tag{52}$$

5.2.2 Proposed Alternative Method (Method 2)

The formulation given above contains all elements of sensitivity matrix S. The calculation of this matrix is very time-consuming. An alternative formulation is proposed to avoid this extra computation burden.

If the weight vector used in the state estimation is the inverse of the random error variances vector ($W = R_z^{-1}$), equation (47) can be simplified as [2]:

$$R_r = S \cdot R_z \cdot S^T = S \cdot R_z \tag{53}$$

Thus, the diagonal elements will simply be related as:

$$\vec{R}_{zi} = \vec{R}_{ri} / S_{ii} \tag{54}$$

.

In this formulation, only the diagonal elements of S are needed and they are typically available from the bad data processing function, which utilizes the normalized residual test.

It can be seen from (48) and (54) that only the diagonal elements of the covariance matrix are needed for both formulations. Hence, the variances of the residuals of individual measurements are estimated by computing their sample variances corresponding to a set of historical data. The system model and the measurement variances are assumed to be constant during the given period. In order to make (48) or (50) valid, S matrix and the weight vector W must be the same for all those snapshots. Even though the system state continuously varies during the computation period, the fast decoupled state estimation method is used to approximate a constant S matrix. It is observed that S is not too sensitive to changes in the states but is affected significantly by changes in network topology.

5.3 Iterative Initialization Procedure

The proposed method requires the state estimation results for several past time steps. When there is no prior information about the measurement error variances, the method will have to initialize the weights. This is accomplished via the below given iterative procedure which starts with an arbitrarily assumed set of weights:

1) Save k time samples of the system measurements. Those snapshots should be taken reasonably close to each other to ensure steady random error variances for all the measurements. The system topology must also remain unchanged;
2) Initialize the weight vector. If no prior information is available, use a value of 1.0 for all measurements;
3) Run WLS state estimator using the same weight vector for all of those k snapshots. Compute the time series for each measurement residual and their sample variances;
4) Use *method 1* or *method 2* to estimate the random error variances for all the measurements;
5) Update the weights using the reciprocals of the estimated random error variances. Compute the maximum absolute deviation in the weights with respect to the previous iteration. Go to step 3 and continue with iterations until the computed maximum deviation falls below a chosen threshold or the iteration limit is reached.

Simulation results indicate that the convergence of the above iterative procedure remains sensitive to the number of snapshots up to a certain minimum number after which it is not improved significantly with an increase in the sample size. This minimum number is independent of the system size; hence once it is determined it can be used for any system. Some simulation results on this iterative procedure will be presented in later section.

5.4 Recursive Updating Procedure

The above described initialization procedure will yield a set of estimated measurement error variances, which are subsequently used to compute the measurement weights. However, the measurement error variances are known to vary in time due to various external factors as well as the deterioration of equipment. Correspondingly, in order to follow the changes in the variance, the weight vectors also need to be updated frequently. Although the initialization process can be used to re-estimate the variance once a change is detected, it cannot be easily executed as frequently as required due to its heavy computational requirements. It is observed that having initial values close to the true values for the majority of the measurement variances greatly reduces the iteration count for the estimation procedure described in section 5.2 to converge. Hence, a

recursive updating procedure, which can be easily integrated into the conventional state estimator without significantly increasing the computational burden, is designed to solve this problem. The steps of this updating procedure are as follows:

1) Choose the weight vector using the reciprocals of the estimated error variances obtained from the iterative initialization process;
2) Choose an updating window size, *k*. It can be chosen as the number of snapshots used in the initialization process or any other number. Initialize the counter ($i = 0$);
3) Run the conventional WLS state estimator using the current weight vector. Record the residuals for all the measurements. Increment the counter by 1 ($i = i + 1$);
4) If the number of snapshots included in the recorded set is equal to *k* ($i = k$), go to step 5. Else, check if the system topology is changed. If yes, go to step 2. Otherwise go to step 3;
5) Calculate the sample variances of residuals for *k* snapshots;
6) Use *method 1* or *method 2* to estimate the random error variances for all the measurements;
7) Compare the newly estimated variances and the current used one. If the different is significant enough (satisfies specified criterion) or the system topology is changed, update the current weight vector corresponding to the new estimation, trigger next updating process by going to step 2. Otherwise, continue.
8) Run state estimator for the next snapshot. Replace the 1st residual vector in the recorded list by this one. Go to step 5.

The only extra computation in the above given recursive updating procedure is the calculation of the sample variances for measurement residuals and the solution of (51) for *method 1* or (54) for *method 2*.

It should also be noted that the procedure needs to be re-initialized each time a topology change is detected as indicated in step 4. Any topology change will result in a change of the S matrix. As long as the system topology remains constant, the weight vector used in state estimator will be updated automatically every *k* snapshots. In addition, detection of variances' change means the current S matrix doesn't fit the real condition

thus it will also trigger a new updating process. The changes of variances can be detected by checking whether the differences of the new estimation and currently used estimation satisfies specified criterion. We will discuss the selection of this criterion along with the simulation results later.

5.5 Observability Problem

The proposed procedure will require sufficiently high measurement redundancy for successful estimation of all measurement variances. It will encounter observability problems mainly under the following conditions:

- Existence of critical measurements. If there are critical measurements, the corresponding rows and columns in S will all be zero.
- Existence of critical *k-tuples* [48]. The rows and columns of S corresponding to these measurements will be linearly dependent.

In the following sections, we will discuss the influences of these situations on the estimation results of *method 1* and *method 2*, respectively.

5.5.1 Observability Analysis for Method 1

The variances of critical measurements can simply not be estimated by this method because the zero rows and columns in S will result in zero rows and columns in M. However, there is practically no need to estimate the variance of a critical measurement since the weight of the critical measurement will have no influence on the state estimation result. Some arbitrary values can be assigned as weights for the critical measurements to avoid ill-conditioning of the matrix during the state estimation process.

On the other hand, there is a chance for M to be singular when there is a critical *k-tuple*. In such a case, equation (48) or (51) cannot be directly solved. The algorithm shown in section II can be slightly modified to account for such cases with singular M. The original formulation of (48) will be used instead of the weighted formulation (51) for simplicity of notation.

Consider equation (48) where M is a $m \times m$ singular matrix with rank l ($m>l$). Furthermore, define a full-rank sub-matrix of matrix M consisting of l rows and l columns as M'. Those l elements in vector $\overline{R}_z$ which correspond to these l columns can be estimated by:

$$\vec{R}'_z = [M(S)']^{-1} \cdot \vec{R}'_r \tag{55}$$

where:

$\vec{R}'_z$ is a subset of vector $\overline{R}_z$ corresponding to l columns in $M(S)'$;

$\vec{R}'_r$ is a subset of vector $\overline{R}_r$ corresponding to l rows in $M(S)'$.

The sub-matrix M' of rank l can be easily identified via the triangular factorization of M with pivoting.

For those measurements whose variances cannot be estimated, we can use the initial values, if they exist, or the average of variances of other measurements belong to the same residual error spread area [49]. The simulation result shows that even under this circumstance, we still can get a good estimation of most of the measurements.

The fact that there are pseudo-measurements, such as zero-injection measurements, can be exploited to improve the estimation procedure for the remaining measurement variances. These zero injections are considered as perfect measurements thus their variances need not be estimated. They can be excluded at the outset from the variance estimation procedure.

5.5.2 Observability Analysis for Method 2

Variances of critical measurements cannot be estimated because the zero values in the denominator in (54). Hence, this case is handled the same as done in *method 1*.

For critical *k-tuples*, no further problems are encountered since the corresponding denominators in (54) will be nonzero, their variances can be estimated. However, these values will not individually reflect true variances, due to the linear dependencies existing between these measurements.

It can be seen that compared to *method 1*, the handling of low redundancy situation is quite simple. It only needs to identify the critical measurements, which has been done automatically during the calculation of the diagonal elements of S matrix.

5.6 Simulation Result

5.6.1 Simulation Results of the Initialization Process

The initialization procedure is tested using simulated measurements on different size IEEE systems. The results of initialization obtained after 6 iterations for the IEEE 14 bus system are shown in Table XV. Simulation parameters for this case are as follows:

Bus number: 14

Number of snapshots: 200

Tolerance to converge: 10^{-4}

Measurement Setting: Fully measured

Load Setting: Slow Changing

Method: Method 1

Standard Deviation Setting:

Voltage: 0.004, except bus3,8 (0.080) and bus5,9 (0.001);

Injection: 0.01, except bus4 (0.05) and bus 7,10 (0.001);

Flow: 0.008, except branch3,5,9 (0.1) and branch 10 (0.001);

In the above list, "Fully measured" means that a voltage magnitude measurement and a power injection measurement is assigned to every bus. Also, every branch is assigned a power flow measurement at one end.

In order to generate realistic simulation data, bus loads are varied by treating them as random variables distributed according to a Normal distribution *N(Mean, STD)*. The values in the base case are chosen as means. Using different standard deviations, the load settings in the simulations are divided into "slow changing" and "fast changing" categories with 1% and 100% of the mean value specified as the STD respectively.

In Table XV, the first two columns indicate the type of measurement and its location. The third column shows the measurement standard deviations used when generating simulation data. Although only one standard deviation value is used for both active and reactive parts of the same measurement, two different estimation results are obtained due to the use of fast-decoupled algorithm. Column 4 and 5 show the estimation results for the active and reactive measurements, respectively. Note that, column 5 is also used to show the results for voltage measurements after the flow measurements.

TABLE XV
SIMULATION RESULT FOR INITIALIZATION PROCESS (METHOD 1)

Type	*NO.*	$\sqrt{R_Z}$	*Comp* $\sqrt{R_a}$	*Comp* $\sqrt{R_r}$
Injection	1	0.010	0.0098	0.0109
Injection	2	0.010	0.0079	0.0086
Injection	3	0.010	0.0101	0.0125
Injection	4	0.050	0.0521	0.0501
Injection	5	0.010	0.0105	0.0088
Injection	6	0.010	0.0104	0.0108
Injection	7	0.001	0.0014	0.0023
Injection	8	0.010	0.0104	0.0104
Injection	9	0.010	0.0079	0.0115
Injection	10	0.001	0.0030	0.0050
Injection	11	0.010	0.0091	0.0101
Injection	12	0.010	0.0112	0.0087
Injection	13	0.010	0.0090	0.0097
Injection	14	0.010	0.0087	0.0102
Flow	1-2	0.008	0.0089	0.0069
Flow	1-5	0.008	0.0092	0.0079
Flow	2-3	0.100	0.1066	0.1000
Flow	2-4	0.008	0.0083	0.0080
Flow	2-5	0.100	0.1012	0.0984
Flow	3-4	0.008	0.0079	0.0074
Flow	4-5	0.008	0.0067	0.0077
Flow	4-7	0.008	0.0074	0.0083
Flow	4-9	0.100	0.1017	0.0942
Flow	5-6	0.001	0.0032	0.0019
Flow	6-11	0.008	0.0080	0.0086
Flow	6-12	0.008	0.0068	0.0085
Flow	6-13	0.008	0.0081	0.0079
Flow	7-8	0.008	0.0078	0.0085
Flow	7-9	0.008	0.0083	0.0081
Flow	9-10	0.008	0.0077	0.0071
Flow	9-14	0.008	0.0072	0.0074
Flow	10-11	0.008	0.0087	0.0085
Flow	12-13	0.008	0.0080	0.0074
Flow	13-14	0.008	0.0083	0.0078
Voltage	1	0.004		0.0038
Voltage	2	0.004		0.0042
Voltage	3	0.080		0.0853
Voltage	4	0.004		0.0038
Voltage	5	0.001		0.0009
Voltage	6	0.004		0.0039
Voltage	7	0.004		0.0039
Voltage	8	0.080		0.0820
Voltage	9	0.001		0.0010
Voltage	10	0.004		0.0038
Voltage	11	0.004		0.0035
Voltage	12	0.004		0.0039
Voltage	13	0.004		0.0040
Voltage	14	0.004		0.0041

While the simulated weights for most of the same types of measurements are chosen to be the same, for few measurements these weights are intentionally simulated as different. For instance, injection at bus 7, flow 2-4, flow 1-5, voltage at 5, etc. are assumed to have much smaller errors compared to the remaining measurements. As evident from Table XV, the proposed estimation procedure can closely track the simulated weights, differentiating between the more and less accurate measurements.

In addition, from Table XV we can draw the following conclusions for the estimation of variances.

1) For those measurements have normal variances, the estimations are very good.
2) For those measurements have relatively low accuracy, the estimations are also very good.
3) For those measurements have relatively high accuracy, the performances are different for different kinds of measurement.
   A. For voltage magnitude measurements, the estimation is pretty close to the true value.
   B. For power injection and power flow measurements, some of them are not very close to the true value. However, the estimated variances of them are relatively smaller than the average values.

Similar results are obtained for all the other larger size systems and these results are not shown here due to space limitations. The number of iterations required for different size test systems remains insensitive to system size as shown in Table XVI.

TABLE XVI
NUMBER OF ITERATIONS FOR DIFFERENT SYSTEM SIZES

Number of Buses	14	30	57	118
Iterations Needed	6	8	8	6

Since only the diagonal elements (the variances of individual measurement residuals) in the covariance matrix of residuals are used in this method, it is expected that the number of required snapshots for a given accuracy will not increase with increasing system size.

TABLE XVII
SIMULATION RESULT FOR INITIALIZATION PROCESS (METHOD 2)

Type	NO.	$\sqrt{R_Z}$	Method 2		Method 1	
			Comp $\sqrt{R_a}$	Comp $\sqrt{R_r}$	Comp $\sqrt{R_a}$	Comp $\sqrt{R_r}$
Injection	1	0.010	0.0102	0.0112	0.0098	0.0109
Injection	2	0.010	0.0088	0.0093	0.0079	0.0086
Injection	3	0.010	0.0102	0.0123	0.0101	0.0125
Injection	4	0.050	0.0521	0.0481	0.0521	0.0501
Injection	5	0.010	0.0076	0.0086	0.0105	0.0088
Injection	6	0.010	0.0092	0.0105	0.0104	0.0108
Injection	7	0.001	0.0045	0.0035	0.0014	0.0023
Injection	8	0.010	0.0104	0.0103	0.0104	0.0104
Injection	9	0.010	0.0085	0.0122	0.0079	0.0115
Injection	10	0.001	0.0043	0.0049	0.0030	0.0050
Injection	11	0.010	0.0091	0.0101	0.0091	0.0101
Injection	12	0.010	0.0112	0.0089	0.0112	0.0087
Injection	13	0.010	0.0089	0.0100	0.0090	0.0097
Injection	14	0.010	0.0088	0.0109	0.0087	0.0102
Flow	1-2	0.008	0.0087	0.0065	0.0089	0.0069
Flow	1-5	0.008	0.0092	0.0082	0.0092	0.0079
Flow	2-3	0.100	0.1065	0.0967	0.1066	0.1000
Flow	2-4	0.008	0.0082	0.0081	0.0083	0.0080
Flow	2-5	0.100	0.1012	0.0991	0.1012	0.0984
Flow	3-4	0.008	0.0079	0.0071	0.0079	0.0074
Flow	4-5	0.008	0.0084	0.0079	0.0067	0.0077
Flow	4-7	0.008	0.0067	0.0081	0.0074	0.0083
Flow	4-9	0.100	0.1017	0.0946	0.1017	0.0942
Flow	5-6	0.001	0.0013	0.0020	0.0032	0.0019
Flow	6-11	0.008	0.0081	0.0089	0.0080	0.0086
Flow	6-12	0.008	0.0068	0.0086	0.0068	0.0085
Flow	6-13	0.008	0.0083	0.0079	0.0081	0.0079
Flow	7-8	0.008	0.0077	0.0086	0.0078	0.0085
Flow	7-9	0.008	0.0078	0.0078	0.0083	0.0081
Flow	9-10	0.008	0.0073	0.0073	0.0077	0.0071
Flow	9-14	0.008	0.0071	0.0071	0.0072	0.0074
Flow	10-11	0.008	0.0086	0.0082	0.0087	0.0085
Flow	12-13	0.008	0.0080	0.0077	0.0080	0.0074
Flow	13-14	0.008	0.0083	0.0080	0.0083	0.0078
Voltage	1	0.004		0.0039		0.0038
Voltage	2	0.004		0.0042		0.0042
Voltage	3	0.080		0.0856		0.0853
Voltage	4	0.004		0.0038		0.0038
Voltage	5	0.001		0.0008		0.0009
Voltage	6	0.004		0.0039		0.0039
Voltage	7	0.004		0.0040		0.0039
Voltage	8	0.080		0.0811		0.0820
Voltage	9	0.001		0.0011		0.0010
Voltage	10	0.004		0.0039		0.0038
Voltage	11	0.004		0.0035		0.0035
Voltage	12	0.004		0.0038		0.0039
Voltage	13	0.004		0.0041		0.0040
Voltage	14	0.004		0.0041		0.0041

Simulations are also carried out for rapidly changing loads. It is observed that the required number of iterations to converge to the same tolerance will increase for these cases. However, the accuracy of the estimation results remains similar to those shown in Table XV. This validates the applicability of the proposed technique to systems irrespective of their type of load variations.

The above given simulation results are obtained by using *method 1*. Similar results are given by *method 2* when the procedure is used for the same cases except for an increase in the number of iterations. For the IEEE 14 bus system, the required number of iterations is 17 for *method 2* and 6 for *method 1*. However, since there is no need to calculate all the elements of *S* matrix in *method 2*, the total computation time may not actually be more especially for larger systems. The estimation results of *method 2* are shown in Table XVII. For comparison, the estimation results of *method 1* for the same system are also shown in last two column of Table XVII.

Furthermore, it should be noted that the estimation tolerance used in terminating the iterations is 10^{-4}, which is rather small. This tolerance can be relaxed to reduce the iterations further. The simulation results show that a good estimation can be reached after only 5 or 6 iterations. Table XVIII shows the maximum error after each iteration for *method 1* and *method 2*.

TABLE XVIII
MAXIMUM ERRORS AFTER EACH ITERATION

Iter. Index	1	2	3	4	5	6	7	8	9	10	…
Method 1	0.9989	0.0157	0.0011	0.0010	0.0006	0.0001	-	-	-	-	-
Method 2	0.9953	0.0282	0.0091	0.0031	0.0010	0.0004	0.0003	0.0003	0.0002	0.0002	…

It can be seen that the maximum error of *method 2* before 6^{th} iteration are similar to *method 1*. And after iteration 5^{th}, the maximum error becomes very small. This implicit that only several iterations are needed to get an accurate estimation. Table XIX shows the estimation results of *method 2* after only 5 iterations. For comparison, the estimation results of *method 1* after converge are also shown in last two columns.

TABLE XIX
SIMULATION RESULT FOR INITIALIZATION PROCESS (FEWER ITERATIONS)

Type	NO.	$\sqrt{R_Z}$	Method 2 (5 Iterations)		Method 1	
			Comp $\sqrt{R_a}$	Comp $\sqrt{R_r}$	Comp $\sqrt{R_a}$	Comp $\sqrt{R_r}$
Injection	1	0.010	0.0113	0.0118	0.0098	0.0109
Injection	2	0.010	0.0113	0.0110	0.0079	0.0086
Injection	3	0.010	0.0105	0.0117	0.0101	0.0125
Injection	4	0.050	0.0519	0.0478	0.0521	0.0501
Injection	5	0.010	0.0075	0.0079	0.0105	0.0088
Injection	6	0.010	0.0084	0.0095	0.0104	0.0108
Injection	7	0.001	0.0060	0.0053	0.0014	0.0023
Injection	8	0.010	0.0101	0.0102	0.0104	0.0104
Injection	9	0.010	0.0098	0.0123	0.0079	0.0115
Injection	10	0.001	0.0060	0.0059	0.0030	0.0050
Injection	11	0.010	0.0088	0.0099	0.0091	0.0101
Injection	12	0.010	0.0109	0.0090	0.0112	0.0087
Injection	13	0.010	0.0089	0.0099	0.0090	0.0097
Injection	14	0.010	0.0091	0.0107	0.0087	0.0102
Flow	1-2	0.008	0.0076	0.0057	0.0089	0.0069
Flow	1-5	0.008	0.0092	0.0082	0.0092	0.0079
Flow	2-3	0.100	0.1065	0.0966	0.1066	0.1000
Flow	2-4	0.008	0.0080	0.0079	0.0083	0.0080
Flow	2-5	0.100	0.1011	0.0992	0.1012	0.0984
Flow	3-4	0.008	0.0077	0.0074	0.0079	0.0074
Flow	4-5	0.008	0.0082	0.0083	0.0067	0.0077
Flow	4-7	0.008	0.0064	0.0079	0.0074	0.0083
Flow	4-9	0.100	0.1017	0.0946	0.1017	0.0942
Flow	5-6	0.001	0.0030	0.0031	0.0032	0.0019
Flow	6-11	0.008	0.0082	0.0090	0.0080	0.0086
Flow	6-12	0.008	0.0069	0.0086	0.0068	0.0085
Flow	6-13	0.008	0.0084	0.0080	0.0081	0.0079
Flow	7-8	0.008	0.0080	0.0086	0.0078	0.0085
Flow	7-9	0.008	0.0072	0.0073	0.0083	0.0081
Flow	9-10	0.008	0.0065	0.0069	0.0077	0.0071
Flow	9-14	0.008	0.0068	0.0071	0.0072	0.0074
Flow	10-11	0.008	0.0085	0.0081	0.0087	0.0085
Flow	12-13	0.008	0.0080	0.0076	0.0080	0.0074
Flow	13-14	0.008	0.0083	0.0080	0.0083	0.0078
Voltage	1	0.004		0.0039		0.0038
Voltage	2	0.004		0.0042		0.0042
Voltage	3	0.080		0.0856		0.0853
Voltage	4	0.004		0.0038		0.0038
Voltage	5	0.001		0.0009		0.0009
Voltage	6	0.004		0.0039		0.0039
Voltage	7	0.004		0.0040		0.0039
Voltage	8	0.080		0.0811		0.0820
Voltage	9	0.001		0.0011		0.0010
Voltage	10	0.004		0.0039		0.0038
Voltage	11	0.004		0.0035		0.0035
Voltage	12	0.004		0.0038		0.0039
Voltage	13	0.004		0.0041		0.0040
Voltage	14	0.004		0.0041		0.0041

In practical implementation, it is not necessary to require the estimation result converge to a small tolerance as 10^{-4}. Several iterations are enough for getting a satisfied estimation.

5.6.2 Sensitive Study of Estimation Errors

The effect of choosing the wrong weights for the measurements on the solution of the WLS state estimation will be investigated here. Two types of errors will be considered. The first type occurs when large estimated variances are used for measurements which are in fact highly accurate. The second type represents the opposite case where small variances are assumed for measurements that are actually not very accurate.

The following four cases will be discussed to illustrate these effects. Plots of relative errors between the state estimation solutions obtained using the incorrect and correct weights will be presented for comparison of effects of different types of errors.

1. Case1: Low weights are assigned to highly accurate power measurements including power injection measurements and power flow measurements. The errors in the following measurements are simulated according to the correct variances while the state estimation uses the wrong ones:
    1) Power injections in buses 4 and 7. Their correct standard deviation is 0.001, which is wrongly set to 0.01.
    2) Power flows in 1-5 and 4-5. Their correct standard deviation is 0.001 which is wrongly set to 0.01.
2. Case2: High weights are assigned to inaccurate power measurements including power injection measurements and power flow measurements. The measurements used for this simulation are:
    1) Power injections in buses 4 and 7. Their correct standard deviation is 0.1 which is wrongly set to 0.01.
    2) Power flows in 1-5 and 4-5. Their correct standard deviation is 0.1 which is wrongly set to 0.01.
3. Case3: Same as Case 1, but instead of the power measurements, the following voltage magnitude measurements are used:

Voltage magnitude at buses 4 and 7. Their correct standard deviation is 0.001 which is wrongly set to 0.01.

4. Case4: Same as Case 2, but instead of the power measurements, the following voltage magnitude measurements are used:

   Voltage magnitude at buses 4 and 7. Their correct standard deviation is 0.1 which is wrongly set to 0.01.

In all these cases, the remaining measurements are assumed to have a standard deviation of 0.01 and their weights are set consistently.

Since it is not possible to show the results of state estimation for all the system states, one example will be presented. Similar results are obtained for all state variables in all the simulations. The chosen state variable for illustrations is the voltage magnitude at bus 1. Fig. (a) through (d) show the plots of relative errors between the estimated voltage using the correct and incorrect weights for the indicated measurements for the four cases over a period covering 500 state estimation runs. Table XX shows the summary of these results. The second row in Table XX is the average value of the relative errors. Third row is the standard deviation. The fourth and fifth rows are maximum and minimum value, respectively.

By comparing column 2, 4 to 3, 5 in Table XX, it is evident that the effects of the first type of errors are relatively smaller than those of the second type, irrespective of the type of measurements used. On the other hand, a comparison of columns 2, 3 to 4, 5, implies that the incorrect choice of weights for the voltage magnitude measurements will have a much greater effect on the state estimation solution than choosing the incorrect weights for the power measurements.

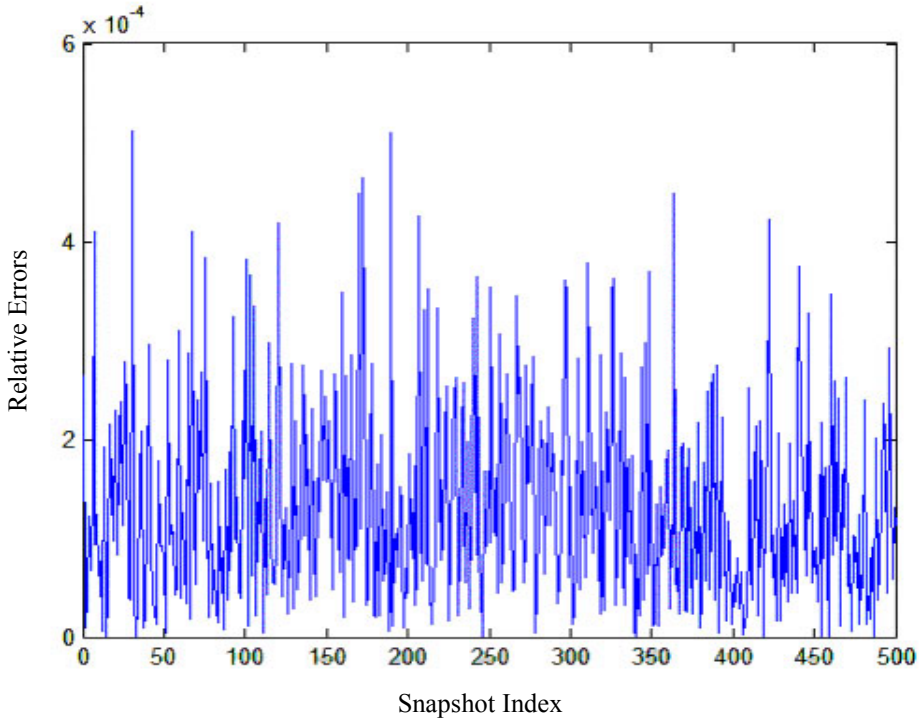

(a)

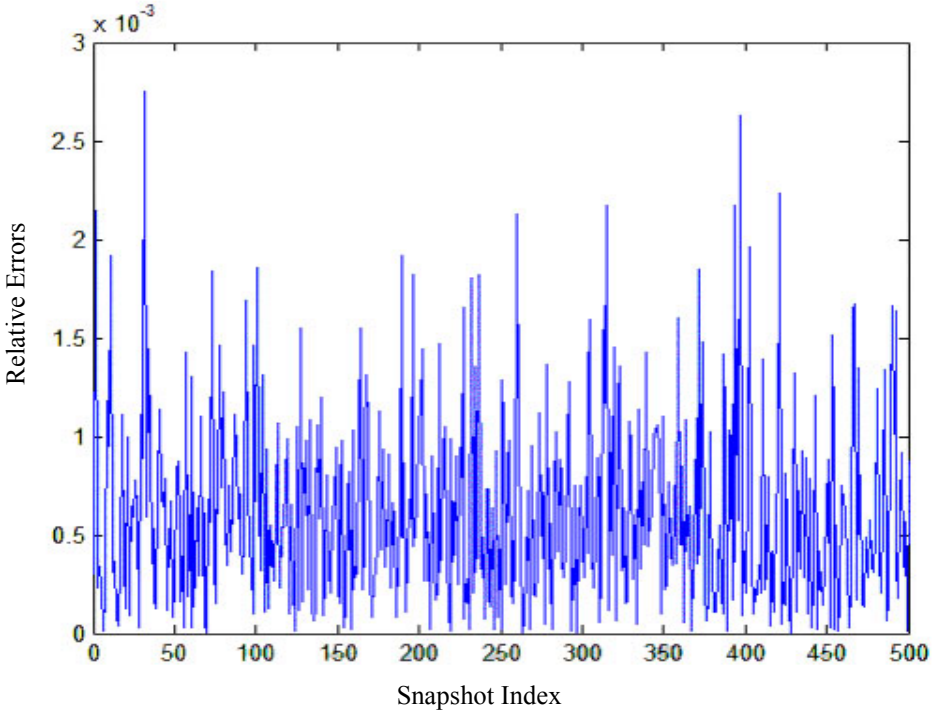

(b)

Fig. 17. Sensitivity study results

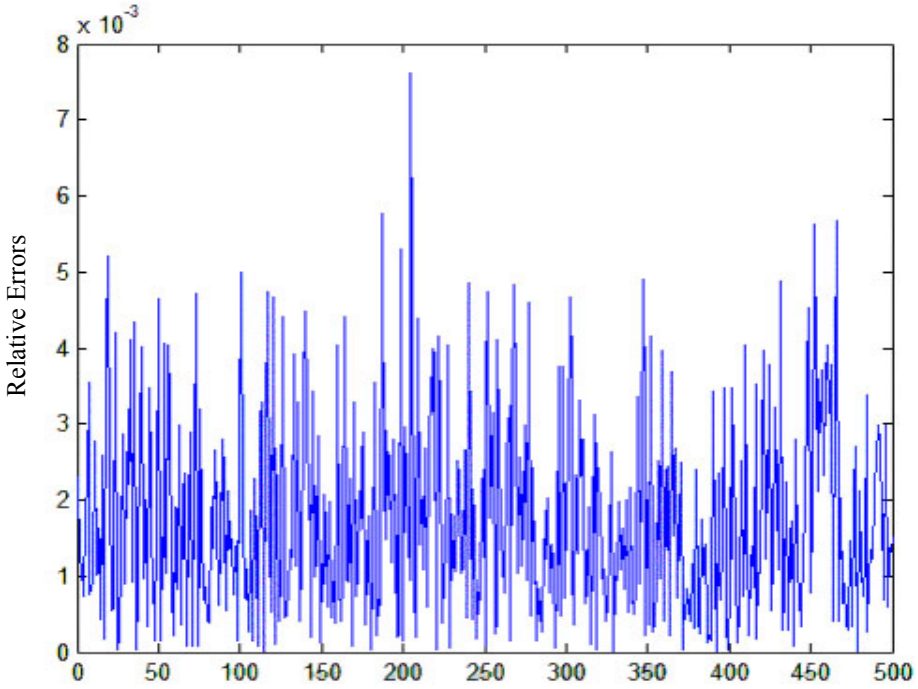

(c)

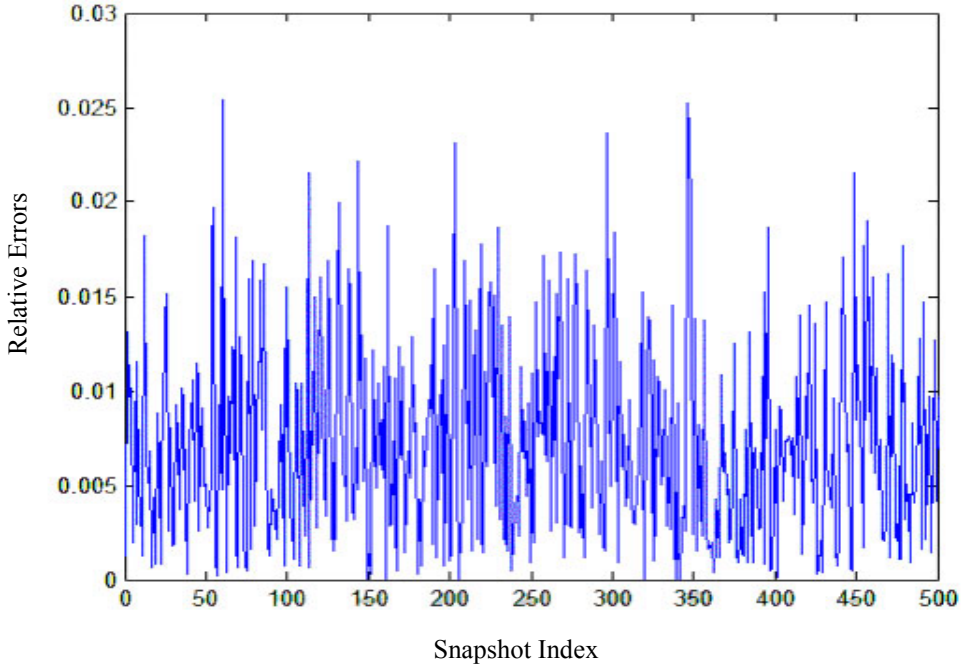

(d)

Fig.17. Continued

TABLE XX
RELATIVE ERRORS OF VOLTAGE MAGNITUDE IN BUS1

Cases	*Case1*	*Case2*	*Case3*	*Case4*
Average Value	0.00013	0.00060	0.00184	0.00526
STD	0.00010	0.00048	0.00132	0.00484
Maximum Value	0.00051	0.00267	0.00758	0.02510
Minimum Value	0.00000	0.00001	0.00004	0.00010

Considering the results of section 5.6.1 as displayed in Table XV, it can be observed that the proposed initialization method can track the weights associated with the voltage magnitude measurements at higher estimation accuracy than the power measurements. Since the results from this section suggest that the solution of state estimation is less sensitive to errors in power measurement weights, it can be concluded that the benefits of the proposed method will remain effective even when some of the power measurements' error variances can not be estimated very accurately by this method.

5.6.3 Recursive Updating Process

In order to test the performance of the proposed recursive updating procedure, time dependent standard deviations are introduced for selected measurements during the generation of the simulation data. The standard deviations of some measurements are abruptly changed as shown in Table XXI.

TABLE XXI
LIST OF VARIANCES CHANGES

Meas.	*Injection*			*Flow*			*Voltage*		
	3	5	7	2-5	4-5	6-11	2	6	9
Old Value	0.01	0.01	0.001	0.10	0.008	0.008	0.004	0.004	0.001
New Value	0.05	0.05	0.008	0.05	0.03	0.001	0.01	0.001	0.01
Time	600	700	800	600	700	800	600	700	800

The simulation data contain a total of 2000 consecutive snapshots. The first 200 snapshots are used to complete the initialization procedure. The results of this stage are similar to the results shown in Table XV. The updating procedure is applied starting with the 201'st time step. Depending on which estimation method is chosen, two possible procedures can be used and they are both tested on the same simulation data.

For convenience, we suppose the system topology is constant during the simulation period. Thus the only event to restart the updating process is the detection of the significant variances' changes. As mentioned in step 7) of the updating process' procedure, this can be done by compare the new estimation after each snapshot and the current used one. The relative errors between these two estimation results will be used as indicators. In addition we must specify a criterion to test the variances' changes. Suppose we set the criterion as:

1) At less one of the relative errors is greater than 5 and;
2) At less five of the relative errors are greater than 1.

The profile of new estimated standard deviation after every snapshot for reactive power injection in bus 3, whose standard deviation is changed at 600th point from 0.01 to 0.05, is shown in Fig. 18. The updating process uses *method 1* in this case.

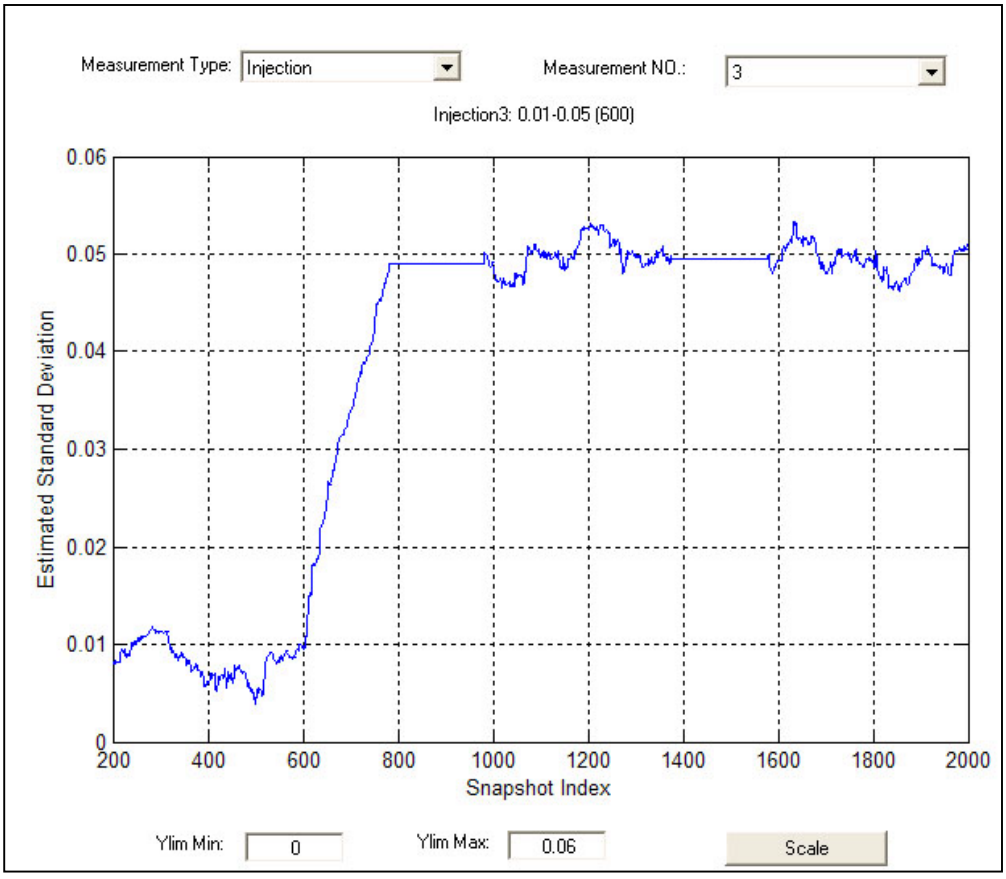

Fig. 18. Simulation result of updating process (method 1)

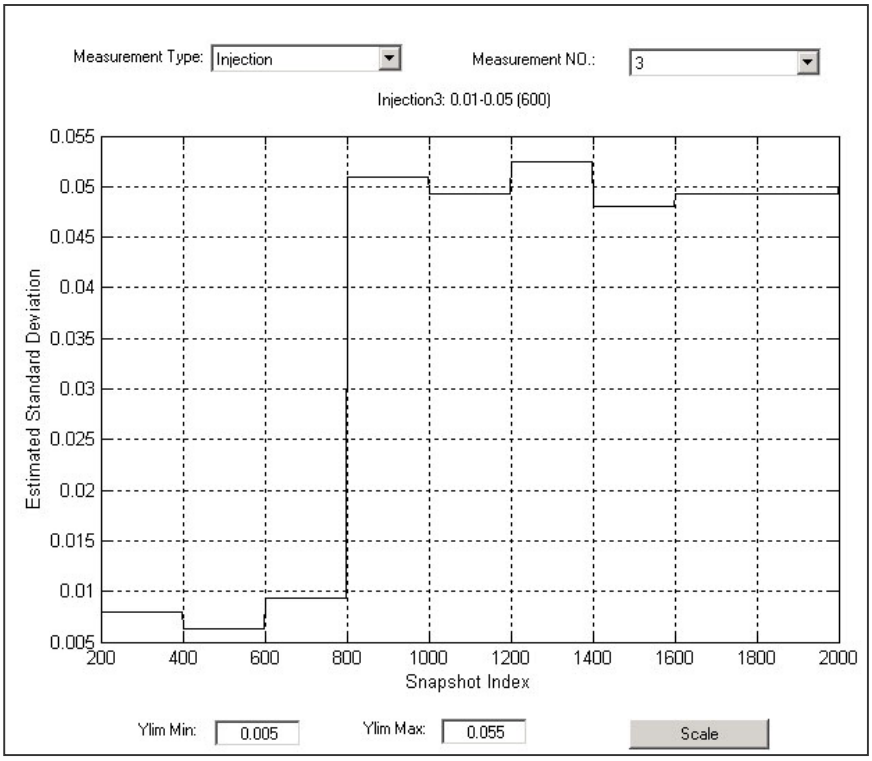

Fig. 19. Simulation result of updating process without criterion (method 1)

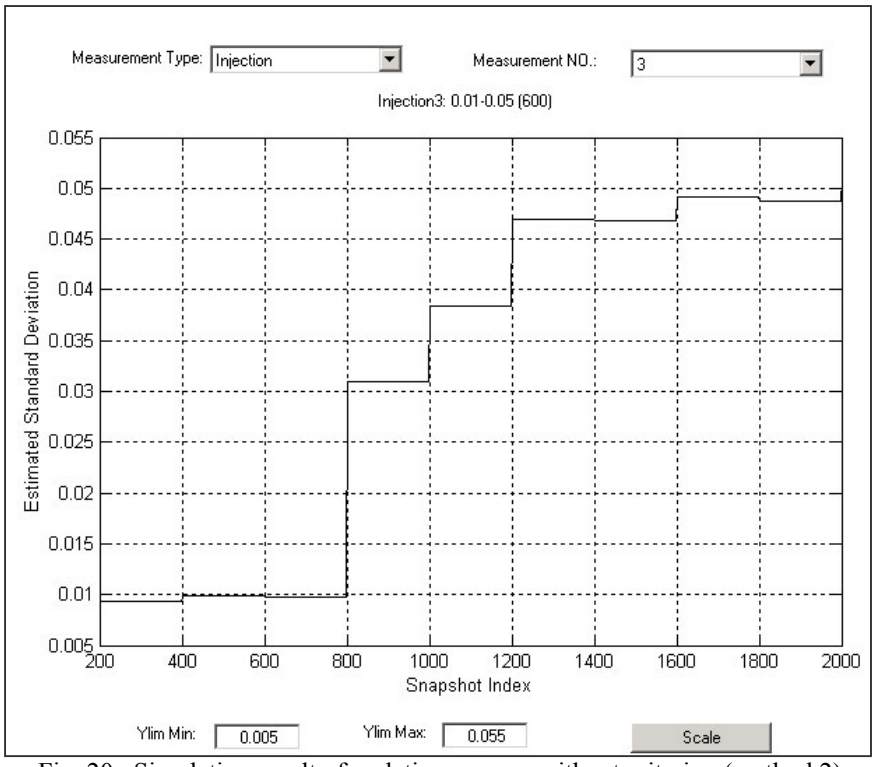

Fig. 20. Simulation result of updating process without criterion (method 2)

However, it is not easy to define the criterion appropriately in a practical system. A simple solution for this matter is to update the weight vector at the end of every updating process, no matter there are significant changes of the variances or not. In our simulation, since we use the window size as 200, the measurement weight vector will be updated every 200 measurement scans. The simulation results based on this idea are shown in Fig. 19 and Fig. 20 for the updating process using *method1* and *method2*, respectively. Similar to Fig. 18, only the profile of estimated standard deviation for power injection in bus 3 is shown. The simulation results indicate that both methods can keep track of the change in the standard deviation and update the corresponding weight correspondingly.

Note that for one cycle (200 time steps) estimation, *method 1* is computationally more demanding however it requires fewer cycles to converge to a new value than *method 2* in case of a sudden jump in the measurement variance. Actually, this is a highly unlikely worst case situation. A more common situation is a gradual drift in the measurement error variances in which case *method 2* can track the changes at a lower computational cost. Assuming that the state estimator can be executed every several seconds, the updating process can capture even the abrupt changes in the measurement error variances in less than few hours. Furthermore, if the variance changes gradually, the proposed updating process will track the changes much faster.

5.6.4 Critical Measurements/Critical K-Tuple of Measurements

It can be argued from the above discussion that the proposed technique performs satisfactorily both in initialization and updating modes, provided that there is sufficiently high redundancy in the measurement set. In the simulation example the measurement/state redundancy is 34/13. Now, its performance under reduced redundancy configurations will be studied.

As shown in Fig. 21, the measurement set is modified to include 10 power injections, 9 power flows and 3 voltage magnitude measurements. These measurements are also specified in the first two columns of Table XXII. The redundancy ratio for this configuration is 19/13. The structure of the sensitivity matrix for the active part is shown in (56). For convenience, the row sequence of S_a is rearranged to form a block diagonal structure.

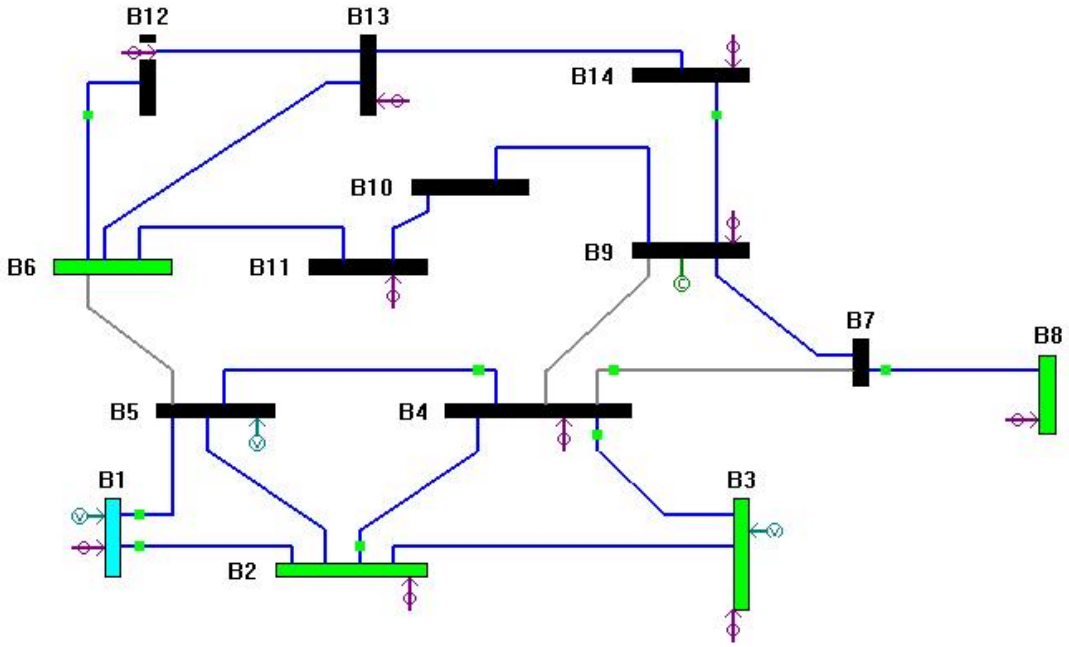

: Power Injection : Power Flow : Voltage Magnitudes

Fig. 21. Studied system with measurement configuration

TABLE XXII
SIMULATION RESULT FOR LESS REDUNDANCY CONFIGURATION

Type	*NO.*	$\sqrt{R_Z}$	*Comp* $\sqrt{R_a}$	*Comp* $\sqrt{R_r}$
Injection	1	0.010	0.0098	0.0114
Injection	2	0.001	0.0131	0.0107
Injection	3	0.050	0.0453	0.0442
Injection	4	0.010	0.0211	0.0245
Injection	8	0.010	0.0093	0.0091
Injection	9	0.010	0.0211	0.0245
Injection	11	0.010	0.0211	0.0245
Injection	12	0.010	0.0064	0.0055
Injection	13	0.010	0.0063	0.0056
Injection	14	0.010	0.0064	0.0055
Flow	1-2	0.008	0.0079	0.0060
Flow	1-5	0.008	0.0077	0.0081
Flow	2-4	0.001	0.0031	0.0038
Flow	3-4	0.100	0.1018	0.0982
Flow	4-5	0.008	0.0086	0.0064
Flow	4-7	0.008	0.0211	0.0245
Flow	6-12	0.001	0.0064	0.0055
Flow	7-8	0.008	0.0093	0.0091
Flow	9-14	0.008	0.0063	0.0056
Voltage	1	0.004		0.0033
Voltage	3	0.080		0.0814
Voltage	5	0.001		0.0026

$$S_a = \begin{bmatrix} 0 & 0 & 0 & 0 & 0 & 0 & 0 \\ 0 & 0 & 0 & 0 & 0 & 0 & 0 \\ 0 & 0 & 0 & 0 & 0 & 0 & 0 \\ 0 & 0 & 0 & 0 & 0 & 0 & 0 \\ 0 & 0 & 0 & 0 & S_2 & 0 & 0 \\ 0 & 0 & 0 & 0 & 0 & S_3 & 0 \\ 0 & 0 & 0 & 0 & 0 & 0 & S_4 \end{bmatrix} \tag{56}$$

where:

S_2: A 2x2 sub matrix with rank 1.

S_3: A 5x5 sub matrix with rank 1.

S_4: A 8x8 sub matrix with rank 4.

As can be seen from (56), for the active sub problem, this measurement set contains the following:

1) Critical subset 1: 4 critical measurements, injections at 4,9,11 and flow 4-7. They correspond to the first four rows of S_a in (56).
2) Subset 2: Critical pair including injection 8 and flow 7-8, which correspond to the sub matrix S_2 in (56).
3) Subset 3: Residual spread component containing 5 measurements, injections at 12,13,14 and flows 6-12,9-14. Any two of these five measurements form a critical pair. They correspond to the sub matrix S_3 in (56).
4) Subset 4: Remaining 8 measurements. Any five of them form a critical *5-tuple*. They correspond to the sub matrix S_4 in (56).

The initialization procedure is tested for this case using both *method 1* and *method 2*. Again, the estimation results are similar except for the fact that *method 2* converges in more iterations. Table XXII shows the results of *method 2*.

For critical measurements, the weights have no influence and there is no way to estimate their variances. These are assigned the average value of all other measurements (0.0211) in order to avoid any ill conditioning.

For critical pairs, such as the subset 2 and those pairs in subset 3, the corresponding sub-matrix of S has a rank of 1, and hence the estimation results of measurements

belonging to the same set are equal. This is a limitation imposed by the measurement configuration and can not be avoided without further meter placement.

The estimation results for the weights of measurements in subset 4 are closer to the true values than those in subset 3. This can be explained by the higher local redundancy in subset 4 compared to that of subset 3.

Moreover, low redundancy has less of an influence on the estimation results for the voltage magnitude measurements. This is verified by the results in Table XXII, where the weights for all three voltage magnitude measurements each having a different error variance, can be closely estimated.

5.7 Conclusions

This chapter is concerned about the estimation of measurement error variances for their subsequent use in state estimation. A simple method is proposed based on the sample variances of the measurement residuals calculated using the historical records. An off-line iterative initialization and an on-line recursive updating procedure are developed and illustrated by simulated examples. The chapter also illustrates the limitations of the proposed method imposed by the measurement configuration using observability analysis. The presented approach can be used at desired intervals in order to maintain properly tuned weights for the measurements.

CHAPTER VI

THREE-PHASE STATE ESTIMATION STUDY

6.1 Introduction

Power systems are generally configured in three phases, and are designed to operate in an almost balanced manner. Balanced three-phase operation implies the following conditions to be met:

- Transposition of the transmission lines
- Even distribution of bus loads
- Maintaining balanced generator outputs

Analysis of balanced three-phase systems is relatively simple compared to the full detailed three-phase solution of the network equations. A symmetrical component transformation will decompose the balanced three-phase system into three independent systems, commonly referred to as the positive, negative and the zero sequence networks. Absence of negative and zero sequence signals under perfectly balanced three-phase operating conditions, allows the analysis to be carried out in the single phase, using only the positive sequence model. State estimators are no exception, making use of the positive sequence network model and the measurements in solving for the best estimate for the system state.

In practice, most high voltage systems are nearly balanced and depending on the system configuration and loading conditions, they can be modeled and solved in the positive sequence. However, there may be cases where the balanced system assumptions no longer hold, when bus loads have an uneven distribution among the three phases, or relatively long but non-transposed transmission lines, carrying significant power flows exist in the system. Such lines will have different mutual coupling among the pairs of phase conductors and consequently the power flows through each of the three conductors of the lines will not be the same.

Unbalanced operating state of a power system can be obtained using a more detailed network model and measurement set containing all three-phase quantities of interest. The problem of three-phase state estimation for transmission and distribution systems

operating under unbalanced conditions is described in several papers [60], [62]-[69]. Some of them [62]-[63] describe the general three-phase state estimation algorithms, while others [64]-[69] focus on the application of three-phase state estimation in distribution systems utilizing special characteristics. However, any phase unbalances in loads and/or any existing non-transposed transmission lines are commonly ignored in state estimators which are used for power systems today. As indicated in [60], such simplifying assumptions may affect the accuracy and numerical robustness of the estimator.

This chapter therefore studies the effects of such simplifying assumptions on the estimated state of the systems under varying operating conditions. A state estimator based on the full three-phase network model is developed first. This estimator is then utilized to evaluate cases of load unbalance as well as lack of line transposition. IEEE 30 bus test system is modified to generate these cases. A three-phase power flow program is used to generate the measurement data, which are then corrupted with Gaussian errors to simulate measurement deviations. True three-phase state of the system is compared against those obtained based on different assumptions on the measurements. Details of these cases will be described after an overview of the system modeling.

The results of sensitivity study give rise to a new method to get the full detailed three-phase solution. The sequence domain three-phase state estimation algorithm is developed in this chapter. The main idea of this method is to model the power system in positive-negative-zero sequence domain. Three-phase measurements are transformed into sequence domain. The single-phase WLS (Weighted Least Square) state estimation is run in each sequence domain and the estimated sequence domain results are converted back to three-phase domain. Utilizing this method, we can get three-phase solution by conducting three independent single-phase state estimations. Since the relation between time consuming and system size for a normal state estimation algorithm is nonlinear, this method should have better efficiency compare to the conventional three-phase state estimation algorithm. The detailed formulations and implementation of this method will be described in this chapter.

A current injection method (CIM) formulated in rectangular coordinates is utilized to further increase the efficiency. The advantage of using current injection method in power

flow or state estimation problems is discussed in many papers. It will be faster than Newton-Raphson (NR) or fast-decoupled (FD) algorithm [71]-[72]. In addition, writing the network equations in rectangular coordinates make the Jacobian and gain matrix constant, thus further lessen the computation time.

However, due to time limit, some of the important issues for this method have not been completely studied. Further research is needed in order to make it applicable to real-time environment.

Sections 6.2 - 6.7 in this chapter will discuss the algorithm and simulation results of the sensitivity study. The other sections will briefly introduce the sequence domain three-phase state estimation algorithm and give the primitive simulation results.

6.2 Algorithm and System Modeling

The weighted least squares (WLS) algorithm is used in the implementation of the three-phase state estimator. The details of the measurement equations and Jacobian entries can be found in [62]. Sparse matrix techniques are used to improve the computational efficiency and memory savings. All system components such as transmission lines, loads, transformers and generators are modeled in three-phase as described below.

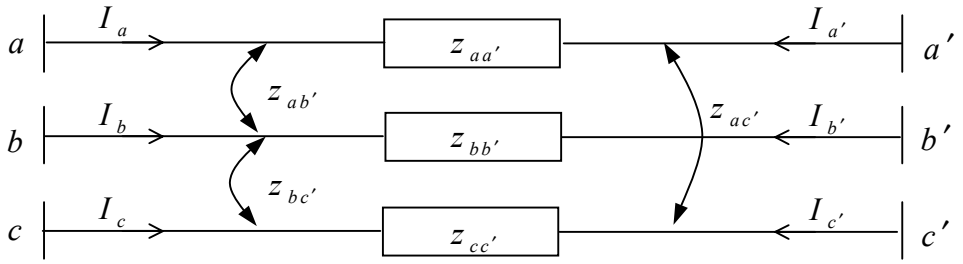

Fig. 22. An example of three-phase transmission line

6.2.1 Three-Phase Transmission Lines

A typical three-phase transmission line is given in Fig. 22. The network equations for this line can be written in compact form, according to the procedure described in [70]. The effect of the ground wire is included in the self and mutual impedance of the three-phase conductors. The primitive series impedance matrix of the line is given:

$$Z_P = \begin{bmatrix} z_{aa'} & z_{ab'} & z_{ac'} \\ z_{ba'} & z_{bb'} & z_{bc'} \\ z_{ca'} & z_{cb'} & z_{cc'} \end{bmatrix} \tag{57}$$

Defining the primitive admittance matrix $Y_P = Z_P^{-1}$, the nodal equations for the system of Fig. 22 can be written as:

$$\begin{bmatrix} I_a \\ I_b \\ I_c \\ I_{a'} \\ I_{b'} \\ I_{c'} \end{bmatrix} = \begin{bmatrix} & & \\ Y_P & -Y_P & \\ & & \\ & & \\ -Y_P & Y_P & \\ & & \end{bmatrix} \begin{bmatrix} V_a \\ V_b \\ V_c \\ V_{a'} \\ V_{b'} \\ V_{c'} \end{bmatrix} \tag{58}$$

If the susceptances associated with the line charging exist, they will be added to the diagonal elements of the admittance matrix corresponding to the end nodes. The susceptances of all shunt elements in three phases are assumed equal.

6.2.2 Three-Phase Loads and Generators

Each three-phase bus consists of three single-phase buses with loads connected in Wye and modeled by negative power injections in the state estimation measurement equations. Similarly, generated real and reactive power at each single-phase bus is modeled as a positive injection. Generator buses may have unbalanced injections assigned to them as measurements if the operating conditions are not balanced.

6.2.3 Transformers

The winding-connection type of transformer becomes critically important in the three-phase study [70]. While all transformers considered in this study are assumed to be Wye connected at both sides, any other combination can be modeled as shown in [70]. Transformers with off-nominal tap settings are represented as shown in Fig. 23.

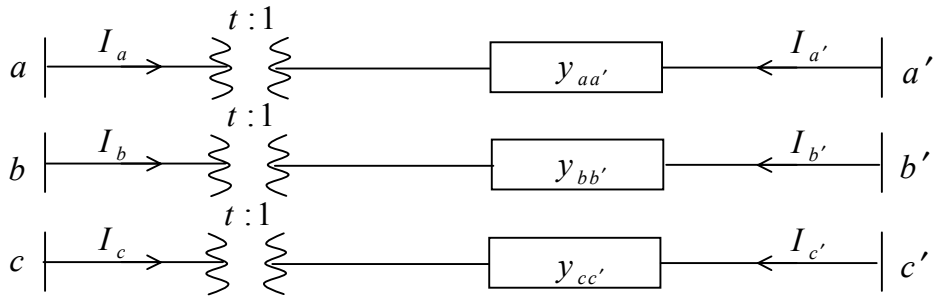

Fig. 23. Typical three-phase transformer model

Accordingly, the node equations of transformer can be described as (59).

$$\begin{bmatrix} I_P \\ I_S \end{bmatrix} = \begin{bmatrix} A/t^2 & C/t \\ C^T/t & B \end{bmatrix} \begin{bmatrix} V_P \\ V_S \end{bmatrix} \tag{59}$$

where:

I_P and I_S are primary and secondary three-phase current;

V_P and V_S are primary and secondary three-phase voltages;

t is the off-nominal tap;

$$A = B = -C = \begin{bmatrix} y_{aa'} & 0 & 0 \\ 0 & y_{bb'} & 0 \\ 0 & 0 & y_{cc'} \end{bmatrix}.$$

For the admittance matrices corresponding to other kinds of winding connections, please refer to [63].

6.2.4 Bus Shunts

Bus shunts are assumed to be decoupled in each phase and they are modeled by adding appropriate susceptance values to the diagonal elements corresponding to the buses.

6.3 Studied Cases

All studied cases are built using the IEEE 30 bus system. Loading unbalances as well as the non-transposed line effects on the network model are studied. In order to create a

three-phase network model for the IEEE 30 bus system, several assumptions are made regarding the sequence component data that are not readily available. This will be explained below.

6.3.1 Convert Positive Sequence Model to Three-Phase Model

IEEE 30 bus system data are available only in the positive sequence. The following steps are followed to generate the three-phase network model based on the positive sequence model.

1) Transmission lines

We assume the relationship between negative, zero and positive sequence impedances of all the transmission lines is as follows:

$$Z_0 = 3Z_1;\ Z_2 = Z_1 \tag{60}$$

where:

Z_0, Z_1, Z_2 are the zero, positive and negative sequence impedances, respectively.

Then the three-phase impedance matrix will become:

$$Z_{abc} = K^{-1} \cdot \begin{Bmatrix} Z_0 & 0 & 0 \\ 0 & Z_1 & 0 \\ 0 & 0 & Z_2 \end{Bmatrix} \cdot K \tag{61}$$

where:

Z_{abc} is the 3×3 three-phase impedance matrix;

$K = \begin{Bmatrix} 1 & 1 & 1 \\ 1 & a & a^2 \\ 1 & a^2 & a \end{Bmatrix}$, and $a = e^{j120^o}$

2) Transformers

All phase to phase coupling are ignored for the transformers as shown in Fig. 23. The off-nominal taps and branch impedances are obtained directly from IEEE 30 bus data file.

6.4 Cases of Unbalanced Operation

Following cases are investigated. Each case involves a different type of unbalance and severity.

1) Case T1

In this case, all transmission lines are assumed to be non-transposed. The amount of coupling asymmetry among the three-phase conductors is chosen based on the mutual impedance between phase A and phase C. This quantity is set equal to 90% of the mutual impedances between the other two phases.

2) Case T2

This case is identical to Case 1, except for the severity of the coupling asymmetry. The mutual impedance between phase A and phase C is set equal to 60% of other two mutual impedances.

3) Cases L1-L4

These are a set of four cases where all bus loads in the system are assumed to be unbalanced. The amount of unbalance between phase loads, is varied by keeping the phase A and B loads equal, and changing phase C load to 90%, 80%, 70% and 60% of that of the other phase loads for the cases L1 through L4 respectively.

6.4.1 Generation of Three-Phase Measurements

A three-phase power flow program is used to generate the measurements corresponding to all the cases described above. These perfect measurements are in turn corrupted by Gaussian distributed random errors with zero mean and standard deviation of 0.004, 0.01 and 0.008 for the voltage magnitude, power injection and power flow measurements respectively.

6.5 Investigation Methodology

The investigation concerning the above described cases is carried out by performing three state estimation solutions using different assumptions and available measurements, which are outlined below:

1) Estimate1 (Three-phase)

A three-phase state estimation is performed using the full set of three-phase measurements, assuming that the necessary instrumentation is available to have access to the measurements in all three phases. Once the three-phase estimates are obtained, their positive sequence components are evaluated and recorded.

2) Estimate2 (Single-phase)

In this case, it is assumed that only phase A measurements are available at the control center where the state estimator is run. The positive sequence network model, similar to the one used by the common single-phase state estimators, is employed. The resulting state estimate, which is a single-phase result, is recorded.

3) *Estimate3 (Single-phase)*

This is identical to the *Estimate2*, except for the measurement set, which now contains the positive sequence values of the three-phase measurements. This would correspond to a case where three-phase instrumentation and the corresponding measurements are available, yet a single-phase state estimator is to be run.

These three sets of estimated results will be referred respectively as *Estimate1, Estimate2* and *Estimate3* in the presented tables below. The estimated states in *Estimate2* and *Estimate3* are compared with *Estimate1* to quantify the effects of the assumptions involved. A flowchart of overall investigation procedure is summarized in Fig. 24.

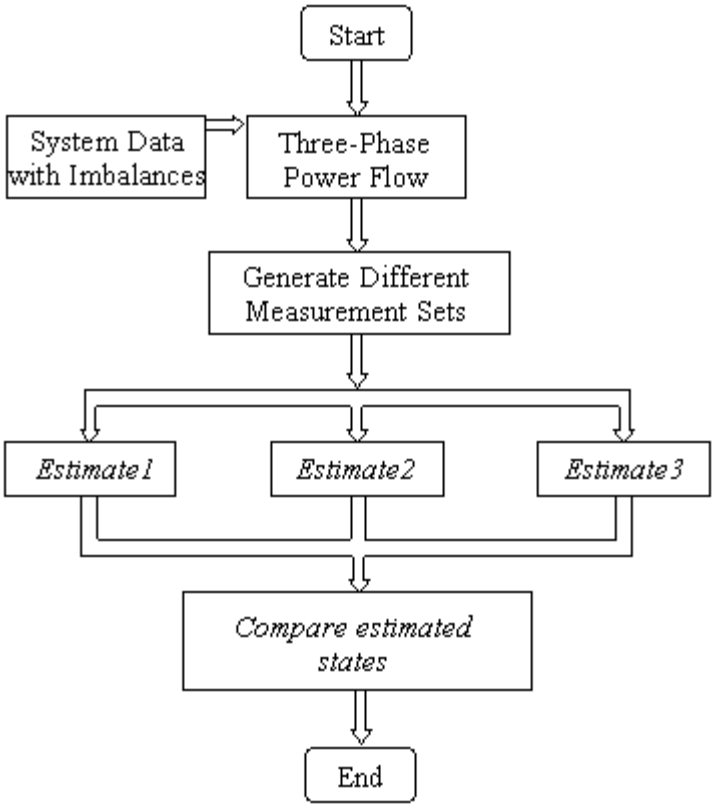

Fig. 24. Flowchart of investigation process

The following indices are used for the comparisons:

1) Normalized residuals

The normalized residuals for all measurements are computed for both kinds of state estimators. Those measurements with normalized residual great than 3.0 are recorded as the suspected bad data.

2) Maximum Absolute State Mismatches

Absolute mismatches between the states obtained as *Estimate1* and as *Estimate2, Estimate3* are computed. Maximum absolute mismatches of voltage magnitude and phase angles are recorded.

3) Freq. of Relative Errors Greater Than 3σ

The relative errors given by (62) are computed for *Estimate2* and *Estimate3*.

$$err = \left| \frac{S_{estimated} - S_{true}}{S_{true}} \right| \tag{62}$$

where $S_{estimated}$ is the estimated states and S_{true} is true states.

The number of times these relative errors exceed three times the corresponding measurement standard deviation will be referred to as *Freq. of* $err > 3\sigma$.

4) Costs

The values of objective functions evaluated after convergence are referred here as *Costs*. For comparing, the costs get from three-phase state estimator are divided by 3. The value of the cost is compared against the corresponding Chi-square test threshold in order to detect bad data. Chi-square test thresholds are looked up from Chi-square distribution table as 139 for the single phase and 127 (383/3) for the three-phase estimation cases. Those values greater than threshold are noted in the tables.

6.6 Results of Sensitivity Simulations

All of the cases mentioned in section 6.4 are simulated and compared according to the procedure shown in Fig. 24. The detailed results of estimation will be presented for *case T1* (table I), and for brevity only the corresponding indices calculated for the other cases will be shown. In these tables, all the voltage magnitudes will be given in per-unit and phase angles in degrees.

6.6.1 Non-transposed Cases

In the first two cases: *case T1* and *case T2*, the loads are balanced but the transmission lines are non-transposed. Table XXIII shows all three estimation results for *case T1*. The indices of these two cases are presented in Table XXIV and Table XXV, respectively.

Note that, the use of single phase (phase A) measurements to estimate the state of a system operating under unbalanced conditions, may lead to some bias in the state estimate. However, for both *cases T1* and *T2*, Chi-square test thresholds are not hit, i.e. modeling errors due to the non-transposed lines are not detected by the estimator.

TABLE XXIII
ESTIMATED STATES OF *CASE T1*

Bus No.	***Estimate1***		***Estimate2***		***Estimate3***	
	|V|	**Ang.**	**|V|**	**Ang.**	**|V|**	**Ang.**
1	1.060	0.00	1.054	0.00	1.060	0.00
2	1.043	-5.40	1.039	-5.45	1.043	-5.40
3	1.020	-7.58	1.017	-7.67	1.020	-7.58
4	1.011	-9.33	1.009	-9.44	1.011	-9.33
5	1.009	-14.27	1.008	-14.39	1.009	-14.27
6	1.009	-11.11	1.007	-11.25	1.009	-11.11
7	1.001	-12.92	0.999	-13.08	1.001	-12.92
8	1.009	-11.87	1.008	-12.01	1.009	-11.87
9	1.049	-14.09	1.048	-14.22	1.049	-14.09
10	1.043	-15.64	1.041	-15.81	1.043	-15.64
11	1.080	-14.07	1.081	-14.26	1.080	-14.08
12	1.054	-14.91	1.054	-15.09	1.054	-14.90
13	1.068	-14.94	1.068	-15.16	1.068	-14.94
14	1.039	-15.82	1.038	-15.91	1.039	-15.82
15	1.035	-15.84	1.035	-16.03	1.035	-15.84
16	1.041	-15.46	1.040	-15.59	1.041	-15.46
17	1.037	-15.79	1.036	-15.94	1.037	-15.79
18	1.025	-16.45	1.025	-16.68	1.025	-16.45
19	1.023	-16.57	1.022	-16.79	1.023	-16.57
20	1.027	-16.37	1.026	-16.60	1.027	-16.37
21	1.030	-16.07	1.029	-16.24	1.030	-16.07
22	1.031	-16.06	1.030	-16.23	1.031	-16.06
23	1.025	-16.26	1.025	-16.40	1.025	-16.26
24	1.019	-16.43	1.018	-16.57	1.019	-16.43
25	1.015	-16.08	1.014	-16.09	1.015	-16.08
26	0.997	-16.35	0.999	-16.53	0.997	-16.35
27	1.020	-15.61	1.019	-15.58	1.020	-15.61
28	1.005	-11.73	1.004	-11.87	1.005	-11.73
29	0.999	-16.88	0.998	-16.73	0.999	-16.88
30	0.987	-17.75	0.985	-17.61	0.987	-17.75

TABLE XXIV
COMPARISON INDICES OF *CASE T1*

CaseT1	**Bad Data No.**	**Maximum Mismatch**		**Freq. of err >3σ**		Cost
		|V|	**Ang.**	**|V|**	**Ang.**	
Estimate1	0	-	-	-	-	101.3
Estimate2	0	0.005	0.238	0	9	117.0
Estimate3	0	4E-5	0.002	0	0	49.3

TABLE XXV
COMPARISON INDICES OF *CASE T2*

CaseT2	**Bad Data No.**	**Maximum Mismatch**		**Freq. of err >3σ**		Cost
		|V|	**Ang.**	**|V|**	**Ang.**	
Estimate1	0	-	-	-	-	97.9
Estimate2	0	0.018	0.393	1	28	123.5
Estimate3	0	3E-4	0.031	0	0	41.5

6.6.2 Unbalanced Cases

Cases L1-L4 assume fully transposed transmission lines but unbalanced loads. Table IV shows the results for *case L1*. The results appear similar to the ones reported for case T2, which corresponds to a very extreme form of asymmetry as compared to a relatively mild unbalance (10%) of case L1. When the degree of unbalances increases, the errors will increase significantly. Table XXVI shows the results for *cases L1-L4,* where the cost function for *case L4* exceeds the bad data detection threshold based on the Chi-square test. Hence, in this situation the state estimator may incorrectly identify some measurements as bad and discard them to further deteriorate the accuracy of the estimator.

TABLE XXVI
COMPARISON INDICES OF *CASE L1*

CaseL1	**Bad Data No.**	**Maximum Mismatch**		**Freq. of err >3σ**		Cost
		|V|	**Ang.**	**|V|**	**Ang.**	
Estimate1	0	-	-	-	-	90.6
Estimate2	0	0.011	0.455	0	6	125.9
Estimate3	0	4E-5	5E-4	0	0	42.5

TABLE XXVII
INFLUENCE OF UNBALANCED LOADS

CaseL1	Bad Data No.	Maximum Mismatch		Freq. of err >3σ		Cost
		|V|	Ang.	|V|	Ang.	
L1	0	0.011	0.455	0	6	125.9
L2	1	0.017	0.868	12	29	127.5
L3	0	0.025	1.103	19	29	131.1
L4	4	0.030	1.243	24	29	159.1*

**: This value exceeds Chi-square test threshold.*

Fig. 25 shows how the error increases with the severity of unbalances.

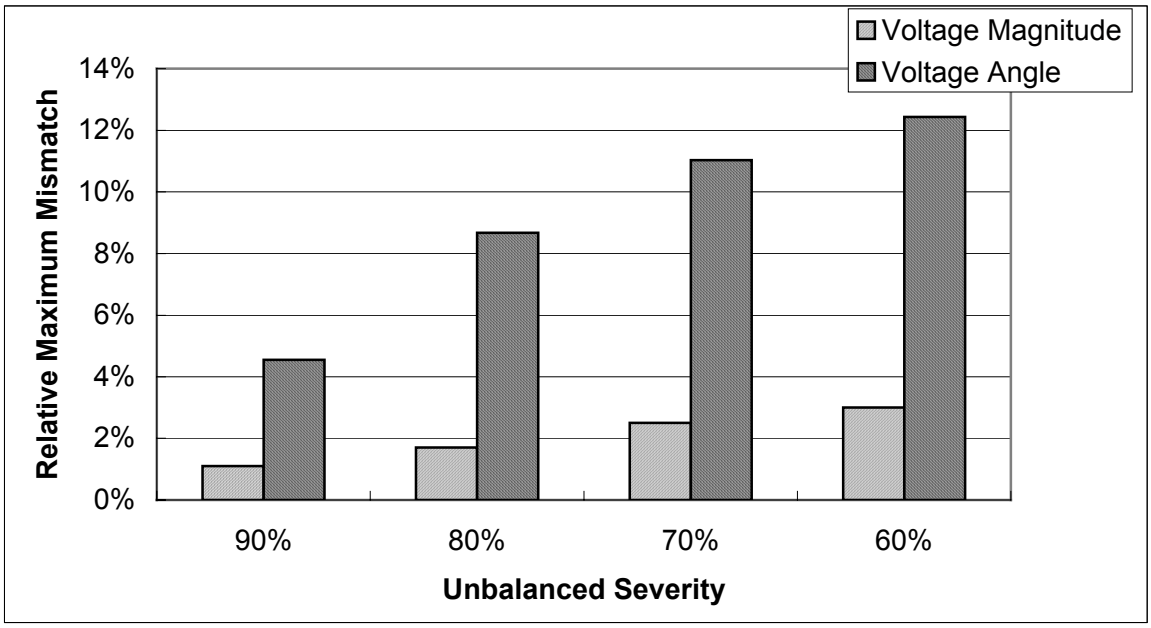

Fig. 25. Relative error caused by unbalances with different degrees

It is evident from these simulation results that the effect of non-transposed lines is less than that of load unbalances, on the state estimates. Fig. 26 and Fig. 27 show the effects of non-transposed lines (*case T2*) and unbalanced loads (*case L4*) on the voltage magnitude and phase angle estimates respectively. In both figures, the curve labeled as *estimate1*, is the true state while the one labeled as *estimate2* represents the estimate. The

mismatches between these two curves reflect the error caused by the assumptions.

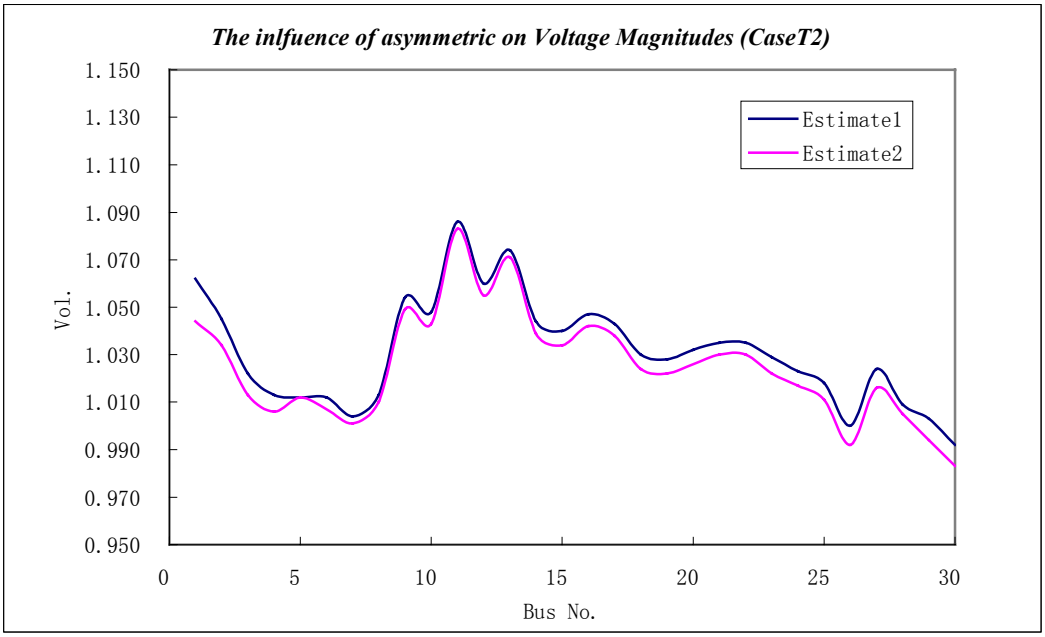

(a)

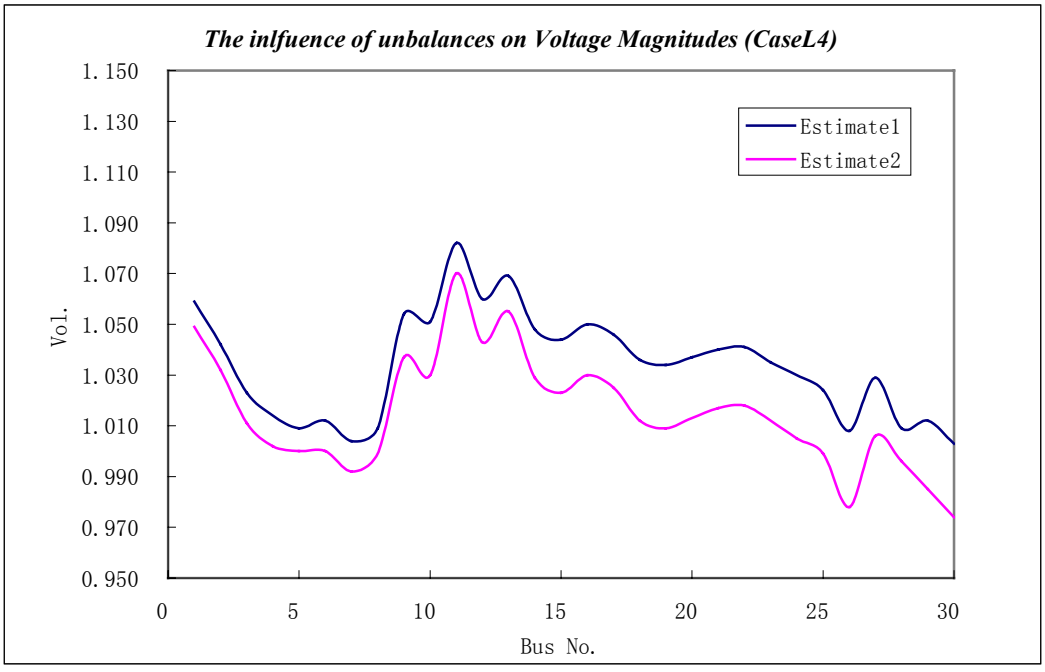

(b)

Fig. 26. Influences of asymmetric and unbalances on voltage magnitudes

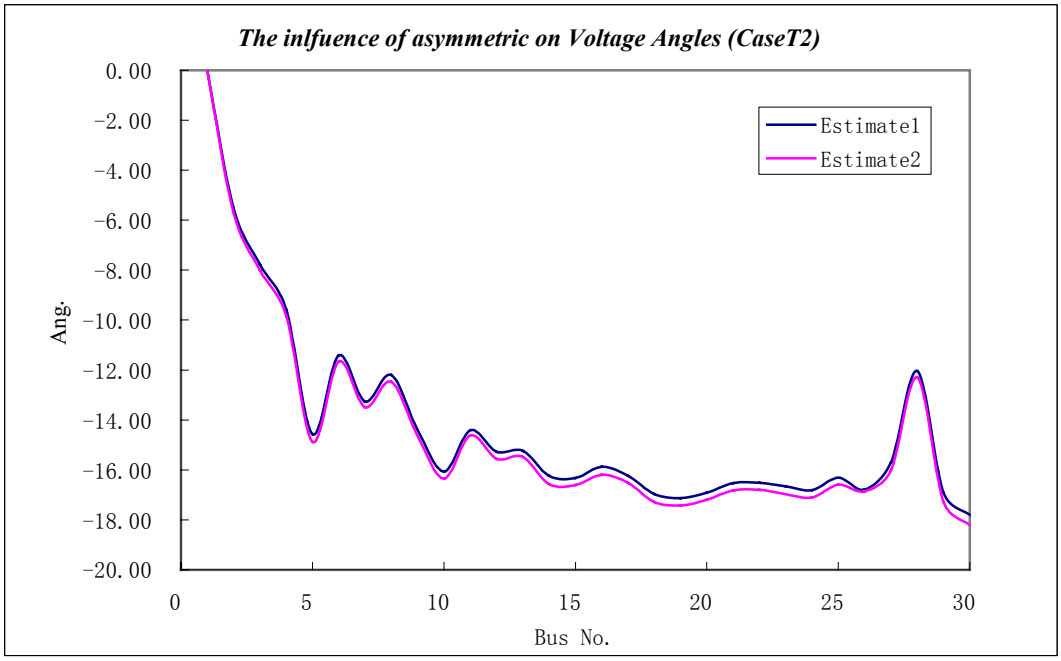

(a)

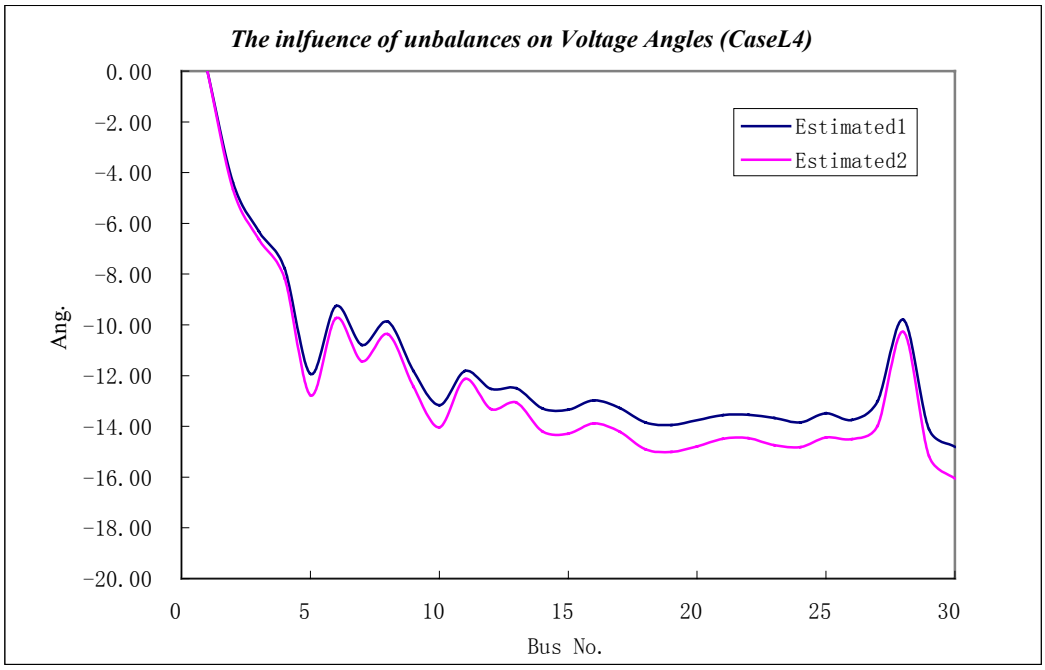

(b)

Fig. 27. Influences of asymmetric and unbalances on voltage angles

6.7 Conclusion of the Sensitivity Studies

The results of the sensitivity studies have been illustrated in the previous section. It is demonstrated that under certain cases, the use of single-phase state estimator may lead to significant biases in the solution due to existing asymmetries or load unbalances. The simulation results also indicate a higher sensitivity of the system state to loading unbalances than to asymmetries in the transmission line conductor configurations. That is to say, under the assumption of symmetrical lines, a good approximation cab be obtained. Motivated by this observation, a new sequence domain three-phase state estimation algorithm is developed in this chapter. The main idea of this method is to model the power system in positive-negative-zero sequence domain. Transform the three-phase measurements into the sequence domain. Run the WLS (Weighted Least Square) estimator for each sequence separately and convert the computed results back to the phase domain. Utilizing this method, we can get three-phase solution by conducting three independent single-phase state estimations. Due to the nonlinear relation between the computation time and system size for the WLS state estimation algorithm, this method is expected to have better efficiency compared with the conventional algorithm. The detailed procedure and implementation of this method will be described in the following section.

A current injection method (CIM) formulated in rectangular coordinates is utilized to further increase the efficiency. The advantage of using current injection method in power flow or state estimation problems is discussed in many papers. It will be faster than Newton-Raphson (NR) or fast-decoupled (FD) algorithm [71]-[72]. In addition, formulating the network equations in rectangular coordinates makes the Jacobian and the gain matrix constant, thus reduces the computation time.

6.8 Development of the Sequence Domain Three-Phase State Estimation

In unbalanced three-phase power system analysis, it is customary to use sequence transformations in order to simplify the computations. This idea can also be introduced to state estimation. By transformation of the phase domain measurements into sequence domain and utilizing the positive, negative and zero sequence domain circuits, it is

possible to transform three-phase state estimation problem into three single-phase state estimation problems, thus to reduce the computation time.

6.8.1 General Procedure

Equation (63) describes the relation between the phase domain system states and sequence domain system states.

$$V_{abc} = T \cdot V_{012} \tag{63}$$

where:

$V_{abc} = (v_a, v_b, v_c)^T$ is the three-phase voltage vector in phase domain;

$V_{012} = (v_0, v_1, v_2)^T$ is the voltage vector in sequence domain. The subscripts 0,1 and 2 represent zero, positive and negative domains, respectively. This naming convention will be used in the sequel.

Let T be the Edith Clarke's transformation matrix [73] given by:

$$T = \frac{1}{\sqrt{3}} \begin{bmatrix} 1 & \sqrt{2} & 0 \\ 1 & -\frac{1}{\sqrt{2}} & \frac{\sqrt{3}}{\sqrt{2}} \\ 1 & -\frac{1}{\sqrt{2}} & -\frac{\sqrt{3}}{\sqrt{2}} \end{bmatrix} \tag{64}$$

Among several well-known transformation matrices, Clarke's matrix has some desirable properties. It is real and orthogonal. For symmetrical lines, Clarke's matrix produces the exact solution while for unsymmetrical lines it produces a very good approximation [74].

Phase domain measurements can be transformed to sequence domain by the inverse Clarke's transformation as below

$$Z_{012} = T^{-1} \cdot Z_{abc} \tag{65}$$

where:

$Z_{abc} = (z_a, z_b, z_c)^T$ is phase domain measurement;

$Z_{012} = (z_0, z_1, z_2)^T$ is transformed sequence domain measurement;

T^{-1} is the inverse of Edith Clarke's transformation matrix.

Similar to single-phase state estimation, the system equations in positive, negative and zero sequence domains are given by:

$$\begin{cases} Z_0 = H_0 X_0 + e_0 \\ Z_1 = H_1 X_1 + e_1 \\ Z_2 = H_2 X_2 + e_2 \end{cases} \tag{66}$$

For convenience, the linear model is used for all three sequences here.

The first step of the sequence domain state estimation algorithm is utilizing single-phase state estimation algorithm to find the solutions for positive, negative and zero domain, using the transformed sequence measurements obtained from (65) and the sequence domain system equations given by (66). After that three-phase solution can be calculated by (63).

6.8.2 Phase Angle Reference

Any state estimation program needs a reference bus. For single-phase state estimation, the angle of the reference bus will be set to zero. Whereas in three-phase state estimation, we consider the reference bus is balanced and its angles will be set to (0^o, -120^o, 120^o). In the proposed sequence domain state estimation, we need to take into account not only the angle reference inside each sequence circuit, but also the angle references between them. Equation (67) can be used to find the angle references between different component models.

$$ref_{012} = angle(T^{-1} \cdot V_{ref-abc}^{Mea} \cdot e^{j\theta_{ref-abc}}) \tag{67}$$

where:

$ref_{012} = (ref_0, ref_1, ref_2)^T$ is the reference angle vector in sequence domain;

$V_{ref-abc}^{Mea} = (v_{ref-a}^{mea}, v_{ref-b}^{mea}, v_{ref-c}^{mea})^T$ is three-phase voltage magnitude measurement vector for reference bus;

$\theta_{ref-abc} = (0^o, -120^o, 120^0)^T$ is three-phase voltage angle vector for reference bus.

It is easily to see that the angle references between different sequence circuits are nothing but the voltage angle vector for the reference bus in the sequence domain and they are constant for a given measurement scan. Their values rely on the voltage magnitude measurements for reference bus. In order to reduce the computation error, the

reference bus must be chosen from those buses which have high accuracy voltage magnitude measurements.

6.8.3 Consideration for Measurements Transformation

Conventional state estimation utilizes three kinds of measurements: power injections, power flows and bus voltage magnitudes. In sequence domain state estimation, they need to be transformed into sequence domain by (65). It is not possible to transform power measurements, including power injections and power flows, into different sequence components directly. The state estimation algorithm utilizing current injection method can solve this problem. Firstly, the power measurements will be transformed to current measurements in the phase domain. After that, the current measurements in different sequence components can be calculated by (65). The current injection state estimation process in each sequence will use these converted current measurements to estimate the system states. The detailed procedure of transforming power measurements to current measurements will be addressed later in this chapter.

Voltage angles are not measured in most of the practical power system. Voltage magnitude measurements cannot be transformed to sequence domain without the voltage angle measurements. In order to apply (65) on voltage magnitude measurements, artificial phase measurements are introduced and their values are set to the estimated voltage angle values after each iteration. Simulation results show that this technique produce satisfactory performance. On the other hand, different kinds of phasor measurement units (PMU) have been installed in power system during the recent decades [75]-[76]. Phase measurements can also be acquired directly by these new devices. The introduction of phase measurement in this method may improve the efficiency and accuracy. However, this issue will not be further discussed in this dissertation.

6.8.4 The Jacobian Matrix

The Jacobian matrix is not required to be constant in a conventional state estimation program. For instance, the Jacobian matrix will change together with the system states if Newton-Raphson method is used. However, in sequence domain state estimation, the state variables may be very close to zero in certain sequence circuits, such as in the zero and negative sequence. If some of the Jacobian matrix elements depend on these variables, the whole matrix will become ill-conditioned. In our study, the current

injection method with rectangular coordinates equations is utilized to make the Jacobian matrix constant, thus to avoid this situation.

6.9 Basic Formulation and Current Injection Method

The state estimation formulation based on current injections, instead of power measurements, is described in this section. All the measurement equations will be formulated in rectangular coordinates.

6.9.1 Measurement Equations for the Current Injection Method

In the current injection method the relation between the measurements and the state variables is linear, as shown in (66). For convenience, here only the equations for one sequence will be given and the sequence subscripts will be ignored.

Equation (66) can be written in detail as:

$$\begin{bmatrix} V_y \\ injI_x \\ flowI_x \\ V_x \\ injI_y \\ flowI_y \end{bmatrix} = \begin{bmatrix} \partial V_y / \partial f & \partial V_y / \partial e \\ \partial injI_x / \partial f & \partial injI_x / \partial e \\ \partial flowI_x / \partial f & \partial flowI_x / \partial e \\ \partial V_x / \partial f & \partial V_x / \partial e \\ \partial injI_y / \partial f & \partial injI_y / \partial e \\ \partial flowI_y / \partial f & \partial flowI_y / \partial e \end{bmatrix} \begin{bmatrix} f \\ e \end{bmatrix} + \varepsilon \tag{68}$$

where:

V_x, V_y are the real and imaginary part of the voltage measurements;

$injI_x, injI_y$ are the real and imaginary part of the current injection measurements calculated from power injection measurements;

$flowI_x, flowI_y$ are the real and imaginary part of the line current measurements calculated from power flow measurements;

e, f are the real and imaginary part of the system state.

ε is the measurement errors

Note here that the Jacobian matrix (H) is constant for fixed network topology.

The WLS estimate for the sequence states will be given by:

$$\begin{bmatrix} f \\ e \end{bmatrix} = (G)^{-1} H^T R^{-1} Z \tag{69}$$

where:

H is the Jacobian matrix obtained from (68);

Z is the measurement vector;

R is the covariance matrix for measurement vector;

$G = H^T R^{-1} H$ is the gain matrix.

6.9.2 Measurement Transformation

The phase domain measurements are power injections, power flows and voltage magnitude. They must be transformed to generate the measurement vector used in (68).

1) Power injection measurement

Three-phase power injection measurement can be transformed to three-phase current injection by:

$$injI^i_{abc} = \left[(P_{inj-i} + jQ_{inj-i}) / V^{i-cal}_{abc}\right]^* \tag{70}$$

where:

$injI^i_{abc}$ is the three-phase current injection vector on bus i;

P_{inj-i}, Q_{inj-i} are real and reactive power injection measurement on bus i;

V^{i-cal}_{abc} is the computed three-phase voltage vector on bus i.

Using (65) $injI^i_{abc}$ can be transformed into sequence domain and its rectangular form will be given by $injI_x, injI_y$ vector in (68).

2) Power flow measurement

Three-phase power flow measurement can be transformed to three-phase line current by:

$$flowI^i_{abc} = \left[(P_{flow-i} + jQ_{flow-i}) / V^{i-cal}_{abc}\right]^* \tag{71}$$

where:

$flowI^i_{abc}$ is the three-phase corresponding line current vector of measurement i;

P_{flow-i}, Q_{flow-i} are i^{th} real and reactive power flow measurement;

V^{i-cal}_{abc} is the computed three-phase voltage vector of the sending-end bus of power flow measurement i.

Using (65) $flowI_i^{abc}$ can be transformed into sequence domain and its rectangular form will be given by $flowI_{x,}flowI_y$ vector in (68).

3) Voltage magnitude measurement

Three-phase power flow measurement can be transformed to sequence domain by:

$$V_{012}^{mea} = T^{-1} \cdot (V_{abc}^{mea} \cdot e^{angle(V_{abc}^{cal})}) \tag{72}$$

where:

V_{012}^{mea} is corresponding voltage vector in sequence domain;

T^{-1} is the inverse of Clarke's transformation matrix shown in (64);

V_{abc}^{mea} is the three-phase voltage magnitude measurement;

V_{abc}^{cal} is the calculated three-phase voltage vector.

The rectangular form of V_{012}^{mea} will be given by $V_{x,}V_y$ vector in (68).

6.9.3 Transformation of Measurement Weights

In conventional state estimation, the weights of measurements are set to the inverse of corresponding measurement variances directly. However, in sequence domain state estimation, the weights of the computed measurements need to be determined by the statistical transformation of the original measurements' covariance matrix.

More attention must be paid to the weights of imaginary part of voltage measurements. From (72), we can see that the computed angle values are used to get the real and imaginary part of voltage measurements. Those artificial phase measurements are introduced without variance information. One solution for this problem is to set lower weights to the imaginary part of voltage measurements. Test results show that setting the weights of imaginary part of voltage measurement as $1/10^{th} – 1/5^{th}$ of other measurements can produce a satisfactory results.

6.9.4 Jacobian Matrix Elements

The elements of the Jacobian matrix for voltage measurements and current injection measurements in (68) are given by the following equations:

$$\frac{\partial V_y}{\partial f} = 1; \frac{\partial V_y}{\partial e} = 0 \tag{73}$$

$$\frac{\partial V_x}{\partial f} = 0 ; \frac{\partial V_x}{\partial e} = 1 \tag{74}$$

$$\frac{\partial injI_x}{\partial f} = -b_{inj} ; \frac{\partial injI_x}{\partial e} = g_{inj} \tag{75}$$

$$\frac{\partial injI_y}{\partial f} = g_{inj} ; \frac{\partial injI_y}{\partial e} = b_{inj} \tag{76}$$

where:

$g_{inj} + jb_{inj}$ is the corresponding element in the nodal admittance matrix;

For the sending-end bus, the elements corresponding to line current measurements are given by:

$$\frac{\partial flowI_x}{\partial f} = -b_{flow} - c_{flow} ; \frac{\partial flowI_x}{\partial e} = g_{flow} \tag{77}$$

$$\frac{\partial flowI_y}{\partial f} = g_{flow} ; \frac{\partial flowI_y}{\partial e} = b_{flow} + c_{flow} \tag{78}$$

While for the receiving-end bus, the elements corresponding to line current measurements are given by:

$$\frac{\partial flowI_x}{\partial f} = b_{flow} ; \frac{\partial flowI_x}{\partial e} = -g_{flow} \tag{79}$$

$$\frac{\partial flowI_y}{\partial f} = -g_{flow} ; \frac{\partial flowI_y}{\partial e} = -b_{flow} \tag{80}$$

where:

$g_{flow} + jb_{flow}$ is the line admittance;

c_{flow} is the line susceptance.

6.10 Implementation

6.10.1 Iterative Procedure

A prototype program utilizing the sequence domain state estimation method was developed. The flow chart of this program is given in Fig. 28.

The power system is given in detailed three-phase model. Clarke's transformation is used to generate the sequence networks. Then the procedure developed in the above sections is run iteratively until convergence to get the full detailed three-phase solution for the given system.

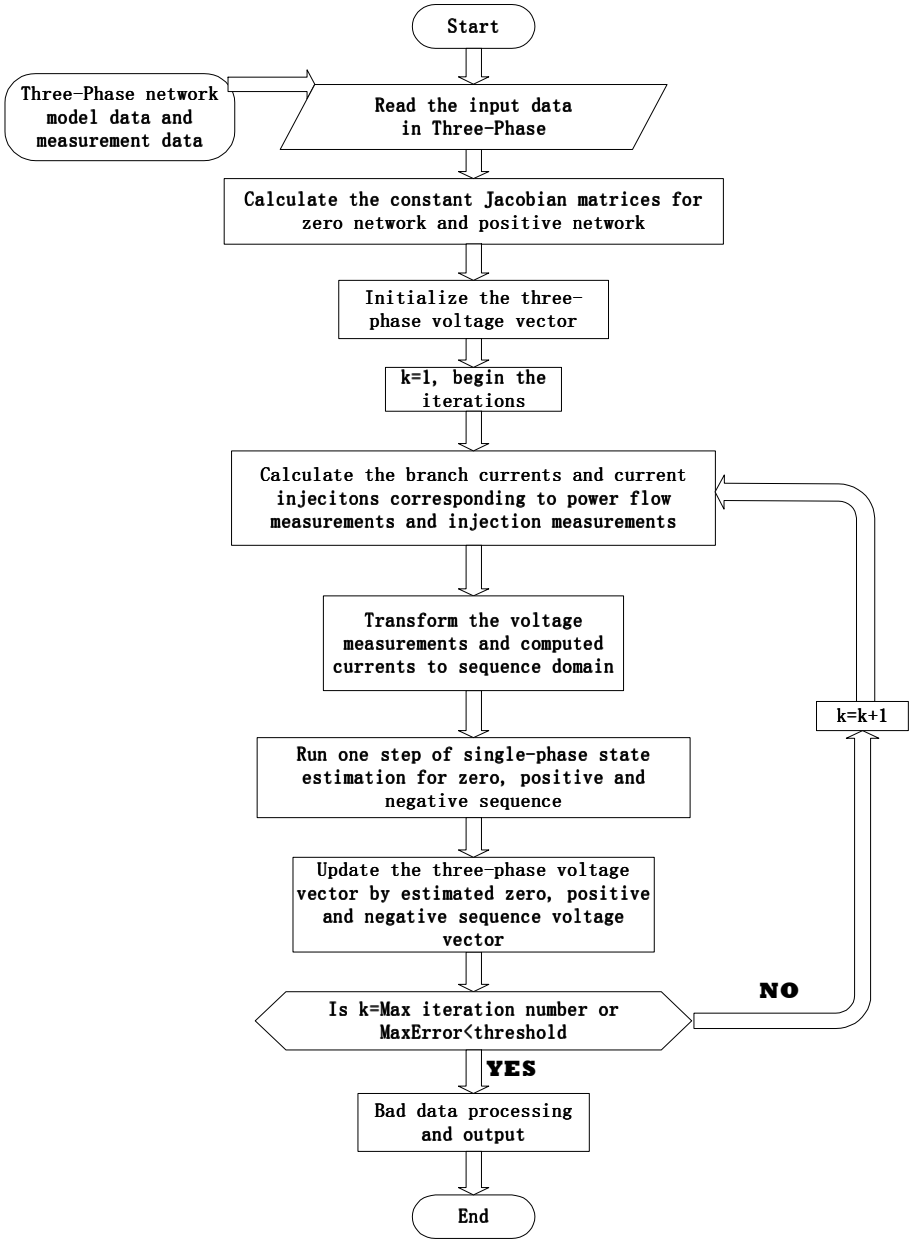

Fig. 28. Flow chart of sequence domain state estimation

All the transformers in the system are assumed to have Y-Y grounded connection. The zero component network of this kind of transformer will have the same connectivity as the other two sequence components. Other types of transformer connections can be accounted for but not done here in this work.

6.10.2 Observability Analysis

When sufficient measurements are available, the state vector of the whole system can be obtained by state estimation. In this case, the network is said to be observable. The conventional numerical observability analysis based on triangular factorization of the gain matrix can be applied in the sequence domain state estimation with little modification. If any zero pivots are encountered during the factorization of any gain matrix, it indicates that the state of the corresponding bus is not observable. This numerical observability algorithm can also be extended to suggest additional meter placement.

6.11 Test Results for Sequence Domain State Estimation

The proposed sequence domain state estimation method was tested on different IEEE testing systems. Section 6.3 describes how to generate the full three-phase simulation data based on IEEE testing systems. In order to simulate the real power system, Gaussian noises are added to all measurements.

6.11.1 Simulation Results for Balanced System

A full balanced system based on IEEE 30 bus system is used in this case. The estimated states of proposed method and conventional three-phase state estimation method [62] are compared. The results are shown in Fig. 29 and Fig. 30.

The profiles of voltage magnitudes and angles show that the estimated states obtained from the proposed method and the conventional three-phase method match closely.

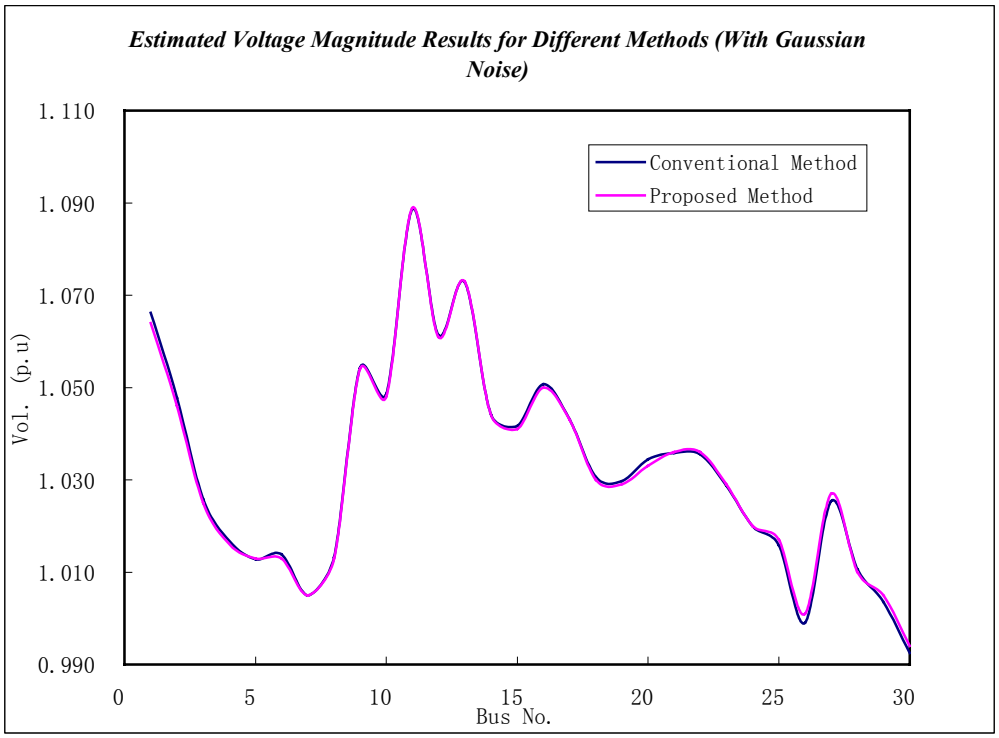

Fig. 29. Voltage magnitude profiles (balanced case)

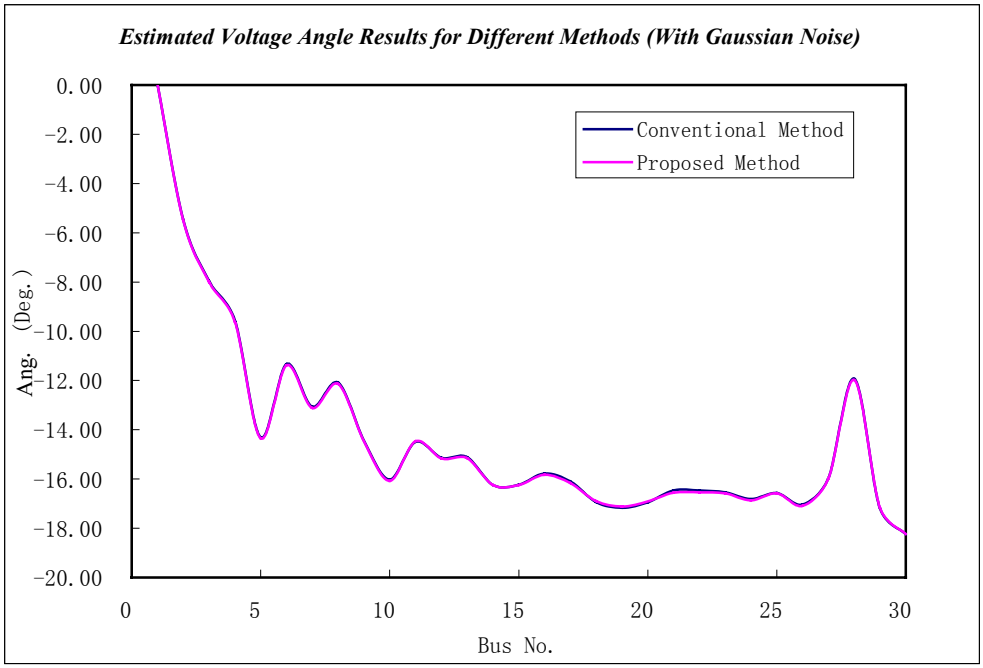

Fig. 30. Voltage angle profiles (balanced case)

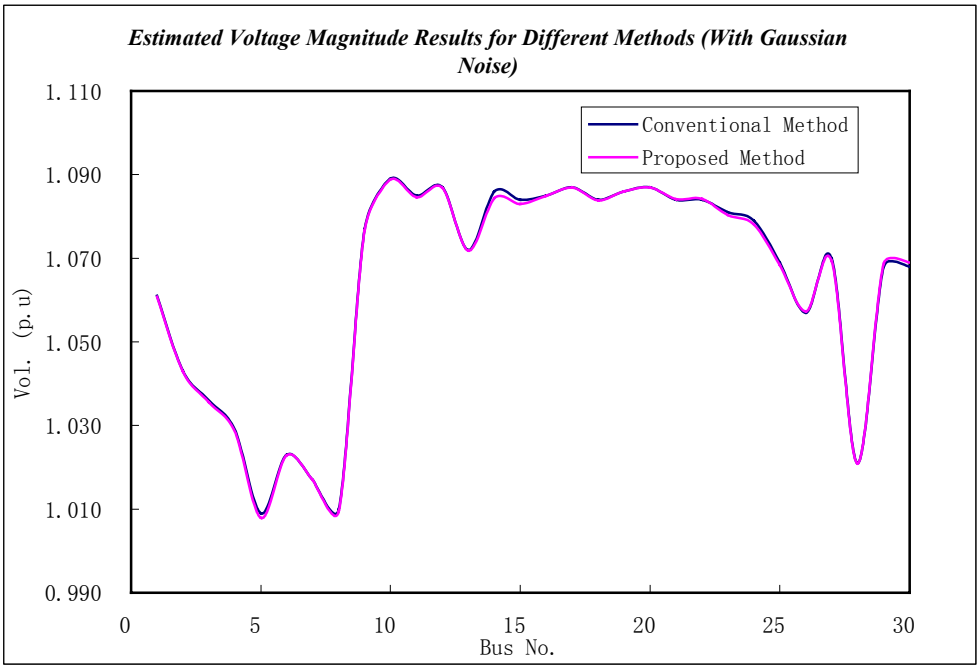

Fig. 31. Voltage magnitude profiles (unbalanced case)

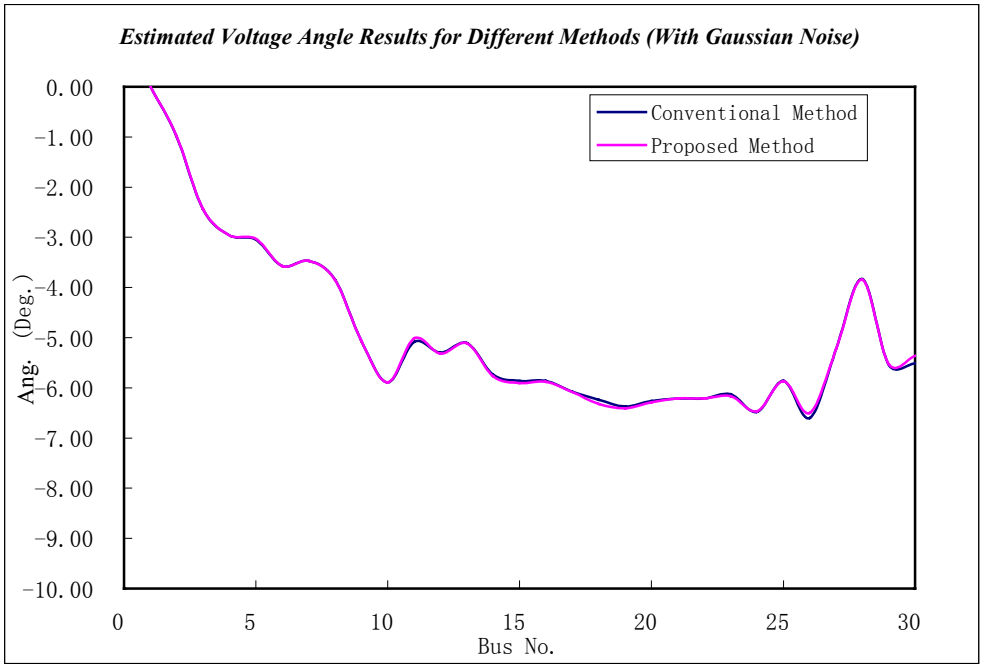

Fig. 32. Voltage angle profiles (unbalanced case)

6.11.2 Simulation Results for Unbalanced System

In this case, unbalanced loads are introduced. The loads in phase A are set to 60% of other two phases. We also get the estimated states by proposed method and conventional three-phase state estimation method. The results are shown in Fig. 31 and Fig. 32.

Fig. 31 and Fig. 32 shows that for the unbalanced case, the proposed method can also produce very good results.

6.11.3 Improved Efficiency

By profiling the running time of the prototype program, we can see that the time spent on transformation between phase domain and sequence domain is trivial compared to the time spent on WLS algorithm. One can conclude that the total time consuming in this method approximate to 3 times the single-phase state estimation method. This claims a great improvement.

The prototype program was tested in different sizes' systems. The iteration numbers and approximate computation times for those systems are shown in Table XXVIII*(The computer used to run the program has a P3 866 inter CPU. Prototype program was developed in matlab6.0. The tolerance for converge is 0.0001 for both magnitude and angle).*

TABLE XXVIII
ITERATION NUMBERS AND COMPUTATION TIMES

Bus No.	**4**	**14**	**30**	**57**	**118**
Meas. No.	72	288	606	1152	2490
Iter. No.	5	6	7	6	6
Times (Sec.)	0.015	0.040	0.080	0.190	0.360

The relationship of measurements numbers and computation times is shown in Fig. 33.

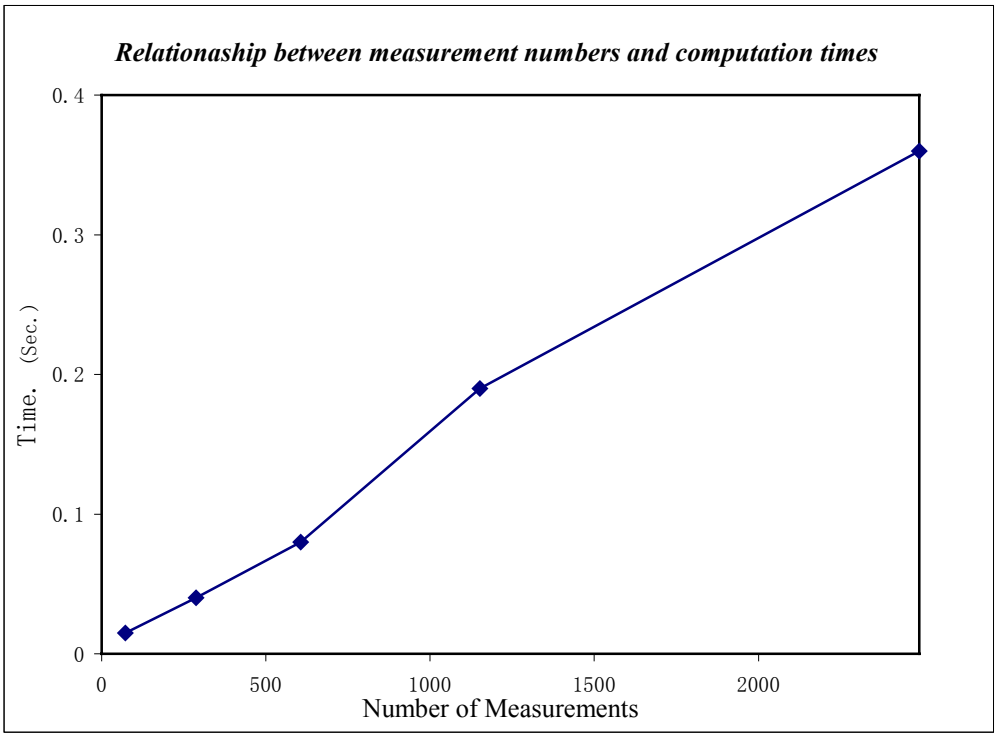

Fig. 33. Relationship of measurement numbers and computation times

We can see from Fig. 33 that the relationship between system sizes (measurement number) and computation time is approximately linear. This also shows a very good property of the proposed method.

6.12 Conclusions

This chapter investigates the effects of unbalanced loads and non-transposed transmission lines on the solution of the positive sequence state estimation problem. A number of simulations are carried out using varying degrees of unbalance among the three phases of bus loads as well as the mutual coupling between pairs of phase conductors. The simulation results indicate a higher sensitivity of the system state to loading unbalances than to asymmetries in the transmission line conductor configurations. It is also demonstrated that under certain cases, the use of single-phase state estimator

may lead to significant biases in the solution due to existing asymmetries or load unbalances.

A novel state estimation approach for unbalanced transmission systems is also presented in this chapter. The system is assumed to be full symmetrical, thus can be represented by three independent sequence component models. Full detailed three-phase measurements are transformed to sequence domain. Single-phase state estimation can be run independently in each sequence domain. The estimated results are transformed back to a-b-c domain to get the three-phase solution. Current injection method and rectangular coordinates equations are also used to further improve the efficiency.

This approach was successfully tested in several systems with different sizes. While limited work is also done on bad data processing aspects of this method, further work is needed in order to fully address the issues of bad data detection/identification in three-phase state estimation.

CHAPTER VII

CONCLUSIONS

The implementation of a two-stage state estimation algorithm capable of topology error identification is discussed in chapter II. A concise substation model and the minimum required extra data set needed to run the two-stage state estimation are defined. With these data structures, a conventional state estimator is updated to support the two-stage algorithm.

Chapter III investigates the part of the two-stage state estimation algorithm involving the suspect bus identification procedure following the first stage estimation. Several possible strategies are developed and comparatively tested by using a topology error library that is created for this purpose based on IEEE 30 bus test system. The performance of each method is evaluated by simulations using this library.

For those cases where status of the CB is assumed to be open while it is actually closed (*type2* and *type3*), most of the methods can identify the suspect buses correctly. On the other hand, for the opposite scenarios, not all of the methods show equally good performance. However, one of the developed methods appears to remain robust by performing consistently well under all studied scenarios. This method is the main contribution of this study and is expected to enhance the performance of the two-stage topology error identification method significantly.

Chapter IV describes a novel remote measurement calibration technique. The measured values are related to the true values by the relationship functions. The detailed formulation of including the coefficients of these functions in a normal state estimation problem is presented. The coefficients will be estimated along with the system state and used to calibrate the measurements. This technique can also be implemented as off-line mode and formulate several snapshots together to suppress the influence of random errors. Moreover, observability of those coefficients under low redundancy measurement configuration is discussed. The pseudo-coefficient-measurements are introduced to solve the numerical problem. This method is tested on different sizes IEEE systems. The simulation results show that the proposed calibration procedure can improve the performance of state estimation even under low redundancy condition.

A systematical solution for estimation of measurement random error variances is described in Chapter V. An initialization process and a recursively updating process realize the auto tuning of the measurement weight in state estimation. The simulation result shows successful performance.

Two different estimation methods are studied together. The current method (*Method 1)* has better performance while is time consuming. The proposed simplified method (*Method 2)* is very efficient and can get satisfied result. Moreover, compare to *method 1*, *method 2* is much easier to be implemented in a practical system.

Chapter VI investigates the effects of unbalanced loads and non-transposed transmission lines on the solution of the positive sequence state estimation problem. A number of simulations are carried out using varying degrees of unbalance among the three phases of bus loads as well as the mutual coupling between pairs of phase conductors. The simulation results indicate a higher sensitivity of the system state to loading unbalances than to asymmetries in the transmission line conductor configurations. It is also demonstrated that under certain cases, the use of single-phase state estimator may lead to significant biases in the solution due to existing asymmetries or load unbalances.

A novel SE approach for unbalanced transmission systems is also presented in this chapter. The system is assumed to be full symmetrical, thus can be represented by three independent sequence component models. Full detailed three-phase measurements are transformed to sequence domain. Single-phase SE can be run independently in each sequence domain. The estimated results are transformed back to a-b-c domain to get the three-phase solution. Current injection method and rectangular coordinates equations are also used to further improve the efficiency.

This approach was successfully tested in several systems with different sizes. While limited work is also done on bad data processing aspects of this method, further work is needed in order to fully address the issues of bad data detection/identification in three-phase state estimation.

7.1 Summary of Contributions

In conclusion, the main contributions of this dissertation are:

1. A two-stage state estimation algorithm for topology error identification on a conventional state estimator is implemented. The substation model and the minimum extra data structure are designed. A program with friendly user interface and program interface is developed;
2. A comprehensive suspected area identification method for two-stage state estimation is proposed. Topology errors library for evaluating the performance of different methods is created;
3. A remote measurement calibration algorithm and a systematical calibration procedure are developed;
4. A systematical method to estimate the standard deviation of the measurements, which result in an auto-tuning process for measurement weights is proposed;
5. The influences of the imbalances of power networks on the conventional positive state estimation process are studied. A novel three-phase state estimation algorithm is developed and preliminary testing is carried out.

7.2 Future Work

We can never claim our work is finished. There is still a lot of room for further developments. In the future, our research work can be improved in the following directions:

1. The proposed methods/processes should be tested on practical power systems. Owing to lack of data from practical systems, all the proposed methods are only tested on simulated systems. The two-stage state estimation algorithm, the comprehensive method for suspected area identification, and process of remote measurement calibration and auto-tuning of the measurement weights are needed to be tested in practical systems in the future before their practical application;
2. Further research on the new sequence domain three-phase state estimation algorithm. The presented method did not completely address the issues of bad data detection/identification, angle reference between different sequences, etc, which can be studied in the future.

REFERENCES

[1] F.C. Schweppe, J. Wildes, and D.B. Rom, "Power system static-state estimation, parts I, II and III," *IEEE Trans. Power Apparatus and Systems,* vol. PAS-89, pp. 120-135, January 1970.

[2] T.E. Dy Liacco, "An overview of power system control centers," *Energy Control Center Design, IEEE Tutorial Course,* TU0010-9PWR, 1977.

[3] T.E. Dy Liacco, "System security: the computer's role," *IEEE Spectrum,* vol. 1, pp. 43-50, June 1978.

[4] A. Monticelli, *State Estimation in Electric Power Systems: A Generalized Approach,* New York: Kluwer Academic Publishers, 1999.

[5] L, Holten, A. Gjelsvik, S. Adm, F.F. Wu, and W.E. Liu, "Comparison of different methods for state estimation," *IEEE Trans. Power Systems,* vol. 3, no. 4, pp. 1798-1806, November 1988.

[6] F.F, Wu, "Power system estimation: a survey," *Electrical Power & Energy Systems,* vol. 12, no. 2, pp. 80-87, April 1990.

[7] A, Monticelli and A. Garcia, "Fast decoupled state estimations," *IEEE Trans. Power Systems,* vol. 5, no. 2, pp. 556-564, May 1990.

[8] A. Abur and M.K. Celik, "Topology error identification by least absolute value state estimation," in *Proc. 7th Mediterranean Electrotechnical Conference,* 1994, pp. 972-975.

[9] A, Abur and M.K. Celik, "A fast algorithm for the weighted least absolute value state estimation," *IEEE Trans. Power Systems,* vol. 6, no. 1, pp. 1-8, February 1991.

[10] M.K, Celik and A. Abur, "A robust WLAV state estimation using transformation," *IEEE Trans. Power Systems,* vol. 7, no. 1, pp. 106-133, February 1992.

[11] A. Monticelli, "Electric power system state estimation," *Proceedings of the IEEE,* vol. 88, no. 2, pp. 262-282, February 2000.

[12] K.A. Clements, G.R. Krumpholz, and P.W. Davis, "Power system state estimation with measurement deficiency: an observability/measurement placement algorithm," *IEEE Transactions on Power Apparatus and Systems,* vol. PAS-102, no. 7, pp. 2012-2020, July 1983.

[13] A. Monticelli and F.F. Wu, “Network observability: identification of observable islands and measurement placement,” *IEEE Transactions on Power Apparatus and Systems,* vol. PAS-104, no. 5, pp. 1035-1041, May 1985.

[14] A. Monticelli and F.F. Wu, “Network observability: Theory,” *IEEE Transactions on Power Apparatus and Systems,* vol. PAS-104, no. 5, pp. 1042-1048, May 1985.

[15] H. Kim, "Power system state estimation enhancements," Ph.D. dissertation, Dept. Electrical Engineering, Texas A&M University, College Station, 1995.

[16] N. Singh and H. Glavitsch, “Detection and identification of topological errors in online power system analysis,” *IEEE Transactions on Power Systems,* vol. 6, no. 1, pp. 324-331, February 1991.

[17] N. Singh and F. Oesch, “Practical experience with rule-based on-line topology error detection,” *IEEE Transactions on Power Systems,* vol. 9, no. 2, pp. 841-847, May 1994.

[18] T. Tian, M. Zhu, and B. Zhang, “An artificial neural network-based expert system for network topological error identification,” in *Proc. 1995 IEEE International Conference on Neural Networks,* vol.2, pp.882-886.

[19] A.S. Costa and J.A. Leao, “Identification of topology errors in power system state estimation,” *IEEE Transactions on Power Systems,* vol. 8, no. 4, pp.1531-1538, November 1993.

[20] K.A. Clements and P.W. Davis, “Detection and identification of topology errors in electric power systems,” *IEEE Transactions on Power Systems,* vol. 3, no. 4, pp.1748-1753, November 1988.

[21] F.F. Wu and W.-H.E. Liu, “Detection of topology errors by state estimation,” *IEEE Transactions on Power Systems,* vol. 4, no. 1, pp.176-183, February 1989.

[22] A. Monticelli, “Modeling zero impedance branches in power system state estimation,” *IEEE Transactions on Power Systems,* vol. 6, no. 4, pp.1561-1570, November 1991

[23] A. Monticelli, “The impact of modeling short circuit branches in state estimation,” *IEEE Transactions on Power Systems,* vol. 8, no. 1, pp.364-370, February 1993.

[24] A. Abur, H. Kim, and M. Celik, "Identifying the unknown circuit breaker statuses in power networks," *IEEE Transactions on Power Systems,* vol. 10, no. 4, pp.2029-2037, November 1995.

[25] K.A. Clements and A.S. Costa, "Topology error identification using normalized lagrange multipliers," *IEEE Transactions on Power Systems,* vol. 13, no. 2, pp.347-353, May 1998.

[26] A.S. Costa and F. Vieria, "Topology error identification through orthogonal estimation methods and hypothesis testing [power system]," in *Proc. 2001 IEEE Power Tech Conference,* vol.3, Paper EDT4-253.

[27] J.C. Pereira, J.T. Saraiva, V. Miranda, A.S Costa, E.M. Lourengo, and K.A. Clements, "Comparison of approaches to identify topology errors in the scope of state estimation studies," in *Proc. 2001 IEEE Power Tech Conference,* vol.3, Paper EDT3-176.

[28] Antonio Gomez Exposito and Antonio de la Villa Jaen. "Reduced substation models for generalized state estimation," *IEEE Transactions on Power Systems,* vol.16, no.4, pp.839-846, November 2001.

[29] A. Abur, "A bad data identification method for linear programming state estimation," *IEEE Transactions on Power Systems*, vol.5, no.3, pp.894-901, August 1990.

[30] M. R. Irving and M. J. Sterling, "Substation data validation," *IEE Proceedings,* vol.129, no.3, pp.119-122, May 1982.

[31] G. Turan, *Electric Power Distribution System Engineering,* New York: McGraw-Hill Book Company, 1986.

[32] A. Abur, F. Magnago, and Y. Lu, "Educational toolbox for power system analysis," *IEEE Computer Applications in Power,* vol.13, no.4, pp. 31-35, October 2000.

[33] A. Abur, *Power Education Toolbox (P.E.T) User Manual,* Texas A&M University, College Station, TX, 1999.

[34] A. Debs, "Parameter estimation for power systems in the steady state," *IEEE Transactions on Automatic Control,* vol. AC-19, no. 6, pp. 882-886, December 1974.

[35] A. Z. Gamm, Y. A. Grishin, A. M. Glazunova, and I. N. Kolosok, "Methods for identification of telemetering random errors variances in electric power systems," in

Proc. 1998 International Conference on Power System Technology, vol.2, pp. 1255-1259.

[36] A. Z. Gamm, A. M. Glazunova, and I. N. Kolosok, "Identification of measurement variances based on test equations using ANN," in *Proc. 2001 IEEE Power Tech Conference,* vol.2, Paper AIT1-084.

[37] G. Liu, E. Yu, and Y.H. Song, "Novel algorithms to estimate and adaptively update measurement error variance using power system state estimation results," *Electric Power Systems Research,* vol. 47, no. 1, pp. 57-64, October 1998.

[38] W. Hubbi, "Computational method for remote meter calibration in power systems," *IEE Proceedings: Generation, Transmission and Distribution,* vol.143, no. 5, pp. 393-398, September 1996.

[39] J.G. Moreno and J.L.M. Vigil-Escalera, R.S. Alvarez, "Statistical measurement calibration based on state estimator results," in *Proc. 1999 IEEE Power Engineering Society Transmission and Distribution Conference,* vol.1, pp. 184-189.

[40] M. M. Adibi and D. K. Throne, "Remote measurement calibration," *IEEE Transactions on Power Systems,* vol. PWRS-1, no. 2, pp. 194-203, May 1986.

[41] M. M. Adibi and R. J. Kafka, "Minimization of uncertainties in analog measurement," *IEEE Transactions on Power Systems,* vol. 5, no. 3, pp. 902-910, August 1990.

[42] M. M. Adibi and J. P. Stovall, "On estimation of uncertainties in analog measurements," *IEEE Transactions on Power Systems,* vol. 5, no. 4, pp. 1222-1230, November 1990.

[43] M. M. Adibi, K. A. Clements, R. J. Kafka, and J. P. Stovall, "Integration of remote measurement calibration with state estimation-a feasibility study," *IEEE Transactions on Power Systems,* vol. 7, no. 3, pp. 1164-1172, August 1992.

[44] N.I. Deeb, "Calibration of measurement sets in an electric power system using an updated broyden method," in *Proc. the American Power Conference,* vol.51, pp. 610-621, 1989.

[45] A. Fallaha, E. Cohen, A. Kayyali, and A. Ming, "Calibration of power flow measurements," *Electric Power Systems Research,* vol. 38, no. 1, pp. 1-10, July 1996.

[46] F. Shoukri-Kourdi and E. Cohen, “Two-stage calibration of power flow measurements without reliable points,” *Electric Power Systems Research,* vol. 52, no. 2, pp. 83-90, May 1999.

[47] L. Mili and A. Ghassemian, “Robust remote measurement calibration in power systems,” in *Proc. 2001 IEEE Power Engineering Society Summer Meeting,* vol.1, pp. 439-441.

[48] K.A. Clements and P.W. Davis, “Multiple bad data detectability and identifiability: a geometric approach,” *IEEE Transactions on Power Delivery,* vol. PWRD-1, no. 3, pp. 355-360, July 1986.

[49] K.A. Clements, G.R. Krumpholz, and P.W. Davis, “Power system state estimation residual analysis: an algorithm using network topology,” *IEEE Transactions on Power Apparatus and Systems,* vol. PAS-100, no. 4, pp. 1779-1787, April 1981.

[50] P. Zarco and A. Gomez, “Off-line determination of network parameters in state estimation,” in *Proc. 12th Power System Computation Conference*, 1996, pp. 1207-1213.

[51] P. Zarco, A. Gomez, “Power system parameter estimation: a survey,” *IEEE Transactions on Power Systems,* vol. 15, no. 1, pp. 216-222, February 2000.

[52] M. Allam and M. Laughton, "A general algorithm for estimating power system variables and network parameters," in *Proc. 1974 IEEE Power Engineering Society Summer Meeting,* Paper C74 331-5.

[53] P. Teixeira, S. Brammer, W. Rutz, W. Merritt, and J. Salmonsen, “State estimation of voltage and phase-shift transformer tap settings,” *IEEE Transactions on Power Systems,* vol. 7, no. 3, pp. 1386-1393, August 1992.

[54] W. Liu and S. Lim, “Parameter error identification and estimation in power system state estimation,” *IEEE Transactions on Power Systems,* vol. 10, no. 1, pp. 200-209, February 1995.

[55] I. Slutsker, S. Mokhtari, and K. Clements, “On-line parameter estimation in energy management systems,” in *Proc. American Power Conference,* 1995, vol. 57-1, pp.161-166.

[56] I. Slutsker and S. Mokhtari, “Comprehensive estimation in power systems: state topology and parameter estimation,” in *Proc. American Power Conference,* 1995, vol. 57-1, pp.149-155.

[57] I. Slutsker and K. Clements, “Real time recursive parameter estimation in energy management systems,” *IEEE Transactions on Power Systems,* vol. 11, no. 3, pp. 1393-1399, August 1996.

[58] O. Alsac, N. Vempati, B. Stott, and A. Monticelli, “Generalized state estimation,” *IEEE Transactions on Power Systems,* vol. 13, no. 3, pp. 1069-1075, August 1998.

[59] S. Zhong and A. Abur, “Remote calibration method for measurements used by the state estimators,” in *Proc. 35th Annual North American Power Symposium,* 2003 [CD-ROM].

[60] A. P. Sakis Meliopoulos, Bruce Fardanesh, and Shalom Zelinger, "Power system state estimation: modeling error effects and impact on system operation," in *Proc. 2001 IEEE 34th Annual Hawaii International Conference on System Sciences,* pp. 1-9.

[61] S. Zhong and A. Abur, "Effects of non-transposed lines and unbalanced loads on state estimation," in *Proc. 2002 IEEE Power Engineering Society Winter Meeting,* vol. 2, pp. 975-979.

[62] H. Kim and A. Abur, "State estimation for three phase power networks," in *Proc. 26th Annual North American Power Symposium,* 1994, pp. 210-220.

[63] C. W. Hansen and A. S. Debs, "Power system state estimation using three-phase models," *IEEE Transactions on Power Systems,* vol. 10, no. 2, pp. 818-824, May 1995.

[64] A. P. Sakis Meliopoulos and F. Zhang, "Multiphase power flow and state estimation for power distribution systems," *IEEE Transactions on Power Systems,* vol. 11, no. 2, pp. 939-946, May 1996.

[65] I. Roytelman and S. M. Shahidehpour, "State estimation for electric power distribution systems in quasi real-time conditions," *IEEE Transactions on Power Delivery,* vol. 8, no. 4, pp. 2009-2015, October 1993.

[66] Mesut E. Baran and Arthur. W. Kelley, "State estimation for real-time monitoring of distribution systems," *IEEE Transactions on Power Systems,* vol. 9, no. 3, pp. 1601-1609, August 1994.

[67] C. N. Lu, J. H. Teng and W. H. E. Liu, "Distribution system state estimation," *IEEE Transactions on Power Systems,* vol. 10, no. 1, pp. 229-240, February 1995.

[68] K. Li, "State estimation for power distribution system and measurement impacts," *IEEE Transactions on Power Systems,* vol. 11, no. 2, pp. 911-916, May 1996.

[69] D. Thukaram, Jovitha Jerome and C. Surapong, "A robust three-phase state estimation algorithm for distribution networks," *Electric Power Systems Research,* vol. 55, pp. 191-200, September 2000.

[70] M. Chen and W. E. Dillon, "Power system modeling," *Proceedings of the IEEE*, vol. 62, pp. 901-915, July 1974.

[71] W.F. Tinney, "A presentation to the workshop in engineering mathematics and computer sciences," in *Proc. Workshop on Advanced Mathematics and Computer Science for Power Systems Analysis*, EPRI EAR/EL-7107 Project 8010, 1991, pp. 1.1-1.13.

[72] S. Carneiro Jr., J.L.R. Pereira, and P.A. Nepomucemo Garcia, "Unbalanced distribution system power flow using the current injection method," in *Proc. 2000 IEEE Power Engineering Society Winter Meeting*, vol. 2, pp. 946-950.

[73] E. Clarke, *Circuit Analysis of AC Power Systems*, vol. I. New York: Wiley, 1950.

[74] M.C. Tavares, J. Pissolato, and C.M. Portela, "New mode domain multiphase transmission line model-Clarke transformation evaluation," in *Proc. 1998 International Conference on Power System Technology*, vol. 2, pp. 860-864.

[75] R.O. Burnett Jr., M.M. Butts, and P.S. Sterlina, "Power system applications for phasor measurement units," *IEEE Computer Applications in Power*, vol. 7, no. 1, pp. 8-13, January 1994.

[76] R.E. Wilson, "PMUs [phasor measurement unit]," *IEEE Potentials*, vol. 13, no. 2, pp. 26-28, April 1994.

VITA

Shan Zhong was born in Mashan, China, on September 25, 1977. He got his B.S. degree from the Department of Electrical Engineering, HuaZhong University of Science and Technology, China, in 1997. In 2000, he received his M.S. degree from the Department of Electrical Engineering, Tsinghua University, China. In August 2000, he began pursuing his Ph.D. degree in the Department of Electrical Engineering at Texas A&M University. He has been a research assistant for his advisor, Dr. Ali Abur. He can be reached at:

Shan Zhong
Power Company
BeiLiu City, GuangXi Province,
China, 537400

The typist for this dissertation was Shan Zhong.